Spring 2020

Modeling Cle Elum Reservoir Shoreline Erosion: GIS Analysis to Support Cultural and Environmental Resource Management, Yakima Basin, Washington

Michael H. Horner
Central Washington University, mihorner@hotmail.com

MODELING CLE ELUM RESERVOIR SHORELINE EROSION: GIS ANALYSIS TO SUPPORT CULTURAL AND ENVIRONMENTAL RESOURCE MANAGEMENT, YAKIMA BASIN, WASHINGTON

A Thesis

Presented to

The Graduate Faculty

Central Washington University

In Partial Fulfillment

of the Requirements for the Degree

Master of Science

Cultural and Environmental Resource Management

---

by

Michael H. Horner

June 2020

CENTRAL WASHINGTON UNIVERSITY

Graduate Studies

We hereby approve the thesis of

Michael H. Horner

Candidate for the degree of Master of Science

APPROVED FOR THE GRADUATE FACULTY

_____ _____
Dr. Karl Lillquist, Committee Chair

_____ _____
Dr. Anthony Gabriel

_____ _____
Dr. Steven Hackenberger

_____ _____
Mr. Shane Scott

_____ _____
Dean of Graduate Studies

ABSTRACT

MODELING CLE ELUM RESERVOIR SHORELINE EROSION: GIS ANALYSIS TO SUPPORT CULTURAL AND ENVIRONMENTAL RESOURCE MANAGEMENT, YAKIMA BASIN, WASHINGTON

by

Michael H. Horner

June 2020

In the Yakima Basin, managers are expanding reservoirs including Cle Elum Lake to increase the availability of water. The objective of this study was to examine areas prone to further shoreline erosion to inform resource management. This research included the use of airphotos and fieldwork to identify erosional shorelines. Erosion was verified in the field using a video survey as well as indicators such as shoreline slope, sediment size, and nearshore width. Near-term erosional segments were identified by more rapidly receding bluffs while long-term erosional segments included both bedrock cliffs and bluffs. Although most of the shoreline is depositional, near-term bluff erosion is most prevalent along the southeastern and northeastern shorelines while long-term erosion is mainly along the northwestern and southeastern shorelines. Potential erosion control variables were identified in the scientific literature and data representing them were acquired from fieldwork and outside sources. Geologic units and slope intervals are statistically significant variables in shoreline erosion. In the near-term shoreline erosion

inventory, low bluffs with sandstone substrates make the largest contribution to the relationship between geologic units and erosional segments. An extensive cliff formed of intrusive igneous rocks is important to the relationship between geologic unit and long-term erosion. Although the nearshore and foreshore zones are largely below 36° reflecting the glacial origins of this basin, intermediate slopes between 11° and 36° and steep slopes between 37° - 49° are mainly responsible for the link between slope intervals and both bluff and cliff erosion. A Geographic Information Systems (GIS) model used these factors to predict relatively limited areas highly susceptible to future erosion, with near-term erosion risk mainly on the eastern and southwestern lakeshore while the southeastern and northwestern shoreline are most susceptible over the long-term. The product of this analysis were hazard maps indicating the relative risk of shoreline erosion. These maps formed the basis of policy recommendations including increased shoreline protection along southeastern shoreline and the implementation of a long-term monitoring program for shoreline erosion to support the management of cultural resources.

ACKNOWLEDGMENTS

This thesis is dedicated to my wife Jamie Bryant Horner and my children Katherine and Natalie Horner whose support and sacrifices made this work possible.

I would like to thank my committee members for their inspiration and assistance in the development of this thesis. In particular, my committee chair Dr. Karl Lillquist was instrumental in the conceptualization of my research topic and methods. In the process of developing this thesis, he taught me the science of geomorphology while proofreading countless drafts. In addition, I would like to thank Dr. Anthony Gabriel for contributing his expertise in coastal environments, field research, and quantitative methods, as well as Dr. Steven Hackenberger and Shane Scott who first suggested studying reservoir erosion and cultural resources.

A number of others also assisted in the development of this thesis. Dr. John Bowen provided invaluable assistance with statistics. David Cordner trained me in the use of field equipment. In the Department of Geology, Dr. Lisa Ely and Dr. Bre MacInnes provided assistance with sedimentology and facilitated access to needed equipment. Finally, Michael Cibicki with the United States Forest Service (USFS) promptly and efficiently provided airphotos when I had difficulty obtaining them elsewhere.

I also thank my colleagues and friends in in the Cultural and Environmental Resource Management program who provided me with valuable assistance in the development of this thesis including sharing ideas, reviewing drafts, and collaborating in course work. This thesis would have been impossible without the support of my work

colleagues at the International Training and Education Center for Health (I-TECH) at the University of Washington, particularly my supervisor Shelly Tonge-Seymour for her remarkable flexibility, encouragement, and support in this endeavor.

Finally, I would like to thank my family and friends. My parents Christine Horner and Dr. Richard Horner always encouraged me in my pursuit of learning and my father provided help with proofreading this work.

TABLE OF CONTENTS

TABLE OF CONTENTS (continued)

Chapter Page

LIST OF TABLES

LIST OF TABLES (Continued)

Table Page

LIST OF FIGURES

LIST OF FIGURES (Continued)

LIST OF FIGURES (Continued)

CHAPTER I

INTRODUCTION

Research Problem

Climate change complicates access to water resources. From 1906 to 2005, global mean temperature increased 0.74° Celsius (C), with the rate of warming doubling over the last fifty years. Climate models predict another increase of 0.4° C by 2030. Higher temperatures will influence the availability of water resources (Hall, Stuntz, and Abrams 2008). More than one-sixth of the world's population in areas such as the American West is dependent on mountain glaciers and seasonal snowmelt for water supplies (Barnett, Adam, and Lettenmaier 2005). Mountain snowmelt feeds many of the Pacific Northwest's river systems (Elsner et al. 2010). Here, snowpack stores more water annually than do artificial reservoirs (Mote et al. 2005). Warmer temperatures will mean that an increased proportion of precipitation will arrive as rain rather than snow (Hall, Stuntz, and Abrams 2008). As the mountain snowpack diminishes, it will only last until early summer (USBOR and WADOE 2012). Early runoff will lead to peak flows in the spring arriving as much as one month earlier by the 2050s (Barnett, Adam, and Lettenmaier 2005). Lower flows will follow during the dry season when demand for water is the highest (Barnett, Adam, and Lettenmaier 2005; Mote et al. 2005). In central Washington State, the Yakima River Basin will lose access to naturally stored water that supplements reservoir storage in the summer for use in the agricultural valleys dependent on irrigation (USBOR and WADOE 2012).

Under the Yakima River Basin Integrated Water Resource Management Plan ("Yakima Plan") adopted in 2011, the Bureau of Reclamation ("Reclamation") is preparing for reductions in snowmelt runoff in several ways including the enlargement of

the Cle Elum and Bumping lake reservoirs (Benson 2012; Yakima Basin Conservation Campaign 2016). Water managers must balance critical instream and offstream uses of the Basin's finite water resources for irrigation, habitat, and municipal supplies. They are unable to fulfill these demands during droughts, leading to major economic losses. Water managers must also fulfill obligations guaranteeing access to fisheries for the Yakama Nation, the Umatilla tribe, the Colville tribe, and the Wanapum Band. These rights were guaranteed to the Yakama Nation and the Umatilla tribe by the Yakima and Walla Walla treaties (1855) (USBOR and WADOE 2012). The 1974 Boldt Decision reaffirmed tribal fishing rights (*United States v. the state of Washington*). Water managers must also ensure access to water on Native American reservations required by *Winters v. United States* (1908) (Cronin and Ostergren 2007). Reservoir enlargement will enable the retention of more water in the basin during the winter. This will compensate for reduced instream flows during the summer to aid the outmigration of juvenile salmon and for use in irrigation (USBOR and WADOE 2011, 2012).

In 2017, Reclamation completed the Cle Elum Pool Raise project (Markell 2017). This increased Cle Elum Lake's maximum elevation by 0.91 m, increasing its capacity 18,008,835 m^3 (14,600 acre-feet), and inundating an additional 0.19 km^3 (46 acres) seasonally (USBOR and WADOE 2015). Reservoir enlargement expanded the zone disturbed by reservoir fluctuations (Bao et al. 2018). The varial zone (Figure 1) lies between the permanent conservation pool, which is the reservoir's minimum average elevation, and the upper floodpool zone that is the maximum elevation occasionally inundated by high levels of runoff storage (Lenihan et al. 1981; Lorang and Stanford

1993). The effects of lake level fluctuations make the varial zone vulnerable to shoreline erosion (Bao et al. 2018).

Because of these fluctuations, the expansion of Cle Elum Lake has the potential to degrade cultural resources. Cle Elum Lake originated as a natural lake during the

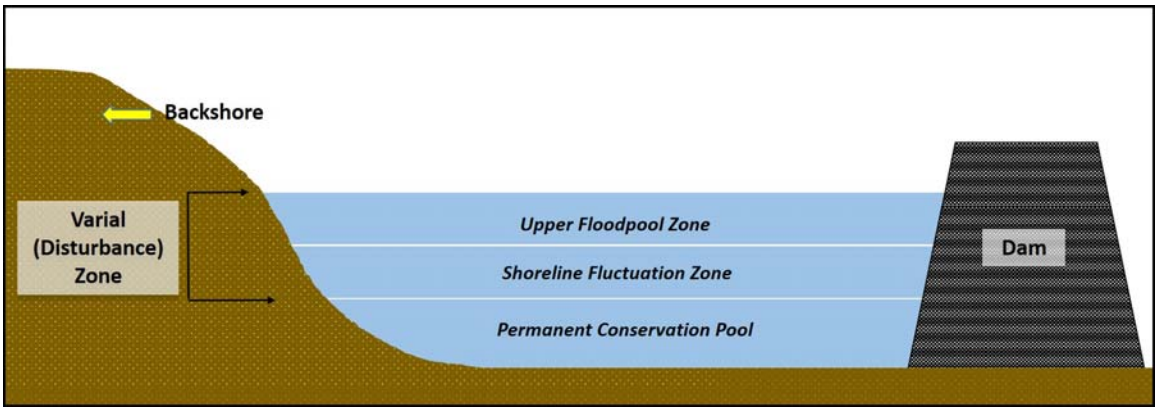

Figure 1: Reservoir zones. Following Lenihan et al. 1981.

Pleistocene (WADOE 2004). It features archaeological evidence of pre-historic cultural activity due to its past role as a fishing ground (USBOR and WADOE 2011). These archaeological sites may require protection under applicable laws including the National Historic Preservation Act (NHPA) (1966), the State of Washington Environmental Policy Act (SEPA), Executive Order 13007: Indian Sacred Sites (1996), the American Indian Religious Freedom Act (1978), and the Native American Graves Protection and Repatriation Act (NAGPRA) (1990) (Harjo 2004; USBOR and WADOE 2015). Both SEPA and NHPA require agencies to survey historically significant features and manage the effects of projects on them. These effects are adverse if they involve cultural resources included in or qualifying for the National Register of Historic Places (NRHP). Under Executive Order 13007, Federal agencies must facilitate the use of sites sacred to Native Americans and prevent impacts to them unless they follow a public notification process. It will also be necessary to prepare for the exposure of graves, regulated by

NAGRPA (USBOR and WADOE 2015). These regulations all require an understanding of the effects of reservoir expansion on cultural resources.

Research Objectives

This study modelled erosion due to the expansion of Cle Elum Lake to support cultural and environmental resource management at in the Yakima Basin. It included five objectives: 1) mapping erosional and depositional shoreline segments; 2) identifying the physical characteristics of erosional sites; 3) determining the physical variables affecting shoreline erosion; 4) modelling erosion susceptibility and creating hazard maps; and 5) making management recommendations based on these findings.

Research Significance

The main significance of this study is that it offers an evaluation of the potential impacts of reservoir expansion to inform future reservoir expansion in the Yakima Basin and other regions facing water scarcity. This is most relevant to the proposed expansion of Bumping Lake, with a natural and cultural history comparable to Cle Elum Lake (Draper and Washington State University 1991; WADOE 2004). With an additional 7.69 km^3 (1,900 acres) inundated, the enlargement of Bumping Lake could lead to more extensive erosion (WADOE and USBOR 2012). Federal and state entities are also enlarging other reservoirs built on rivers in the West including Henry's Fork in Idaho, the Sacramento in California, and the Uintah in Utah to compensate for decreasing summer flows while meeting increasing demands for water (USBOR 2015; USBOR and State of Idaho 2015; Utah Division of Water Resources 2016). The provision of water for habitat and other needs is partially dependent on increasing reservoir capacity (WADOE and USBOR 2012). However, it is important to consider the potential degradation or

destruction of archaeological resources associated with reservoir enlargement projects. Along with impacts to cultural resources, the geomorphic effect of reservoir erosion has important implications for water quality and ecosystem services in an era when massive new storage reservoirs are being constructed worldwide (Su et al. 2017; Bao et al. 2018). Therefore, this project will contribute to the body of research on global climate change adaptation.

CHAPTER II

LITERATURE REVIEW

Modelling the potential impacts of reservoir expansion on cultural resources requires an understanding of the distribution of wave energy in reservoirs, factors controlling wave erosion, and the potential vulnerabilities of cultural resources to erosion. Atmospheric conditions affect wave direction and magnitude. As storm waves shoal, they interact with shorelines characterized by various physical and biological conditions affecting erosion. These factors make it feasible to predict where future erosion may occur and to what extent. With this knowledge, it is possible to mitigate these impacts on cultural resources. The following is an introduction to lacustrine coastal geomorphology and the management of cultural resources in reservoir varial zones.

Shoreline Energy Sources and Wave Generation

Storms winds are the primary sources of energy causing waves, influencing the direction of waves and subsequent sediment movement, and are therefore important factors in lacustrine geomorphic processes (Davies 1977; Jacobsen and Schwartz 1981; Adamo et al. 2014). Mountainous surroundings also generate winds due to thermal variations, making topography a particularly important factor in the shoreline development of many lakes and reservoirs (Kirillin et al. 2015). Winds create shear stress through surface friction. This transfers energy to propagating waves that move more slowly than the wind speed and determines their height and period (Komar 1976; Vosough 2011). They start in a disordered state in which they are out of phase due to wind turbulence and are only visible for short periods before other waves subsume them (Komar 1976). As waves move through the water away from their source area, they

become sorted by period in a process called wave dispersion (Komar 1976). As they move, wind speed and duration as well as fetch (i.e., the distance over which wind blows) determines the amount of energy transferred to water since these factors influence wave height and wave period (Komar 1976; Huggett 2007). Wave height is the distance between one crest and the next trough, measured perpendicular to wave direction. Wave period is the time elapsed as the entire wave length (i.e., distance between two successive crests) passes a given point (Davidson-Arnott 2010). Therefore, wave energy is lower in lakes than in marine environments due to smaller fetch sizes (Gracia 1995).

Offshore, the wave power formula expresses the wave energy flux (i.e., the average rate of energy moving through each wavelength):

$$P = \frac{\rho g^2}{64^{\pi}} H_{m0}^2 T_e$$

where P is the wave energy flux, H_{m0} is the wave height, T_e is the wave period, ρ is the density of water (depending on the temperature), and g is the increase in velocity due to gravity (USGS 2020; Vosough 2011). This formula implies that wave energy is proportionate to wave period and the square of wave height. Wind speed, duration, and fetch also affect the subsequent energy dispersal of shoaling waves (Adamo et al. 2014).

Breaking waves generates currents. When they break, the wave's surplus momentum, called radiation stress, causes the mean elevation of water to rise from the surf zone. This downward slope in the water surface opposite of wave direction creates a pressure gradient that drives return flow (Davidson-Arnott 2010). Return flow is frequently concentrated as rip currents, associated with erosion and deposition onshore and offshore. Radiation stress also drives longshore currents as waves break obliquely.

These are responsible for a major component of sediment transport in the surf zone (Davies 1977).

Shoreline Segments

Shoreline landforms make it possible to identify the dominant processes affecting shoreline segments (Shipman 2008). Coastal geomorphic processes include erosion and transportation due to wave action, creating erosional and depositional shoreline features (Davidson-Arnott 2010). Coastal geomorphologists have historically characterized lakeshores as erosional and depositional segments (Gilbert 1885; Jewell 2016). In their vernacular use, the terms bluffs and cliffs are sometimes used synonymously. However, cliffs are sheer bedrock exposures while bluffs are gentler slopes covered in soil and sediment (Bird 2001). Both may have precipitous gradients (Jacobsen and Schwartz 1981; Bird 2001). Retreating cliffs and bluffs indicate erosional shorelines. Landforms such as barriers, beach ridges, and spits are low-relief features indicating depositional shorelines (Jewell 2016). Shoreline morphology allows for a local classification of shorelines based on various factors such as wave energy and the physical characteristics of shorelines (Davis 1996).

Shoreline Processes

Littoral Drift and Drift Cells

Drift cells or littoral compartments describe zones within which processes of erosion, transportation, and deposition occur (Jacobsen and Schwartz 1981; Chrzastowski, Thompson, and Trask 1994). Waves and currents act in concert to erode and transport sediments (Davidson-Arnott 2010). Drift cells begin with erosional source areas of sediment (Jacobsen and Schwartz 1981). Littoral drift is the movement of

sediment through the transportational zone by longshore currents (Davies 1977; Jacobsen and Schwartz 1981; Chrzastowski, Thompson, and Trask 1994; Amin and Davidson-Arnott 1995; Davidson-Arnott 2010). Depositional areas mark the ends of drift cells (Jacobsen and Schwartz 1981).

These divisions are not absolute since the direction of drift varies over the short term (Jacobsen and Schwartz 1981; Chrzastowski, Thompson, and Trask 1994). However, many factors in the long-term direction of sediment transport influence natural shoreline features. Therefore, these geomorphic features best reflect net littoral drift direction. This makes them useful indicators of erosional, transportational, and depositional areas (Jacobsen and Schwartz 1981).

Erosion

Convex features such as natural headlands and artificial groins form the boundaries of drift cells (Jacobsen and Schwartz 1981; Davidson-Arnott 2010). Here, the shoreline configuration is at a right angle to the direction of net shore drift driven by waves in the surf zone (Davies 1977; Jacobsen and Schwartz 1981; USGS 2004). The wave energy flux (P) decreases to zero as waves break at a normal rather than oblique angle to the headland (Davidson-Arnott 2010). Sediment transport decreases proportionate to the diminished wave energy (Davidson-Arnott 2010). This confines littoral drift between these convex features (Jacobsen and Schwartz 1981).

As wave energy drops, sediment is deposited on the updrift side of convex features (Jacobsen and Schwartz 1981). This leads to erosion on the downdrift side as it is deprived of sediment (Jacobsen and Schwartz 1981; Chrzastowski, Thompson, and Trask 1994). Waves cause most shoreline erosion and shoreline retreat occurs where wave

energy is highest (Lorang, Komar, and Stanford 1993; Gracia 1995). Shoreline erosion occurs when waves take away more sediment than they deposit (O'Halloran and Spennemann 2002). Waves remove sediment through hydraulic and mechanical action (Sunamura 1977; Lenihan et al. 1981). Hydraulic action including scouring, cavitation, compression, tension, and shearing is the direct impact of waves as they strike cliffs and bluffs, transporting sediments away (Sunamura 1977; Davidson-Arnott 2010; Sierra and Casas-Prat 2014; Jewell 2016). Erosion by mechanical action such as abrasion is the indirect result of waves as sediment transported by them impacts cliff and bluff faces (Lenihan et al. 1981; Davidson-Arnott 2010; Keil et al. 2010; Jewell 2016). At the beginning of drift cells, erosion causes beaches to narrow. Waves attack results in landslides (Jacobsen and Schwartz 1981).

Sediment Transport

The transport of sediments follows coastal erosion and mass wasting. Swash and backwash are driven by waves moving up the beach under their own energy and retreating due to gravity, alternately washing sediment up and down the beach. When waves break oblique to the shoreline, beach drift transports this sediment laterally along the shoreline (Davies 1977). Littoral drift, beach drift, swash, and backwash remove sediments from eroded areas (Davies 1977; Davidson-Arnott 2010). Beach drift and littoral drift move sediment through the transportational zone. Shorelines with sediment transport feature a supply of beach sediments (Davies 1977). These may develop migratory beach ridges (Chrzastowski, Thompson, and Trask 1994). Waves deposit these ridges on top of beach sediments parallel to the shoreline (Lewis et al. 2010).

Sediment Deposition

Deposition occurs where wave energy becomes too low to continue transportation. Deposition on the updrift side of cell boundaries causes beaches here to widen, form beach ridges, rise higher, and increase backshore size. Bluffs become gentler as subaerial erosion predominates over wave erosion. Vegetation increases downdrift within the drift cell. Sediment size typically decreases moving downdrift as wave energy also decreases (Jacobsen and Schwartz 1981).

Factors Influencing Erosion in Inland Waters

Fetch

Fetch is a geometric factor strongly correlated with erosion in reservoirs (Su et al. 2017). Fetch determines the amount of time wind transfers energy to water, affecting wave height and period (Komar 1976; Gracia 1995). Wave energy moves in the same direction as wind (Gracia 1995). Since currents determine the direction of sediment movement, fetch is associated with net littoral drift direction, particularly on highly developed shorelines with variable fetch distances (Jacobsen and Schwartz 1981; Adamo et al. 2014).

Fetch limits wave period and height in lakes due to their relatively small sizes compared to marine environments (O'Halloran and Spennemann 2002). Smaller fetch distances generate insufficient wave energy to increase long period wave height (Komar 1976). However, fetch still influences wave height and period in lakes, and therefore wave energy (Gracia 1995; Adamo et al. 2014). In addition, when wind intensity and duration are equal, fetch defines wave period in lakes (Lenihan et al. 1981). These factors

make fetch the most useful predictor of wave energy in lakes. Increased lake elevation creates larger fetches and increased wave energy (Gracia 1995).

Planimetric Shape

The planimetric shape of shorelines is a second geometric factor influencing shoreline processes. Convex lakeward features such as bedrock promontories are subject to the direct force of waves (Yasso 1965). These features are susceptible to greater erosion (Lakhan 1997). Convex-lakeward features also disperse wave energy through reflection and turbulence, and redirect it from other parts of the shoreline through diffraction (i.e., movement of wave energy along the crest perpendicular to wave direction) and refraction (i.e., bending of waves) (Yasso 1965; Davidson-Arnott 2010). Landforms including wave-cut cliffs and bluffs as well as platforms mark these shorelines (Currey and Sack 2009).

Sheltered areas such as bays and other concave-lakeward features generally considered depositional environments are often indicated by fringing and pocket beaches (Jackson et al. 2002; Currey and Sack 2009). However, these "low energy" environments may still experience significant wave heights and periods (Jackson et al. 2002). Shoreline bathymetry causes wave refraction, allowing them to approach parts of the shoreline not perpendicular to shoaling waves (Jackson et al. 2002; Davidson-Arnott 2010). Therefore, shoreline configuration is also an important influence on wave height in these locations, along with wind speed, duration, and fetch (Jackson et al. 2002).

Both the resulting shape of the shoreline and wave direction are predictive of future shoreline change (Adamo et al. 2014). Wave energy redirected and attenuated by convex lakeward features may enlarge a bay, leading to increased shoreline radius. The

equation for a logarithmic spiral describes the shape of this type of shoreline development, featuring concave headland-bay or spiral-log beaches (Yasso 1965; Jacobsen and Schwartz 1981). They form on the lee side of headlands, which form drift cells partially confining sediment movement. Since waves bend here, wave refraction, diffraction, and reflection provide energy to move sediment towards the headland. Further from the headland, the beach's arc widens, and sediment size increases as does slope. Therefore, log-spiral beaches are landforms indicating the direction of littoral drift (Jacobsen and Schwartz 1981).

The shoreline development index quantifies the planimetric shape of lakes (Osgood 2005). It is the ratio of the full shoreline length to the smallest shoreline length necessary to enclose the same area. The shoreline development index ranges from one for circular bodies of water and above for those with irregular shapes (Schiefer and Klinkenberg 2004). An analysis of natural lakes and reservoirs throughout the United States indicates that the mean shoreline development of natural lakes is 2.9 compared to nine for reservoirs. The sinuous shapes of most reservoirs results from their inundation of former meandering river channels and floodplains (Thornton et al. 1981). The high mean shoreline development of reservoirs reflects more convex and concave features subject to erosion and deposition (Yasso 1965; Lakhan 1997).

Slope Angle

A third geometric variable in shoreline erosion is slope angle (O'Halloran and Spennemann 2002). Slope angle influences wave energy (Davidson-Arnott 2010). It is particularly important in fetch-limited areas and is a main control on erosion in reservoirs (Jackson et al. 2002; Bao et al. 2018). As waves travel inshore, they interact with three

zones of the lakefloor depending on the water depth (Figure 2). The first of the zones is the offshore area, also termed the outer shoreface. Here, waves are symmetrical and wavelength is more than twice the depth. Next, they reach the inner shoreface and begin to shoal (Davidson-Arnott 2010). Here, depth is about the same as wave height (Komar 1976). This area, referred to as the wave base, is the maximum depth at which passing waves disturb sediments (Rich 1951). Waves begin to build-up (Lorang, Komar, and Stanford 1993). Contact with the bottom decreases wavelength, increases wave height, and decreases wave speed (Davidson-Arnott 2010). As this occurs, waves become steeper (Komar 1976). Velocity within their crests becomes greater than the waves' overall speed, causing the crest to break and spill forward (Komar 1976). Finally, waves move across the surf zone and run-up the beach face (Lorang, Komar, and Stanford 1993).

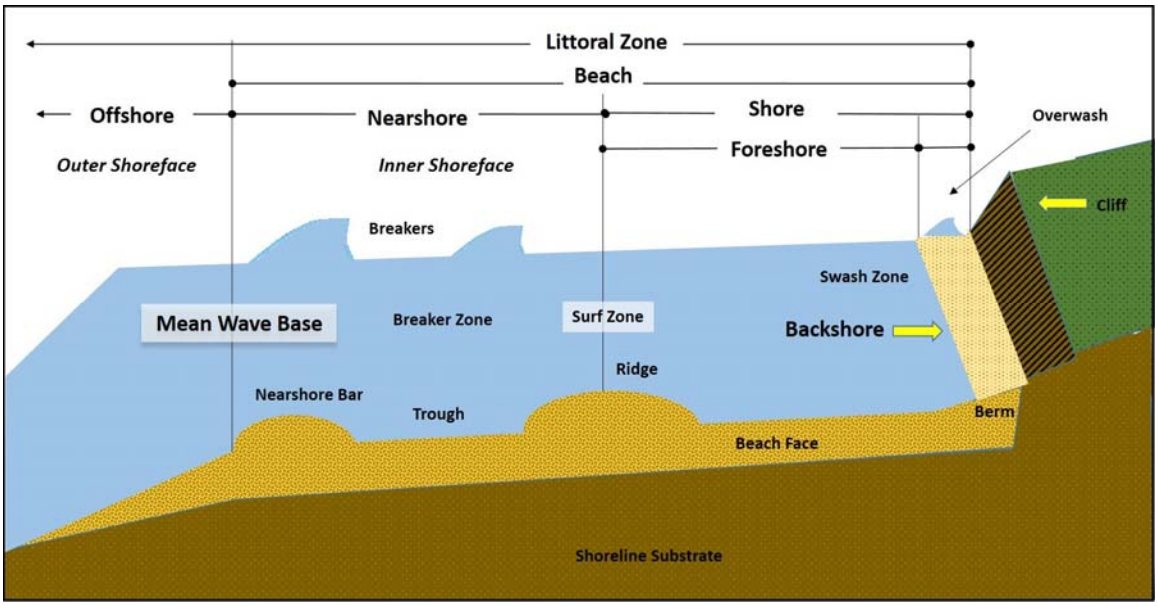

Figure 2: Shoreline profile from outer shoreface to backshore. Summarizing Komar 1976; Ritter, Kochel, Miller 1995; Davis 1996; Davidson-Arnott 2010; Leyva 2020.

Shoreline slope determines breaking wave type. Variations in the bathymetry of the outer shoreface affects the heights of waves. These variations, in turn, influence the height of waves entering shallow areas (Lenihan et al. 1981). Waves enter the surf zone

portion of the nearshore, and break (Davidson-Arnott and Greenwood 1999). Several types of breaking waves may occur including plunging and surging waves (Battjes 1974). Plunging waves occur along shorelines with an intermediate slope between 11° and 36° (O'Halloran and Spennemann 2002; Huggett 2007). Here, they build-up rapidly (Lorang et al. 1993). Internal motion causes these waves to plunge over their crests at a high velocity (O'Halloran and Spennemann 2002). They break at once high on the shore, and expend all of their energy followed by a large runup (Lorang et al. 1993). Plunging waves cause a high degree of shoreline erosion (O'Halloran and Spennemann 2002). Along steeper shorelines with slopes greater than 50°, the bases of surging waves experience high runup (Davies 1977; Huggett 2007). They nearly plunge forward, but instead their bases surge up the beach and they lose their crests (Lenihan et al. 1981; Davidson-Arnott 2010). As a result, there is little turbulence and they repeatedly wash across the foreshore, transferring sediment from the lakefloor onto the upper shoreline, causing deposition (O'Halloran and Spennemann 2002; Davidson-Arnott 2010).

Cliff and Bluff Height

A final geometric factor in shoreline retreat is the height of embankments. Bank height may influence erosion rates. Amin and Davidson-Arnott (1997) found that their height has a small influence on erosion rates, as the toes of lower banks are most susceptible to erosion. Erosion occurs as bluffs recede from the bottom up (Chrzastowski, Thompson, and Trask 1994). The presence of talus temporarily slows the rate of erosion (Kamphuis 1987). Ultimately, waves remove talus from their toes (Komar and Shih 1993). The height of embankments controls the amount of talus since higher banks produce and accumulate more colluvium (Sunamura 1983). Because of their larger

surface areas, bluffs over thirty feet high accumulate triple the volume of talus than those between fifteen and thirty feet (Reid 1992). As a result, they may be more resistant to wave attack (Sunamura 1983). Higher on the bluff face, erosion decreases as the force of waves diminishes. Higher embankments also disperse wave energy over a larger surface (Amin and Davidson-Arnott 1995).

However, other studies question the direct relationship between the height of embankments and erosion or suggest that higher bluffs are actually more vulnerable to erosion (Quigley et al. 1976; Buckler and Winters 1983; Rashid et al. 1989). This is because bluff height becomes less important over time. It is true that a longer time may be required for wave attack starting at the toe to lead to the erosion of higher bluff faces (Buckler and Winters 1983). However, accumulating talus progressively covers its own source. This negative feedback slows the further reinforcement of the bluff (Huggett 2007). Eventually, erosion reaches the top (Buckler and Winters 1983). Higher bluffs' susceptibility to related erosion processes may also offset the protection afforded by larger volumes of talus at their bases (Reid 1992). Bluffs composed of resistant materials such as clay and till become oversteepened by toe erosion (Rashid et al. 1989). Bluffs with high clay content often erode into vertical faces (Chrzastowski, Thompson, and Trask 1994). Eventually these bluffs may experience larger mass wasting events (Rashid et al. 1989). Mass wasting causes their crests to retreat rapidly (Buckler and Winters 1983). Eventually, wave erosion and bluff retreat reach equilibrium (Quigley et al. 1976). At lower lake levels, equilibrium takes longer to reach as higher bluffs continue mass wasting after it has stopped on lower bluffs. These factors may negate the resistance afforded by talus (Sunamura 1983). Therefore, differences in erosion rates are minimized

(Buckler and Winters 1983). As a result, higher bluffs may erode more dramatically due to larger mass wasting events (Rashid et al. 1989).

Vegetation

Vegetation type and coverage also control coastal morphology, since it serves to stabilize shorelines and prevent erosion (Davidson-Arnott 2010). Roots improve the cohesion of soils (Osterkamp, Hupp, and Stoffel 2012). They also increase soil permeability. However, the root systems of various plant species perform these functions to different degrees (Gyssels et al. 2005). For example, areas vegetated by shrubs may be eroded more easily than forest vegetation (Lorang and Stanford 1993).

Vegetation coverage is a related factor in reservoir shoreline erosion (Bao et al. 2018). Reduction of vegetation cover leads to soil erosion (Niu et al. 2014). In reservoirs, varial zones are typically devoid of plants. The lack of vegetation leaves them susceptible to increased erosion by waves. The severity of this problem varies among different portions of the varial zone. The upper floodpool zone is typically not inundated for most of the year and therefore able to support more vegetation than lower areas (O'Halloran and Spennemann 2002). In backshore areas above varial zones, forested areas important for erosion control may be vulnerable to undercutting that weakens tree roots and results in slumping as well as denudation due to overwash resulting from storms (Lorang and Stanford 1993). These are further vulnerable to overland flow erosion (Davidson-Arnott 2010). However, as erosion rates decrease in aging reservoirs, marshes may grow lakeward in low relief portions of the backshore (Lorang, Komar, and Stanford 1993).

Shoreline Substrates

Characteristics of shoreline substrates such as lithology and geologic structure determine the rate and capacity of wave energy to cause shoreline erosion (Davies 1977; Gracia 1995; Amin and Davidson-Arnott 1997; Davidson-Arnott 2010; Adamo et al. 2014). Where few beach sediments exist, shorelines are composed of rock cliffs. In the absence of deposition due to a lack of sediment supply, these cliffs are either static or receding due to erosion (Davidson-Arnott 2010).

The resistance of rocky cliffs to wave erosion varies by lithology. Cliffs composed of metamorphic and igneous rocks are highly resistant to erosion (Davidson-Arnott 2010). These include granite and basalt, which have a high degree of hardness due to their crystalline structures (Davidson-Arnott 2010; Chesterman and Lowe 2018). The strength of sedimentary rock varies. Chemically deposited rocks such as limestone are the strongest sedimentary rocks as they contain dense microscopic grains (Davidson-Arnott 2010; Chesterman and Lowe 2018). Sedimentary rocks with weak cohesion and stratification such as shale and sandstone are moderately resistant (USGS 2004; Davidson-Arnott 2010). Moisture disintegrates cliffs composed of soft, fine-grained sedimentary rocks such as mudstone (Earle 2015; Chesterman and Lowe 2018). First, waves erode their toes and remove talus (Davidson-Arnott 2010). Major landslides follow this (Komar and Shih 1993). As a result, cliffs composed of sedimentary rocks may erode as much as meters per year in contrast to resistant metamorphic and igneous rocks that may only recede centimeters or less each century (Davidson-Arnott 2010).

The weakest cliffs and bluffs are formed of sedimentary deposits (Davidson-Arnott 2010). These may be somewhat bonded by clay or compressed by glaciation

(Davidson-Arnott 2010). Here, sediment supply and grain size indicate the deposition of material such as glacial till and Quaternary alluvium (Synge 1966; Davies 1977; Brandt and Hassan 2000; USGS 2004; Davidson-Arnott 2010). These deposits are very weak and susceptible to mass wasting (USGS 2004). However, some studies indicate glacial clay till bluffs only erode at half the rate of sandy bluffs (Davis, Fingleton, and Pritchett 1975; Buckler and Winters 1983). This is because sediments such as sand and silt are highly subject to transportation by waves (Stanford and Hauer 1992). In reservoirs at increased water elevations, shoreline segments composed of sands, sandy loams, and silts are the most vulnerable to wave-induced erosion (Stanford and Hauer 1992; Brandt and Hassan 2000). Lakes impounded by moraines converted to reservoirs are also subject to erosion by artificially elevated water levels (Brandt and Hassan 2000). This results in straightened shorelines marked by cliff-base and bluff-base beaches (Currey and Sack 2009). However, the increased rate of retreat on sandy shorelines may be offset by sedimentation (Davidson-Arnott 2010). For example, loose sediments are deposited as glacial outwash is exposed to wave action (Synge 1966). This may explain why other studies indicate bluffs bonded by clay are oversteepened and recede more quickly than sandy bluffs (Buckler and Winters 1983; Rashid et al. 1989).

Plunging waves attack bluff toes, initiating subaerial mass wasting (Lorang, Komar, and Stanford 1993; Davidson-Arnott 2010). In glacial till bluffs, sand, clay, and gravel content determine the rate of bluff retreat. Those composed of fine sand and clay sediments are typically more durable and solid. Sediment suspended following the erosion of bluffs potentially results in additional erosion through abrasion (Kamphuis

1987). As bluffs become less stable, surface runoff and chemical weathering cause further degradation (Currey and Sack 2009).

In addition to determining the rate that waves erode shorelines, lithology also influences the degree of shoreline development. Irregular shoreline development is associated with basins featuring resistant bedrock such as andesite and basalt interspersed with weaker sedimentary deposits as well as those with a high degree of bedding, faulting, and jointing (Komar 1976; Schiefer and Klinkenberg 2004; Davidson-Arnott 2010). Resistant material forms headlands while less resistant deposits retreat landward to form bays (Komar 1976). The resulting headlands also cause wave refraction, furthering irregular shoreline development (Chrzastowski, Thompson, and Trask 1994). In contrast, elongated lakes develop in glaciated areas with the presence of faults and weak bedrock (Schiefer and Klinkenberg 2004). Many of these Pleistocene lakes are in valleys oversteepened by glaciers (Schiefer and Klinkenberg 2004).

Despite the resistance to erosion afforded by their lithology, shorelines composed of resistant rocks may still be prone to more rapid erosion depending on their geologic structure (USGS 2004). Rocks with pronounced dips are prone to erosion and mass wasting, especially when the bedding planes and fractures dip towards the water (Davies 1977; Komar and Shih 1993; USGS 2004). Mass wasting may start at joints, faults, and cleavages (Davies 1977; USGS 2004). There is a strong relationship between the incidence of shoreline mass wasting and the spatial distribution of these weak points in the rock (USGS 2004).

Additional Factors in Reservoir Erosion

Water Level Fluctuations and Wave Energy Distribution

The timing of water level fluctuations and storms controls the distribution of wave energy in lakes and reservoirs (Lorang, Komar, and Stanford 1993). Fluctuations in natural lakes only occur for a short time during the spring snowmelt. This causes their elevations to increase briefly and then return to their baseline (Lorang, Komar, and Stanford 1993). As a result, annual wave energy distributes more randomly across the nearshore in natural lakes (Lorang, Komar, and Stanford 1993; Lorang and Stanford 1993). This dissipates wave energy, preventing the erosion of the backshore including cliffs and bluffs (Lorang, Komar, and Stanford 1993). In contrast, the seasonal variation in the amplitude and duration of high water-levels in reservoirs is artificially controlled and extended (Lorang, Komar, and Stanford 1993). Prolonged high water-levels concentrates wave energy against the upper shoreline (Lorang and Stanford 1993).

In conjunction with water level fluctuations, meteorological conditions also play an important role in shoreline processes (Lorang, Komar, and Stanford 1993; Rubensdotter and Rosqvist 2003). This is particularly true in lakes, where waves are otherwise limited by relatively small fetch distances (Gracia 1995). When storms coincide with higher pool levels, wave energy is concentrated against the foreshore (Lorang, Komar, and Stanford 1993). This amplifies erosion at the upper shoreline (i.e., the highest limit of the upper floodpool zone at full capacity) (Lorang, Komar, and Stanford 1993; Sadeghian et al. 2017).

In fluctuating reservoirs, waves break across the entire varial zone from the permanent conservation pool through the upper floodpool zone (Lenihan et al. 1981;

Lorang and Stanford 1993; Bao et al. 2018). This disturbance zone is subject to increased erosion (Bao et al. 2018). Because waves break across the full varial zone, reservoir shorelines may lack a proper beach face and foreshore (Lorang and Stanford 1993). The beach face is a part of the swash zone where waves often deposit a ridge of gravel protecting the shoreline from waves (Lorang et al. 1993). Here, a combination of overwash and undercutting are the most prevalent forms of erosion (Lorang and Stanford 1993). Increased reservoir levels promote erosion at the highest levels of the varial zone where undercutting is the most common form of erosion (Lorang and Stanford 1993; Bao et al. 2018). In a study of the world's largest storage reservoir, the Three Gorges Reservoir in China, erosion rates in the varial zone were up to twenty times that of areas above the high shoreline (Bao et al. 2018).

Wave Energy Distribution and the Morphodynamic State of Beaches

The distribution of breaking wave energy determines the morphodynamic state of shorelines, whose configurations can either reflect energy against the shoreline or dissipate it offshore (Wright and Short 1984; Lorang et al. 1993; Lorang, Komar, and Stanford 1993; Lorang and Stanford 1993). Processes of erosion or deposition lead to one of these two states (Wright and Short 1984). Reflective shorelines develop as waves swash fine-grained sands offshore. The loss of sand leaves a narrow, cobbled nearshore, a steep foreshore with slope angles up to 25°, and beaches composed of gravel. As reflective configurations develop, plunging waves break closer to shore, creating a stepped profile at the breaking point. Here, in this narrow part of the nearshore zone, waves expend all of their energy and runup across the foreshore ending at the beach face (Lorang et al. 1993; Lorang, Komar, and Stanford 1993). As bluff erosion results,

reflective shorelines continue to develop (Kamphuis 1987). In reservoirs, storm waves coinciding with prolonged high pool levels promote the development of reflective shorelines, as breaking wave energy is concentrated against a small portion of the foreshore (Lorang et al. 1993). Because of these morphodynamics, erosion usually increases for a time after the onset of reservoir operations (Lorang, Komar, and Stanford 1993).

Over a period of several decades following this dissipative shorelines may develop. Eventually, erosion expands the nearshore varial zone, leaving a beach composed of fine-grained sand (Lorang et al. 1993; Lorang, Komar, and Stanford 1993). These dissipative shorelines have broad nearshores and surf zones with low gradients, causing waves to break and expend their energy offshore. As a result, erosion rates decrease (Lorang, Komar, and Stanford 1993; Bao et al. 2018). The growth of marshes from the backshore towards the lake may indicate that the reservoir has reached a state of equilibrium between erosion and deposition (Lorang, Komar, and Stanford 1993).

Coastal Landforms as Indicators of Shoreline Processes

Indicators of Erosion

Subaerial erosion of sedimentary bluffs and cliffs by wave action results in their undercutting or oversteepening. In this process, wave action erodes their bases and removes the resulting debris (Davies 1977; Davidson-Arnott 2010). Bluffs made of glacial material erode the fastest (Komar 1976; Davidson-Arnott 2010). Periodic slope failures and retreat follow undercutting (Buckler and Winters 1983; Lorang and Stanford 1993). Cliffs erode more slowly, mainly during storms, which provide the necessary hydraulic and mechanical action (Komar 1976; Lenihan et al. 1981; Keil et al. 2010).

Cliff retreat creates erosional platforms that usually slope lakeward. It also produces headlands, particularly where bedding is vertical and normal to the shoreline (Komar 1976).

Common movement types along coasts include avalanches as well as soil and rock falls. Slides with topples and flows occur less commonly (Highland and Bobrowsky 2008). Rock falls and slides occur where bedding is parallel to the shoreline and dipping towards the water (Komar 1976). Low cliffs and bluffs as well as those lacking complex stratigraphy are most vulnerable to shallow slides and flows. High cliffs and bluffs may be more likely to have complex stratigraphy with water moving between permeable layers and underlying impermeable layers. Here, rotational slides may occur (Davidson-Arnott 2010). These processes create platforms produced from cliff and bluff retreat (Sunamura 1977; Currey and Sack 2009).

Indicators of Deposition

Waves and currents also act to create depositional features (Gracia 1995). Such features include barriers, bars, beaches, deltas, and spits (Komar 1976; Lorang and Stanford 1993; Gracia 1995). These occur as waves enter the inner shoreface and slow due to contact with the bottom. This creates longshore currents carrying sediment that they deposit when energy becomes too low to continue transport (Jacobsen and Schwartz 1981; Gracia 1995). In lakes, deltas formed from littoral drift indicate erosion occurring elsewhere (Lorang and Stanford 1993). Spits develop on top of underwater platforms formed from sediments in the direction of net littoral drift. As the platforms rise above the water, smaller spits continue to develop in the same direction, close to or at the end of

the littoral compartment. Therefore, these depositional landforms may also reveal littoral drift direction (Jacobsen and Schwartz 1981).

A variety of other geomorphic processes also augment or form shoreline depositional features (Davis 2006). Sediment transported downdrift may accumulate at stream mouths if supply exceeds stream's capacities to transport it further, causing stream mouths to bend in the same direction as shore-drift (Jacobsen and Schwartz 1981). Although such depositional landforms occur frequently in lakes, highly developed features such as spits that jut out into the water before curving back to enclose lagoons may indicate that fluvial deposition is more significant than littoral processes (Gracia 1995).

It is important to distinguish landforms resulting from fluvial processes since alluvium is actually the most important source of sediment along depositional shorelines (Davis 1996). Where streams enter low energy lakes and reservoirs, they lose velocity, and begin to deposit alluvium and create deltas (Lenihan et al. 1981; Ritter, Kochel, Miller 1995 Lenihan et al. 1981; Bird 2001). These sedimentary deposits are highly subject to future erosion and can only exist if sediment supply outstrips the capacity of waves to erode them (Lorang and Stanford 1993; Ritter, Kochel, and Miller 1995). Lightweight sediments travel further offshore before settling. Fluvial deposition is responsible for the problem of sedimentation in reservoirs (Lenihan et al. 1981).

In steep-sided, mountain lake basins, mass wasting also plays an important role in the development of depositional features, which can help control erosion (Quigley et al. 1976; Castañeda 2015). These features result from cliff and bluff erosion and failure along lakeshores (Quigley et al. 1976). Debris flows also occur frequently in

mountainous areas. They move rapidly down pre-existing channels and accumulate in debris fans (Hungr, Leroueil, and Picarelli 2014). Debris fans can extend offshore as much as twice the height of their source area (USGS 2004). Although these result from mass wasting, they may also protect bluffs from further erosion (Quigley et al. 1976).

Cultural Resources on Reservoir Shorelines

Impacts of Reservoirs on Cultural Resources

The World Commission on Dams has acknowledged the extensive damage and destruction of cultural resources due to reservoir construction in a number of countries around the world (Brandt and Hassan 2000). These impacts are poorly understood and difficult to predict quantitatively (Brandt and Hassan 2000; Wyskup 2006). It was not until the publication of the National Reservoir Inundation Study that formal investigation of these impacts began (Lenihan et al. 1981). Awareness of this problem only grew decades after the impoundment of many reservoirs, including Cle Elum Lake (USBOR and WADOE 2011).

The type and severity of threats to cultural resources varies depending on an array of factors. One of the best predictors of their risk of erosion is the elevation of archaeological sites in reservoirs, where wave erosion is the greatest threat to cultural resources (Lenihan et al. 1981). Here, wave erosion mainly occurs in the fluctuating shoreline zone. However, waves can only reach the lowest sites in the permanent conservation pool as reservoirs first fill. In addition, lower sites are also less vulnerable due to shorter fetch lengths (O'Halloran and Spennemann 2002). Instead, deposition is most prevalent offshore. Deposition can actually help preserve sites by burying them (Lenihan et al. 1981).

During the initial inundation and subsequent annual fluctuations, the shoreline zone advances upwards. The size of this zone and its duration depends on the annual amplitude of water levels and the speed with which reservoirs fill, making these important factors controlling the erosion of archaeological sites (Lenihan et al. 1981). Wave and wind erosion impact archaeological sites along the temporary shoreline for prolonged periods (Garrett 2006). This exacerbates natural shoreline erosion through both wave attack and overland flow (Lenihan et al. 1981). Wave attack exposes artifacts to subaerial processes and overland flow transports sediments bearing them (Lenihan et al. 1981; O'Halloran and Spennemann 2002). Within the shoreline fluctuation zone, sites at the highest elevations are subject to the greatest wave energy due to artificially increased fetch distances (Gracia 1995). Since the waterline rises up steeper shorelines more slowly, waves attack sites here for the longest period. While the risk of erosion is highest along the fluctuating shoreline, it is also more accessible than lower areas making these impacts more apparent (Lenihan et al. 1981).

Surging and plunging waves both damage cultural resources. Contact with steep shorelines causes the bases of shoaling waves to runup high (Davies 1977; Davidson-Arnott 2010). The resulting surging waves deposit sediment and bury artifacts as well as transport sediments containing them (O'Halloran and Spennemann 2002). Plunging waves erode archaeological sites and transport abrasive gravel and sand, causing additional damage (Kamphuis 1987; O'Halloran and Spennemann 2002).

Artifact composition and materials also affects the risk of erosion posed by reservoirs. Vertical structures such as walls are more vulnerable to wave action and undercutting than horizontal features such as floors. Waves easily transport less

consolidated and substantial remains such as middens, charcoal, and bone. At higher sites, increased wave energy can move heavier objects (Lenihan et al. 1981). Bone degrades after prolonged inundation with increasing risk in areas subject to erosion. Similarly, erosion damages pictographs and petroglyphs (Garrett 2006). Masonry structures and floors hardened by compaction through use or heat exposure are more resistant to erosion (Lenihan et al. 1981). For areas exposed to the greatest inclement forces, the long-term preservation of cultural resources is especially dependent on these site-specific factors (Lenihan et al. 1981).

Erosion also poses several secondary risks to cultural resources. Erosion and transportation disperses artifacts, destroying site context (Lenihan et al. 1981). The risk of erosion through reservoir operations can create a justification for preventative archaeological excavations. Exposure of these sites places them at risk for vandalism (Garrett 2006). Soil erosion also promotes bioturbation due by burrowing animals (Lenihan et al. 1981).

Managing Cultural Resources in Reservoirs

Archaeological surveys can be included in reservoir project planning. This includes an evaluation of sites' erosion risk based on their elevation within the varial zone relative to expected water levels ranging from average years to one hundred flood events (Brandt and Hassan 2000). Another risk factor assessed is the vulnerability of specific material types to degradation (Lenihan et al. 1981). In addition to these preliminary assessments, the continued monitoring of sites is also important (Brandt and Hassan 2000). This risk assessment forms the basis for mitigation strategies. Prioritizing the most

vulnerable facets of sites, including artifacts as well as environmental and contextual information, enables nuanced policy decisions to be made (Lenihan et al. 1981).

Although protecting cultural resources *in situ* has proven to be prohibitively expensive in the past, this approach may be preferable to excavation as it preserves site contexts (Brandt and Hassan 2000). Various coverings, including soil with sealants applied and concrete, prevent erosion (Lenihan et al. 1981). Managers can also construct protective structures around sites to reduce wave energy, particularly in the permanent conservation pool and along the shoreline fluctuation zone (Lenihan et al. 1981; USBOR and WADOE 2015). These structures are appropriate for mitigating shoreline erosion in general (USBOR and WADOE 2015). Managers mainly employ rock barriers in the highest energy environments (Michigan Natural Shoreline Partnership 2018). For example, rip-rap is composed of broken rocks while rockery walls use interlocking angular rocks. They lay against slopes and are between about 8 feet and 10 feet high. Perched beaches are soil filled in against slopes creating a new beach above the floor of reservoirs. This approximates slopes found in natural lakes (USBOR and WADOE 2015).

However, many of these structural approaches have disadvantages. The hardening of shorelines interrupts littoral drift (Zelo, Shipman, and Brennan 2000). As previously discussed, sediment transport is required to supply beach sediments, leading to erosion in downdrift areas starved of sediment (Davies 1977; Jacobsen and Schwartz 1981; Chrzastowski, Thompson, and Trask 1994).

Seawalls direct wave energy down and to the side of the wall. This redirected wave energy can cause scouring of the lakefloor (Michigan Natural Shoreline Partnership 2018). This may impact archaeological sites within the varial zone. Eventually, scouring

may undercut the seawall. Outflanking also results in erosion in adjacent areas. This may encourage the construction of more seawalls, and the expansion of shoreline erosion (Michigan Natural Shoreline Partnership 2018).

Shoreline protection structures are also prone to costly failures. Rip-rap may fail due to incorrect placement, scouring at the toe, settling, and outflanking although engineered rip-rap is less prone to failure. Rip-rap also requires maintenance to avoid failure (Griggs and Fulton-Bennett 1988).

Several bioengineered options utilize wooden barriers to reduce wave energy. Anchored logs are whole trees placed parallel or perpendicular to the lakeshore. Log revetments are clusters of logs placed perpendicular to the lakeshore. Log terraces are tiers of anchored logs placed parallel to the lakeshore and backed by sediment that allows drainage. Other methods are used where wave energy is lower, such as in bays and other areas with fetch less than 4 km. Examples include slope reshaping, slash and soil (i.e., the placement of alternating levels of woody debris and soil on the lakeshore), and fell and anchor (i.e., cutting down trees on top of slopes subject to erosion and anchoring them in place to retain soil) (USBOR and WADOE 2015).

To improve the condition of lakeshores, the Michigan Natural Shoreline Partnership recommends the least invasive intervention possible depending on wave energy. Where wave energy is lower, the best solution is to restore native plant coverage (Michigan Natural Shoreline Partnership 2018). Fast growing vegetation is also used to stabilize archaeological sites (O'Halloran and Spennemann 2002). Vegetation has the added advantage of obscuring archaeological materials from pothunters (Lenihan et al.

1981). Coir fiber logs are useful for promoting strongly rooted vegetation able to withstand wave energy (Michigan Natural Shoreline Partnership 2018).

In addition to on-site preservation methods, various policy options exist to prevent site erosion. Wave erosion can be limited by lowering the speed, size, and number of boats, or prevented by limiting recreational boating to certain locations (Mosisch and Arthington 1998; Brandt and Hassan 2000). Reservoir operators can also limit maintenance work in sensitive areas (Lenihan et al. 1981). They can also minimize fluctuations by filling reservoirs more quickly and limiting drawdowns as much as possible, in order to lower the number of sites exposed to wave action (O'Halloran and Spennemann 2002).

If protecting sites in their context is not feasible, archaeologists can retrieve artifacts uncovered by erosion (Brandt and Hassan 2000). Retrieving these artifacts as quickly as possible may protect them from further erosion and disturbance by pothunters (Lenihan et al. 1981). Technological advances allow archaeologists to locate, access, record, and excavate submerged sites (Garrett 2006). Precluding this approach may be cultural prohibitions against disturbing ancestral sites and the attitude that inundation provides protection against some forms of disturbance (Ferri 2015).

CHAPTER III

STUDY AREA

Cle Elum Lake (Figure 3) lies within the Yakima River Basin (Figure 4), a 15,941-km^2 watershed in south-central Washington (USBOR and WADOE 2012). The Yakima River runs 345 km from Lake Keechelus near the Cascade crest to its confluence with the Columbia River at Richland (Yakima Subbasin Fish and Wildlife Planning Board 2004). The Yakima's main sub-basins include the Roslyn, Kittitas, Selah, Yakima, Toppenish, and Benton basins (USBOR and WADOE 2012). The entire Yakima Basin lies within the ceded area of the Yakama Nation and its reservation (Yakima Subbasin Fish and Wildlife Planning Board 2004).

Figure 3: Cle Elum Lake view towards the northeast. Photograph by Michael Horner, August 2014.

Cle Elum Lake (Figure 5) lies within the Okanogan-Wenatchee National Forest. It is located in Kittitas County, 13 km northwest of Cle Elum (USBOR and WADOE 2015). It is on the Cle Elum River in the Roslyn sub-basin of the upper Yakima Basin, 13 km upstream of the confluence of the Cle Elum and Yakima Rivers (Cohen 1998; USBOR and WADOE 2012; Gendaszek, et al. 2014).

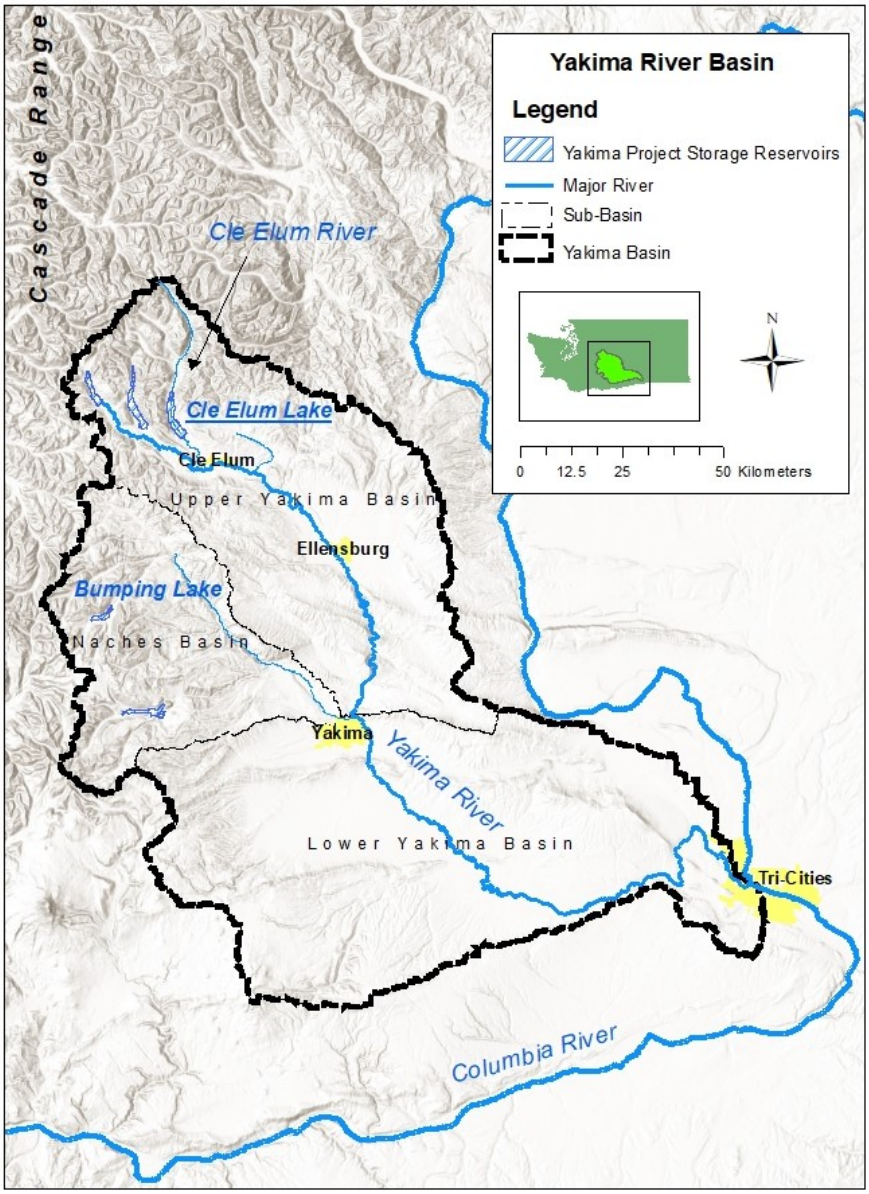

Figure 4: Yakima River Basin (ESRI 2006; USGS 2008; ESRI 2015; WADOE 2015; USGS 2016).

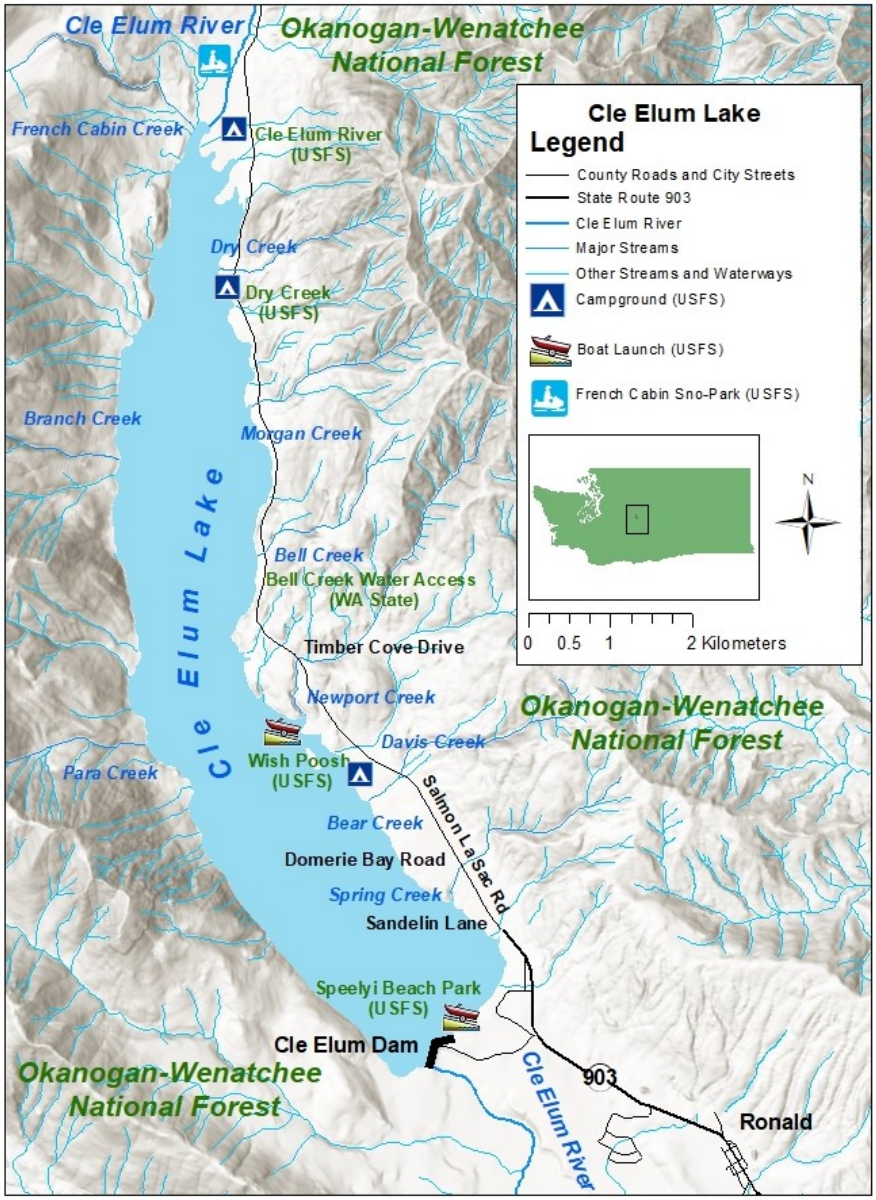

Figure 5: Cle Elum Lake (ESRI 2006; USGS 2016; ESRI 2015; WADOE 2015; Google Maps 2018; WADOT 2020).

Topography

Cle Elum Lake lies within the southern portion of the North Cascade Range. Parabola-shaped glacial valleys characterize this area (Porter 1976). This includes the U-shaped Cle Elum River valley, formed by successive Pleistocene alpine glaciers (USBOR and WADOE 2015). Glacial valleys such as this feature a variety of slope angles (Porter 1976). Cle Elum Lake's outer shoreface has little variation in depth (Figure 6). However,

both the eastern and western shorelines have intermediate slopes of about 12°, while areas at the north end near the inlet and the south end near the dam have low slopes under 5° (Figure 7) (Lieberman and Grabowski 2007).

Fluvial processes and mass wasting also shaped the basin's topography. Fluvial deposition is important as fifty-three streams enter the lake. For example, a low gradient alluvial fan exists where Morgan Creek North enters the lake (Steinkraus et al. 2014). Mass wasting deposits also exist along the southwest and eastern shorelines in particular (see Figure 7) (Frizzell et al. 1984; Tabor et al. 2000; USBOR and WADOE 2015).

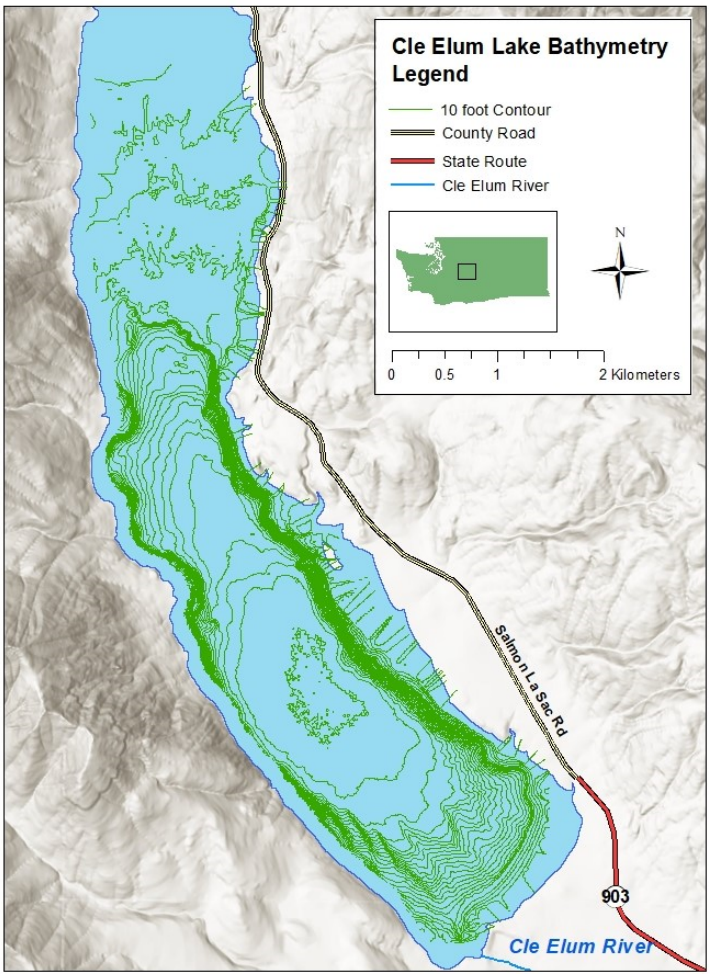

Figure 6: Cle Elum Lake bathymetry (ESRI 2006; Manning 2016; USGS 2016; ESRI 2015; WADOT 2020).

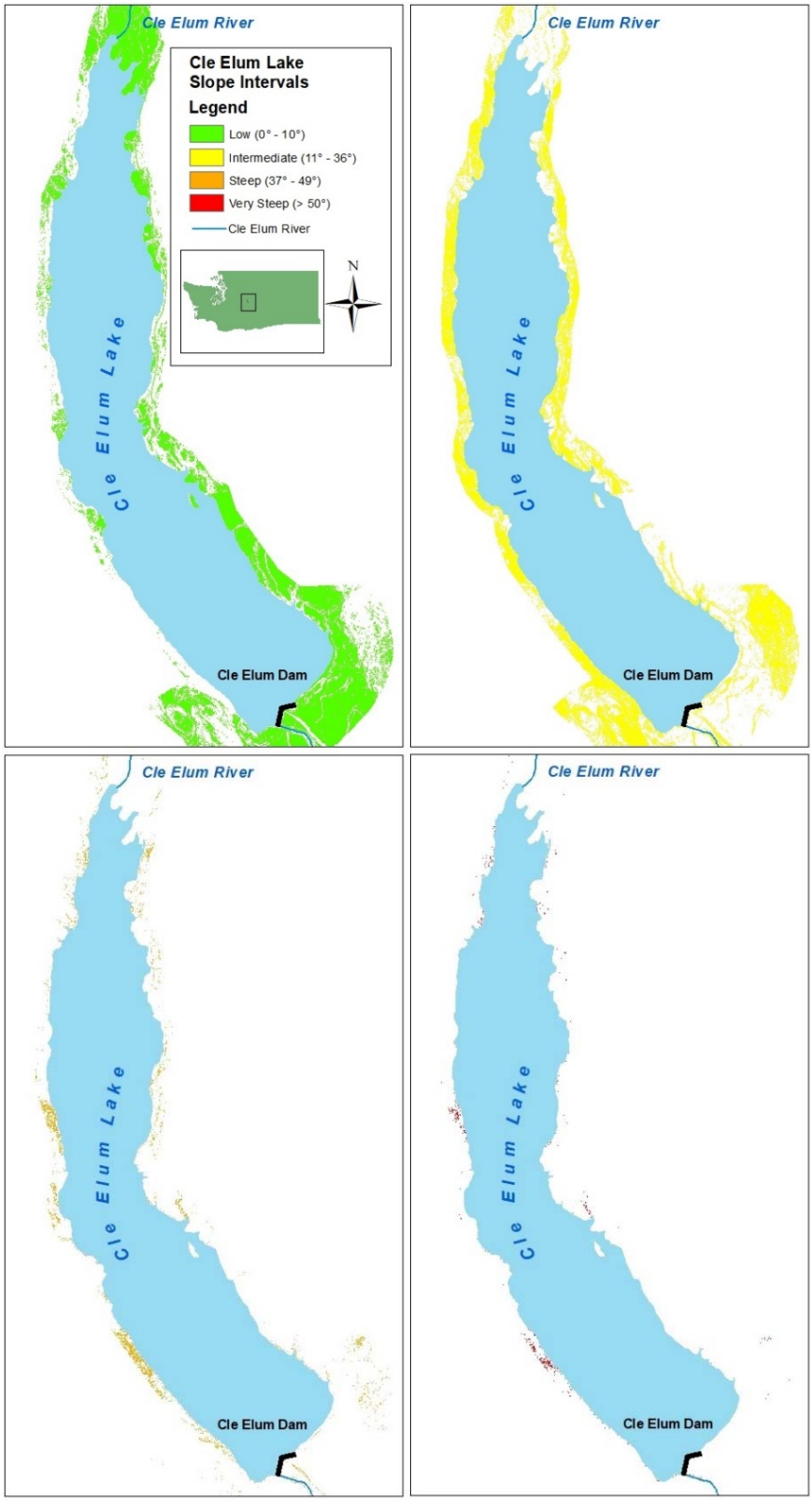

Figure 7: Cle Elum Lake slope intervals (ESRI 2006; WADNR 2014; USGS 2016).

Shoreline Substrates

Underlying much of the Cle Elum Lake basin is the sedimentary and volcanic Teanaway River Block (Figure 8) (Tabor et al. 2000; USBOR and WADOE 2015). This

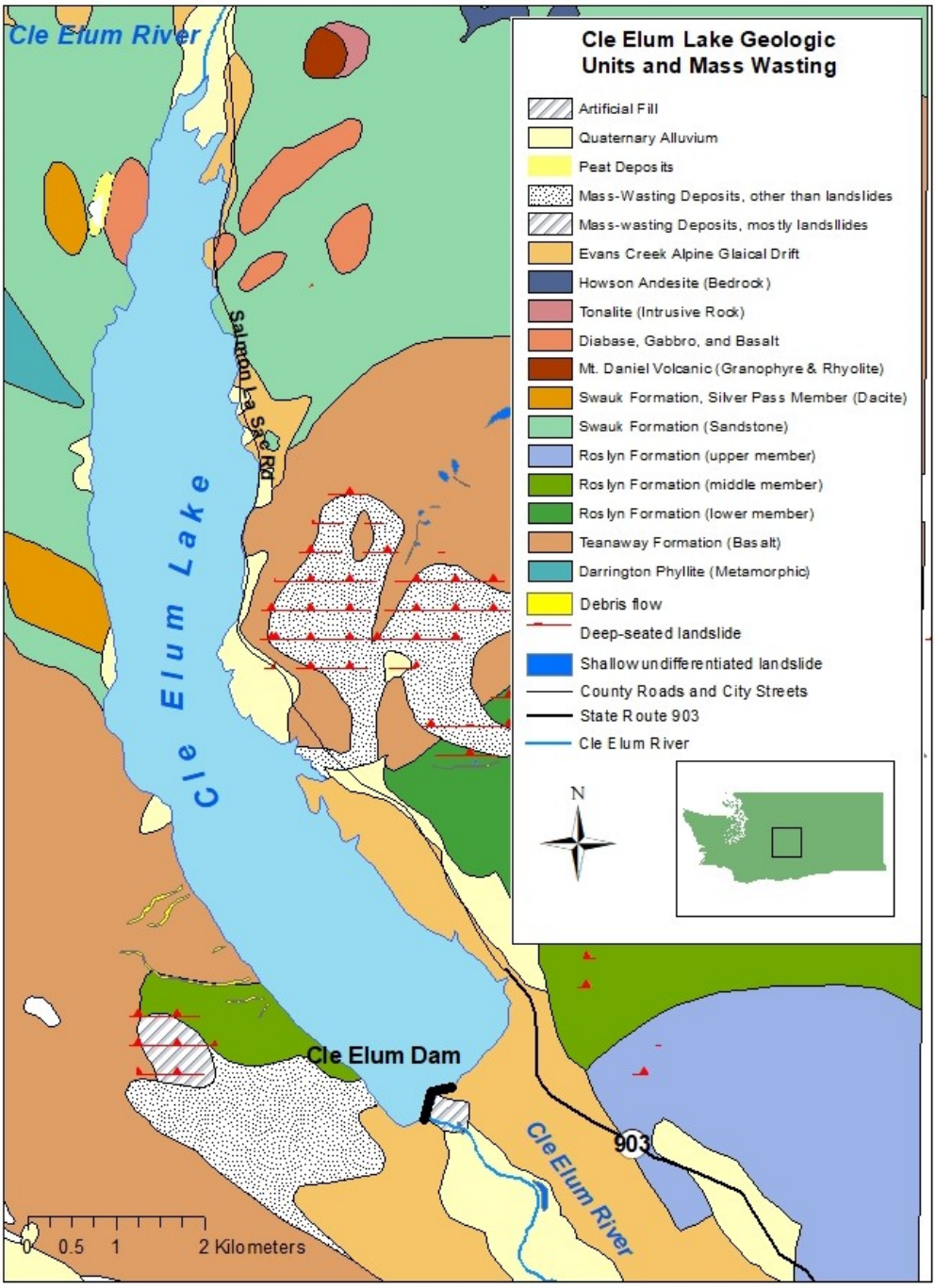

Figure 8: Cle Elum Lake geologic units and mass wasting (Frizzell et al. 1984; Tabor et al. 2000; ESRI 2006; USGS 2016; WADOT 2020).

includes three formations. The Swauk Formation is a prominent sandstone-dominated unit along most of the northern lakeshore. This unit includes the dacitic Silver Pass Volcanic Member (Tabor et al. 2000). Among this are small pockets of diabase, gabbro, and basalt (Tabor et al. 2000). The basaltic Teanaway Formation lies along the western shoreline and a small portion of the eastern shoreline (Frizzell et al. 1984; Tabor et al. 2000). The sandstone Roslyn Formation composes a short stretch of the southwest shore (Tabor et al. 2000).

Glacial, alluvial, and mass wasting deposits overlie much of the bedrock of the Cle Elum Lake basin. During the Fraser glaciation, just under 19,150 ± 250 years ago, the last of the successive glaciers that formed the Cle Elum Lake basin deposited the Evans Creek alpine glacial drift (Tabor et al. 2000; USBOR and WADOE 2015). This is correlated with glacial drift deposited elsewhere at the maximum extent of the Fraser glaciation (Porter 1976). The Cle Elum River cut through these deposits, leaving moraine and outwash in pockets along the eastern and western shorelines (Frizzell et al. 1984; Tabor et al. 2000; USBOR and WADOE 2015). Stream mouths expose Quaternary alluvium here and at the northern inflow (Frizzell et al. 1984; USBOR and WADOE 2015). The mass wasting deposits in the southwestern and eastern parts of the lake result from both landslides and debris flows that descended the steeper slopes on the western side of the lake (Frizzell et al. 1984; USBOR and WADOE 2015).

Climate and Weather

The Yakima Basin has pronounced seasonal temperature differences. Prevailing westerly maritime winds and mountains to the northeast block cold air from the north and moderate winter temperatures. Summers are warm as continental air intrudes (Yakima

Subbasin Fish and Wildlife Planning Board 2004). At Cle Elum (Figure 9), the 1981-2010 climate normal mean annual temperature was about 8.2° C. The mean temperature in January was -1.3° C while it was 19.2° C in July (NCEI 2018).

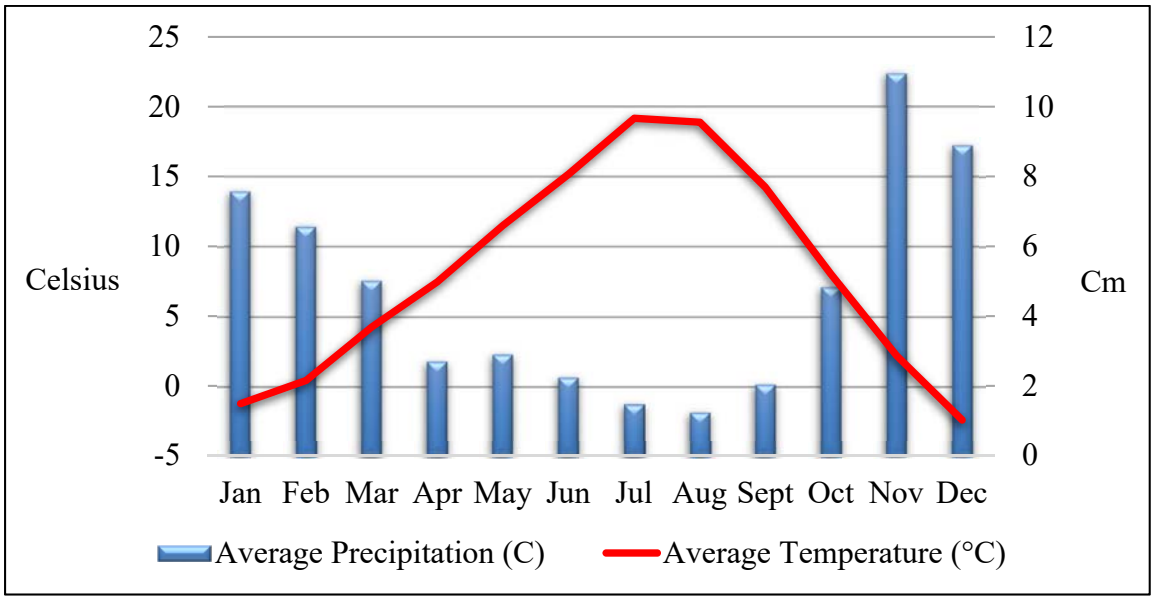

Figure 9: Cle Elum climograph: 1981-2010 climate normal (NCEI 2018).

In the Yakima Basin, precipitation is highly seasonal and geographically variable. Low pressure over the North Pacific exposes the Northwest interior to mid-latitude cyclones during the colder months while storms track to the north in the summer (Wise 2012). As a result, half of the annual precipitation arrives between November and January (Yakima Subbasin Fish and Wildlife Planning Board 2004). Orographic cooling of humid, marine air rising over the Cascades produces approximately 300 cm of precipitation annually at the Cascade crest (Rinella, McKenzie, and Fuhrer 1992; Yakima Subbasin Fish and Wildlife Planning Board 2004). At Cle Elum, which lies about halfway between the Cascade crest and the eastern edge of the Yakima Basin, the average annual precipitation from 1981 to 2010 was 56.6 cm (NCEI 2018). However, the precipitation from October through March was 43.8 cm, which is more than 77 percent of

the normal mean annual precipitation (NCEI 2018). Due to the Cascade rain shadow, semi-arid conditions prevail in the Basin's eastern portion with precipitation averaging between 20 cm and 25 cm annually (Yakima Subbasin Fish and Wildlife Planning Board 2004).

Snowpack is a critical component of the Basin's hydrology, and is described as the Yakima Basin's "sixth reservoir" (USBOR and WADOE 2012). In the mountains, the majority of precipitation is snow between November and March. It remains in snowpack through the winter or in permanent snowfields and glaciers beyond this, often retaining the bulk of water into early summer (Rinella, McKenzie, and Fuhrer 1992; USBOR and WADOE 2012). Snowmelt feeds most of the Basin's streams that start in the mountains (Rinella, McKenzie, and Fuhrer 1992). The spring snowmelt is when the streams of the basin often experience peak flows (Figure 10) (Taylor and Gazis 2014). Another 2° C

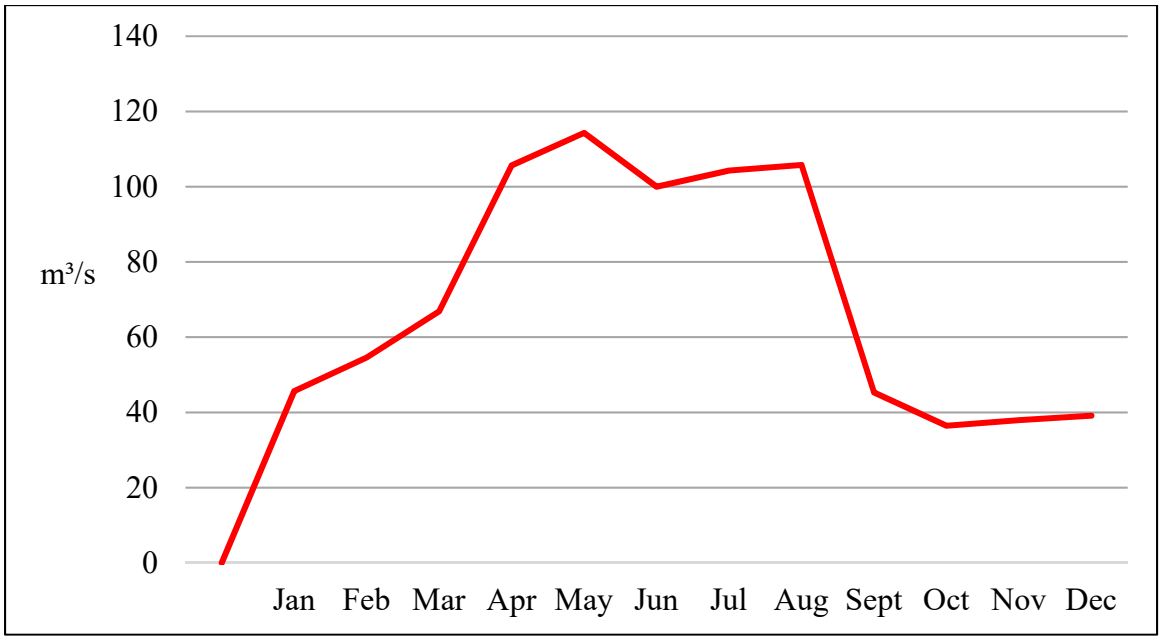

Figure 10: Average annual flow of the Yakima River near Umtanum 2010-2019 (BOR 2020).

increase of average temperature by the 2040s could cause more rain resulting in diminished snowpack, permanent snowfields, and glaciers (USBOR and WADOE 2011, 2012; Osborn 2012). Changes to the climate and hydrologic regime would increase streamflows in the winter and early spring, followed by lower flows in the late spring and summer (USBOR and WADOE 2012).

Prevailing winds at Cle Elum Lake are westerly (Table 1) (USBOR 2018). With a mean normal angle of 280°, it is likely that the Cle Elum valley walls funnel these winds towards the southeastern corner of the lake (Dey 1988; Kirillin et al. 2015; USBOR 2018). Mean monthly wind directions vary with westerly winds in February and April through September. The highest mean winds during are in April. From 2013-2016, the average annual wind speed was 3.2 kph, while the average seasonal wind speed was 3.4 kph between January and June (USBOR 2018).

Table 1: Cle Elum Lake wind speed and direction (BOR 2018).

	Speed (km)	Direction
Monthly		
January	3.4	ESE
February	3.5	W
March	3.3	WNW
April	3.6	W
May	3.2	W
June	3.3	W
July	3.3	W
August	3.2	W
September	3	W
October	2.9	ENE
November	3.1	SSE
December	3.4	ESE
Annual	3.2	W

Hydrology

In the Yakima Basin, the seasonal and geographic variability of water supplies necessitated the construction of reservoirs to store runoff (USBOR and WADOE 2012). Although instream flows are the highest in the spring, demand for offstream uses of water is greatest in the summer (Mote et al. 2005; Taylor and Gazis 2014). The five major reservoirs operated by Reclamation under the Yakima Project store up to 1,320,689,022 m^3 (1,070,700 acre-feet), or 30 percent of the basin's average yearly runoff. Artificial storage of major runoff ending in late June followed by snowmelt provides water to the dry valleys in the eastern part of the basin where irrigation is required to support agriculture. Reservoirs also supply water for hydroelectricity, salmon habitat, and migration, as well as retain floodwaters (Dick 1993; USBOR and WADOE 2012). Changes in the basin's hydrology due to climate change could prevent Cle Elum Reservoir from filling to its original capacity (Vano 2010).

A glacial moraine formed Cle Elum Lake (USBOR and WADOE 2015). Settlers built an earth dam to block a channel incised by the Cle Elum River through the moraine, resulting in the lake's expansion (Dick 1993; USBOR and WADOE 2015; Yakama Nation Fisheries 2015). Settlers also impounded other natural lakes in the basin to store irrigation water for farmlands. However, a lack of comprehensive planning or capacity to store runoff for dry months led to an over-appropriation of the river's water, which dropped to historically low levels (Dick 1993). The Department of Interior authorized the Bureau of Reclamation to construct the Yakima Project in 1905 to resolve water rights in the basin and improve irrigation (Dick 1993; USBOR and WADOE 2012). As part of the

Yakima Project, Reclamation built a permanent dam at Cle Elum Lake. This dam created a reservoir with a surface area of 18.48 km^2 (USBOR and WADOE 2011).

Cle Elum Lake has the greatest volume of any of the Yakima Project's storage reservoirs. This accommodates the largest mean yearly runoff of any these reservoir's basins, due to its large watershed (Lieberman and Grabowski 2007; USBOR and WADOE 2011). It is fed by the Cle Elum River, along with major streams including Spring Creek, Bear Creek, Davis Creek, Newport Creek, Bell Creek, Dry Creek, French Cabin Creek, Branch Creek, and Para Creek (Google Maps 2018). In addition, 44 minor streams enter the lake (USGS 2016). Its main inflow is at the north end of the lake (Lieberman and Grabowski 2007). As with the Yakima Basin as a whole, runoff here is highly seasonal. Between 2008 and 2019, the river's highest average volume at the inflow (Figure 11) occurred in the middle of May, when its average daily flow was

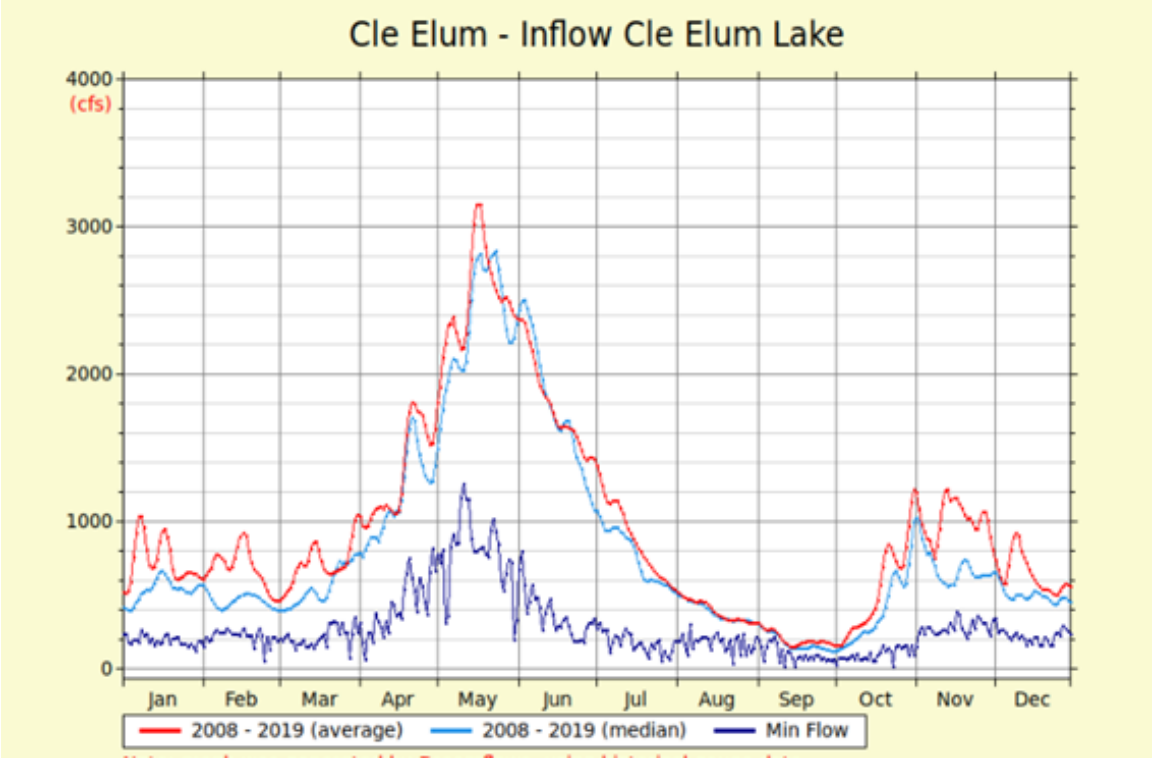

Figure 11: Average monthly Cle Elum Lake inflow 2008-2019 (Dreamflows 2020).

approximately 90.61 m^3/s (3,200 cfs). In contrast, the average daily flow was less than 5.66 m^3/s (200 cfs) in September, rising to over 33.98 m^3/s in the late fall (1,200 cfs) (Dreamflows 2020). The lake's highest average discharge (Figure 12) from December 2018 to December 2019 was in July at 84.43 m^3/s (2,982 cfs) while its lowest discharge was during October and November (USBOR 2020). Because of this hydrologic regime, the lake's maximum elevation in June follows the river's maximum inflow (Figure 13). Beginning with its maximum discharge in July, it declines to its lowest elevation by the beginning of September (USBOR 2018).

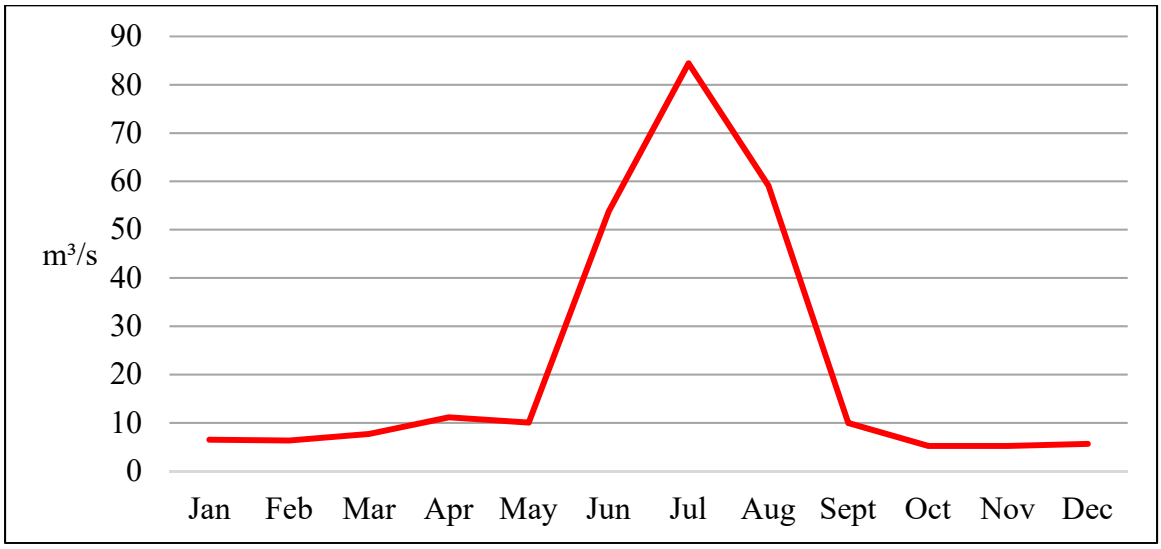

Figure 12: Average monthly Cle Elum River discharge at Cle Elum Lake 2018-2019 (BOR 2020).

Vegetation

The upper third of the Cle Elum Lake basin above the reservoir's original maximum elevation of 682.75 m features mature forest. This includes stands of Pacific silver fir (*Abies amabilis*), western hemlock (*Tsuga heterophylla*), and mountain hemlock (*Tsuga mertensiana*). The lower two-thirds has stands of grand fir (*Abies grandis*)

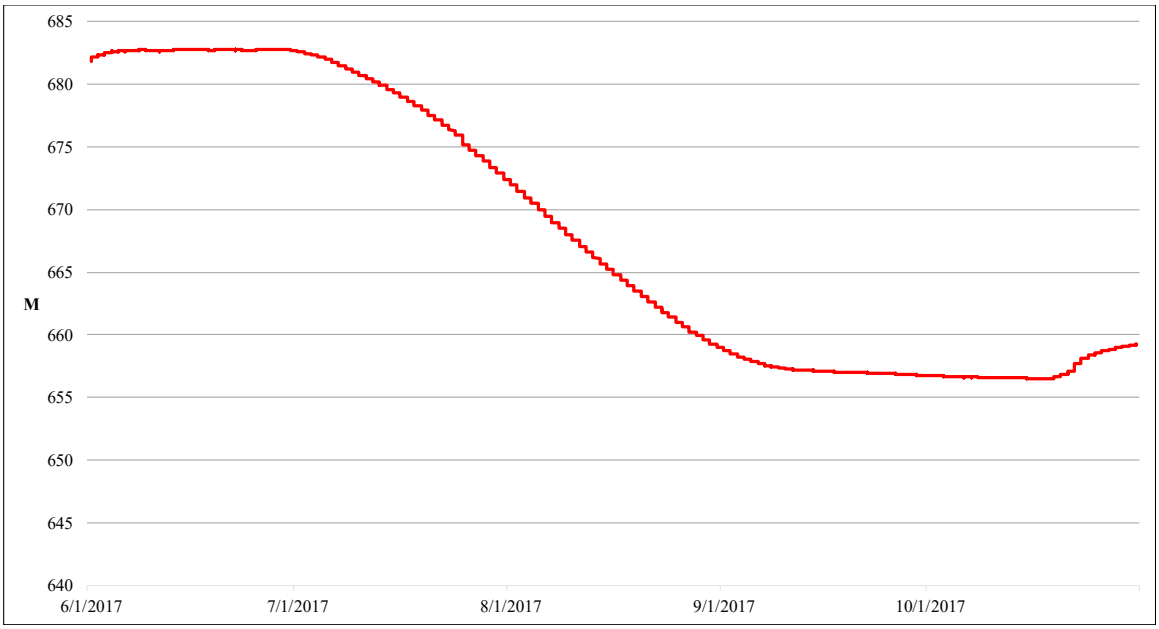

Figure 13: Cle Elum Lake reservoir elevations (BOR 2018).

and ponderosa pine (*Pinus ponderosa*) habitat (Figure 14) (Franklin and Dyrness 1973; USBOR and WADOE 2015).

The Cle Elum Pool Raise project will seasonally inundate the area from the current varial zone up to 683.67 m (USBOR and WADOE 2015). The project area includes non-vegetated areas, low ground cover, deciduous trees, and mature coniferous forests dominated by Douglas fir (*Pseudotsuga menziesii),* especially on the western shoreline (Franklin and Dyrness 1973; USBOR and WADOE 2015). The Pool Raise Project includes the replacement of existing conifers with shrubs and deciduous trees that can withstand flood conditions. Within the varial zone, minimal vegetation exists due to its rocky substrate and fluctuating water levels (USBOR and WADOE 2015). The steeply sloping western shore is particularly barren while isolated areas of red alder (*Alnus rubra*), black cottonwood (*Populus trichocarpa*), and various willow species (*Salix* spp.) exist by the lake's inlet at the north end and lower gradient slopes along the eastern

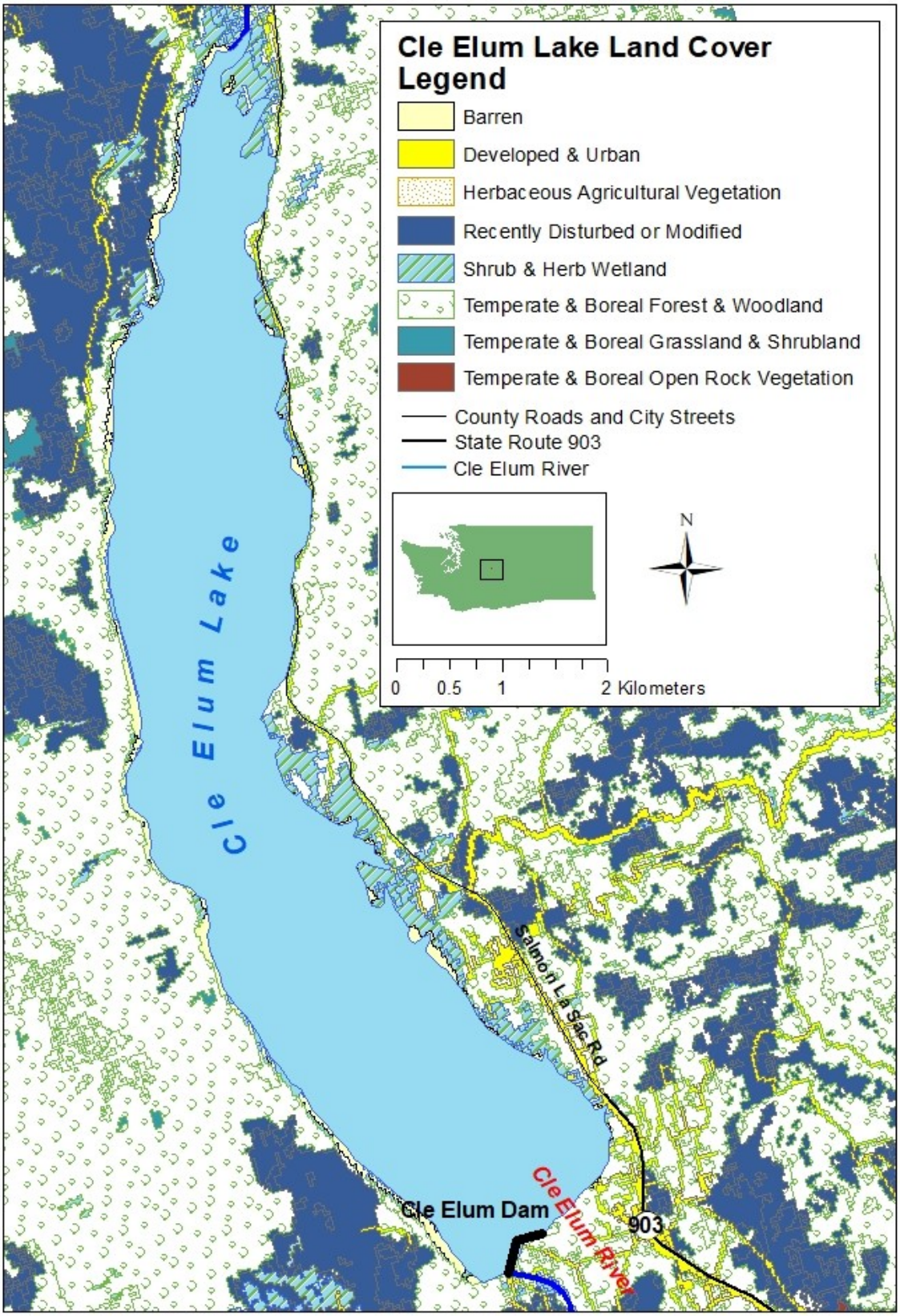

Figure 14: Cle Elum Lake land cover (ESRI 2006; USDA 2013; USGS 2016; WADOT 2020).

shoreline (Figure 15) (Franklin and Dyrness 1973; USBOR and WADOE 2015). The reservoir's shoreline prior to the raising of its pool level included 188 acres of palustrine wetland habitat, about 4.1 percent of the total surface area of the lake. In some cases, palustrine wetlands are vegetated by vascular or non-vascular plants with or without root systems. In other cases, they lack vegetation (USBOR and WADOE 2015).

Human Occupation

Cle Elum Lake features pre-historic Native American sites associated with the Yakama Nation and the Colville tribe, resulting from intensive use of the lake's natural resources (Steinkraus et al. 2014; USBOR and WADOE 2015). Sites belonging to bands of the Yakama Nation include petroglyphs, artifact caches including a projectile point resembling the Clovis style dating to 11,500 years BP, sacred sites, and burial sites (USBOR and WADOE 2011; USBOR and WADOE 2012). Here, waves have eroded and transported sediments at various elevations because of reservoir fluctuations, dispersing artifacts from their original contexts (Steinkraus et al. 2014). Additional sites may also exist including *Aiyalim* (a reported Yakama camp at Cle Elum Lake), sacred sites, and burial locations protected by the Native American Graves Protection and Repatriation Act (NAGPRA) (USBOR and WADOE 2011).

The USFS manages most of the Cle Elum lakeshore while Reclamation administers the zone around the dam; both share jurisdiction over the Pool Raise project area. Adjacent private properties are vulnerable to erosion due to reservoir enlargement. The state also manages a small segment of the eastern shoreline. Salmon La Sac Road (SR-903) approaches the lake from the south and traverses the entire east side of the lake, in areas just above the maximum elevation of the lake. The west side of the lake

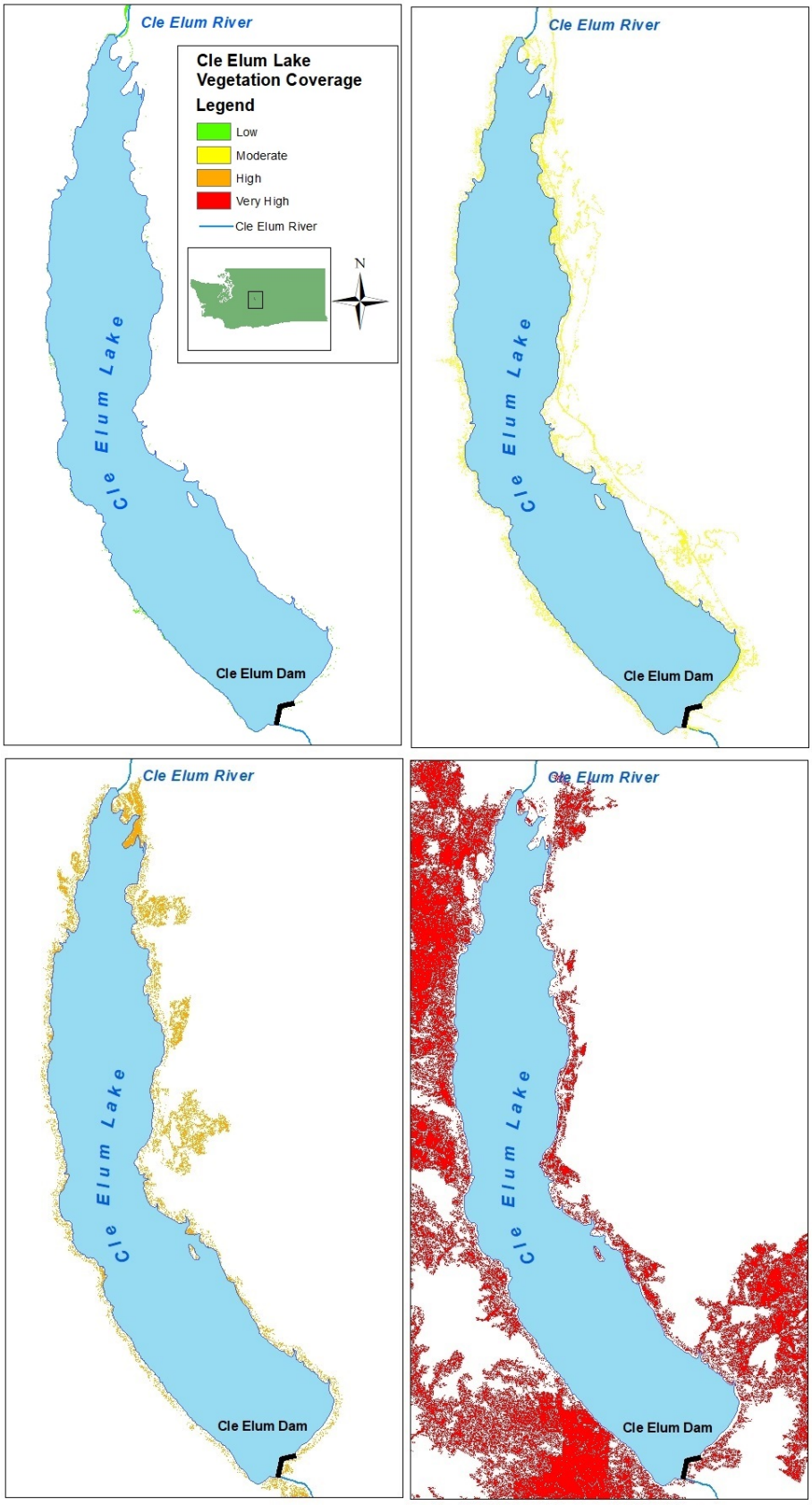

Figure 15: Cle Elum Lake vegetation coverage (ESRI 2006; USDA 2013; USGS 2016).

mostly lacks road access (USBOR and WADOE 2015). There are also a number of private streets in the developed areas at the southeast and northeast corners of the lake. Finally, several recreational facilities exist at Cle Elum Lake including campgrounds and boat launches managed by the USFS (USBOR and WADOE 2015; Google Maps 2018).

CHAPTER IV

METHODS

This assessment of the potential impacts of erosion in Cle Elum Lake included five steps: 1) mapping erosional and depositional shoreline segments using airphoto interpretation and a video survey; 2) identifying the physical characteristics of erosional segments by performing fieldwork and acquiring and synthesizing data on shoreline erosion variables; 3) determining variables in shoreline erosion using statistical analysis; 4) modelling erosion susceptibility using GIS and creating hazard maps indicating the potential erosion risk based on the models; and 5) making management recommendations for stakeholders. Each step of this methodology is described below.

Step 1: Mapping Erosional and Depositional Segments

Airphoto Interpretation

Airphoto interpretation provided the initial basis for an inventory of shoreline erosion for later geospatial analysis to establish the risk of future erosion (Boualla et al. 2017; Irigaray 1995; Irigaray, Fernandez, and Chacon 1996; Jiménez-Perálvarez et al. 2009). I viewed natural color airphotos stereoscopically using a mirror stereoscope to draft geomorphic maps of erosional shoreline segments (Lorang, Komar, and Stanford 1993; Shipman 2008). According to an email dated 24 July 2017 from USFS Biological Technician Michael Cibicki, who provided the airphotos, they were taken on 6 July 2012. They have a scale of 1:15,000 (Valley Air Photos 2012). I manually mapped landforms indicating erosion and deposition visible on hardcopies of the airphotos. Bluffs and cliffs as well as mass wasting (Table 2) were the primary indicators for distinguishing areas of erosion (Davies 1977; Sunamura 1977; Jacobsen and Schwartz 1981). Depositional

Table 2: Airphoto interpretation key.

Landform	Planimetric Form	Cross Sectional Form	Composition	Landform Relationships	Vegetation
Erosional Features					
Headlands	Convex outward	Steep with platforms gently sloping lakeward	Bedrock to consolidated sediments	Associated with cliffs & platforms; landslides and narrow beaches	Vegetated on top, devegetated on the sides
Cliffs/ bluffs	Straight	Steep	Bedrock (cliffs) to consolidated sediments (bluffs)	Associated with headlands & platforms	Evidence of undercut forests
Platforms	Straight or convex outward	Gently sloping lakeward	Bedrock/ consolidated sediments on lakeward side	Associated with headlands & cliffs	N/A
Depositional and Transportational Features					
Beaches (nearshore, foreshore & backshore)	Parallel	Stepped profile (reflective) or gentle beach face (dissipative) rising more steeply up to berm; ridges; level & high backshore	Unconsolidated sand & gravels; fine sediments or organic material between ridges	Updrift of barriers to littoral drift	N/A
Bays	Concave	Gentle beach face; ridges	Unconsolidated sand & gravels	Fringing, pocket & spiral-log beaches	N/A
Spits	Convex, elongate, & parallel	Low; steeper lakeward beach face, flat top, gentler gradient shoreward	Unconsolidated sand & gravels	Found at the entrance to bays	Vegetation if spit stabilized
Barriers	Straight, elongate, & parallel; separate from mainland	Low; gentle lakeward beach face; flat or lumpy top; gentler gradient shoreward	Unconsolidated sand & gravels	Barriers separated by lagoons & wetlands; may form in groups	Beach grasses and shrubs in the center
Other Features					
Fans/ Deltas	Fan-shaped	Low; gentle downward slope in direction of drift	Unconsolidated sediment size decreasing in direction of drift	Diverted stream mouths; associated with depositional features (i.e. spits) at stream mouth	N/A
Rip-Rap	Linear & parallel	Steep	Large boulders	Upper shoreline	N/A

Indicators included barriers, beaches, and spits (Komar 1976; Lorang and Stanford 1993; Gracia 1995; Jewell 2016). Google Earth supplemented airphotos where they were unclear (Fisher et al. 2012).

Ground Truthing Airphoto Interpretation

Next, I verified airphoto interpretation using a video survey conducted during summer 2019. Airphoto interpretation needs corroboration because of the potential for error due to limitations of scale (Fookes, Dale, and Land 1991). To verify the airphoto interpretation, I filmed the entire lake margin using a GoPro HERO3 camera while recording global positioning system (GPS) tracks (Appendix A) with an accuracy within +/-3.65 m using a Garmin eTrex 10 for later georeferencing (Lewis, Fotheringham, and Winstanley 2011; Garmin 2019). These helped to verify and refine the results of the airphoto interpretation.

Shoreline Segments

I digitized shoreline segments based on a variety of sources to serve as an inventory of past shoreline erosion (Irigaray et al. 2007; Jiménez-Perálvarez et al. 2010; Costanzo et al. 2012; Lovrić and Tošić 2017; Tošić et al. 2018). First, ArcGIS software was used to trace the landforms mapped during the airphoto interpretation, using National Agriculture Imagery Program (NAIP) imagery as a base layer for reference purposes (USDA 2013).

Next, I interpreted the video survey. Erosional features were distinguished as either cliffs or bluffs. Later, the time index when each landform was seen on the video was synchronized with the time index of GPS track points recorded during the survey. For each landform, QGIS was used to export a start and end track point along the

shoreline. These were used to export shapefiles representing beaches, bluffs, and bedrock shoreline segments.

Finally, I used this GIS layer of landforms along with other information to refine the results of the airphoto interpretation. First, these landforms were compared to the shoreline segments created from the airphoto interpretation. I used the field measurements, GIS data, and Google Earth where the airphoto interpretation and video survey were unclear. Any corrections were mapped in Google Earth by creating a point marker at the start and end of each revised shoreline segment and exporting it as a KMZ file to QGIS. This was the basis of a final layer of shoreline segments, categorizing landforms as beaches, bluffs, and cliffs.

From this, I created two versions of the shoreline inventory reflecting near-term and long-term erosion. Although both cliffs and bluffs are indicators of shoreline erosion, the erosion of resistant bedrock cliffs is less of a management concern since it occurs over a much longer timeframe than it does for sedimentary bluffs (Davidson-Arnott 2010). In addition, artifacts are typically born in sediment rather than bedrock (Lenihan et al. 1981; O'Halloran and Spennemann 2002; Davidson-Arnott 2010). Therefore, I produced a shoreline inventory of near-term erosion classifying bluffs as erosional, beaches as depositional and excluding bedrock cliffs. For comparison, a second shoreline inventory was produced reflecting both near-term and long-term erosion that classified cliffs and bluffs as erosional segments and beaches as depositional segments. Since this thesis is concerned with littoral erosion and deposition, I excluded the delta of the Cle Elum River since this indicates fluvial deposition. I also excluded infrastructure including the dam and a road embankment (Jacobsen and Schwartz 1981; Bird 2001). In addition,

the shoreline inventory was used to produce a layer of shoreline cross-sectional form categorized as vertical features including bluffs and cliffs as well as beaches with gentle slopes.

Step 2: Identifying the Physical Characteristics of Erosional Segments

Shoreline Survey

The next step was to conduct a field survey of Cle Elum Lake during summer 2019 to identify and measure erosion factors where necessary (Boualla et al. 2017; Irigaray 1995; Irigaray, Fernandez, and Chacon 1996; Jiménez-Perálvarez et al. 2009; USGS 2016). Field work was conducted at sites identified during Step 1. I developed a data sheet to record findings (Appendix B) along with a field manual (Joyce 1978). A pedestrian survey covered most parts of the lakeshore, while a boat provided access to areas of the lakeshore without roads. Reference maps generated from GIS along with Google Earth assisted with orientation, documentation, and interpretation in the field (Joyce 1978; Knodel, Lange, and Voigt 2008; Google Earth 2019).

Since the reservoir and its locale contain both known and unknown archaeological sites, I conducted the pedestrian survey in accordance with applicable cultural resource laws. Because the federal government manages most of the Cle Elum Lake's shoreline (USBOR and WADOE 2015), the Archaeological Resources Protection Act (ARPA) regulates archaeological resources here (King 2013). ARPA only allows excavation permits under certain circumstances. These were not applicable since this was not a survey of archaeological resources (16 U.S.C. 470aa-470mm; Public Law 96-95). I encountered a cultural resource with the Central Washington University (CWU) Central

Washington Anthropological Survey field crew and the find was incorporated into survey project results for Reclamation (Figure 16) (Stilson, Meatte, Whitlam, and DOT 2003).

Figure 16: Projectile point found along southeastern shoreline. Photograph by Michael Horner, May 2019.

Field Measurements

The main purpose of the pedestrian survey was to measure variables in order to further document erosion, deposition, and associated site characteristics (Table 3).

Table 3. Reservoir shoreline erosion variables.

Variable	Source	Classification (Gridcode #)	Comments
Shoreline Planimetric Form*	Airphoto interpretation. Shapefiles drawn by Michael Horner.	• Concave (1) • Convex (2) • Straight (3)	• Concave (bays and stream mouths) • Convex (headlands) – Subject to the direct force of waves and susceptible to greater erosion. Forms the barriers of drift cells • Straight
Shoreline Landforms	Airphoto interpretation supplemented by video survey. Shapefiles drawn by Michael Horner. Also see Slope Intervals.	• Cliff (vertical) • Bluff (vertical) – subject to wave attack • Beach (gently sloping) • Delta	Used to confirm erosion.
Shoreline Segments #	Derived from shoreline composition, planimetric form, and cross-sectional form	• Not Erosional (1) • Erosional (2)	Other shoreline segments such as the dam and delta were excluded from the variable.
Nearshore Width (m)	Field observations using laser rangefinder	-	Reflects morphodynamic state. Determined by break in slope.
Wind			
Fetch (annual average) *	Based on average annual wind direction calculated from Hydromet data using directional statistics in MS Excel.	• Minimum (1) • Medium (2) • Maximum (3)	Determines the amount of energy transferred to water. Defines wave period in lakes making it the most useful predictor of wave energy in lakes.

Table 3 (CONTINUED). Reservoir shoreline

Variable	Source	Classification (Gridcode #)	Comments
	Shapefiles calculated from Cle Elum Lake shoreline shapefile extracted from the USGS National Hydrography Dataset using ArcGIS		
Topography			
Slope Intervals *	Slope shapefiles created from DSMs available from Washington State Department of Natural Resources (WADNR).	• Low (1) • Intermediate (2) • Steep (3) • Very Steep (4)	Influences wave energy and breaking wave type. Reflects morphodynamic state. Classed by intervals of slope angles: • Low (0° - 10°) • Intermediate (11° - 36°) • Steep (37° - 49°) • Very Steep (> 50°)
Foreshore Slope (%)	Field observations using laser rangefinder	-	Reflects morphodynamic state. Determined by break in slope.
Nearshore Slope (%)	Same as above	-	Same as above
Bluff Height (m)	Same as above	-	Bluff height may be a factor in erosion

Table 3 (CONTINUED). Reservoir shoreline

Variable	Source	Classification (Gridcode #)	Comments
Geology			
Geologic Units *	Shapefile available from WADNR	• Ec(1s) - continental sedimentary rocks (Swauk Formation) (1) • Ec(2rl) - continental sedimentary rocks (Roslyn Formation, lower member) (2) • Ec(2rm) - continental sedimentary rocks (Roslyn Formation, middle member) (3) • Ec(2ru) - continental sedimentary rocks (Roslyn Formation, upper member) (4) • Eib - basic intrusive rocks (5) • Eva(ss) – andesite flows (Swauk Formation, Silver Pass Member (Dacite)) (6) • Evb(t) – basalt flows (Teanaway Basalt) (7) • Jph(d) - phyllite, low grade (Darrington Phyllite) (8) • Mit – tonalite (9) • Mva(h) – andesite flows (Howson Andesite) (10) • Oir(d) - intrusive rhyolite (Mount Daniel, volcanic rocks of) (11) • Qa - alluvium (12) • Qad(e) - alpine glacial drift, Fraser-age (Evans Creek Drift) (13)	

Variable	Source	Classification (Gridcode #)	Comments
		• Qf – artificial fill (14)	

Variable	Source	Classification (Gridcode #)	Comments
		• Qls - Mass-wasting Deposits, mostly landslides (15) • Qls(m) - Mass-wasting Deposits, other than landslides (16) • Qp - peat deposits (and bog deposits) (17) • Wtr – water (18)	
Average Sediment Size	Wolman pebble count	-	Influences degree of shoreline development. Sediments such as silts and sands are subject to transportation by waves. Reflects morphodynamic state. Reflects shoreline segment type and littoral compartments with grain size related to wave energy.
Sediment Texture	Samples of bluff material taken during field work. Texture determined using sieve and Mastersizer analysis.	-	Sand, clay, and gravel content determines the rate of bluff retreat. Classified according to USDA categories.
Vegetation			

Variable	Source	Classification (Gridcode #)	Comments
Vegetation Coverage *	Shapefile created from NAIP data using NDVI (ERDAS)	• Low (1) • Moderate (2) • High (3) • Very High (4)	Reduction of vegetation cover leads to soil erosion. Bluff vegetation indicates shoreline segment type.
Vegetation Type *	Shapefile created from NAIP data and supplemented by field observations.	Classified by predominant land cover: • Agricultural & Developed Vegetation (1) • Developed & Other Human Use (2) • Forest & Woodland (3) • Nonvascular & Sparse Vascular Rock Vegetation (4) • Open Rock Vegetation (5) • Open Water (6) • Recently Disturbed or Modified (7) • Shrub & Herb Vegetation (8)	Areas vegetated by shrubs may be eroded more easily than forested areas.

Note. Shoreline Features and Erosion Indicators (* analytical variables, # erosion

I collected data at twenty sites (Appendix C) selected from those identified during step 1 (Figure 17). They are located around the lake and represent an array of erosion factors identified in the literature review. Sites include minimal (three), medium (ten), and maximum (seven) fetch distances (USGS 2016; USBOR 2018). Planimetric form

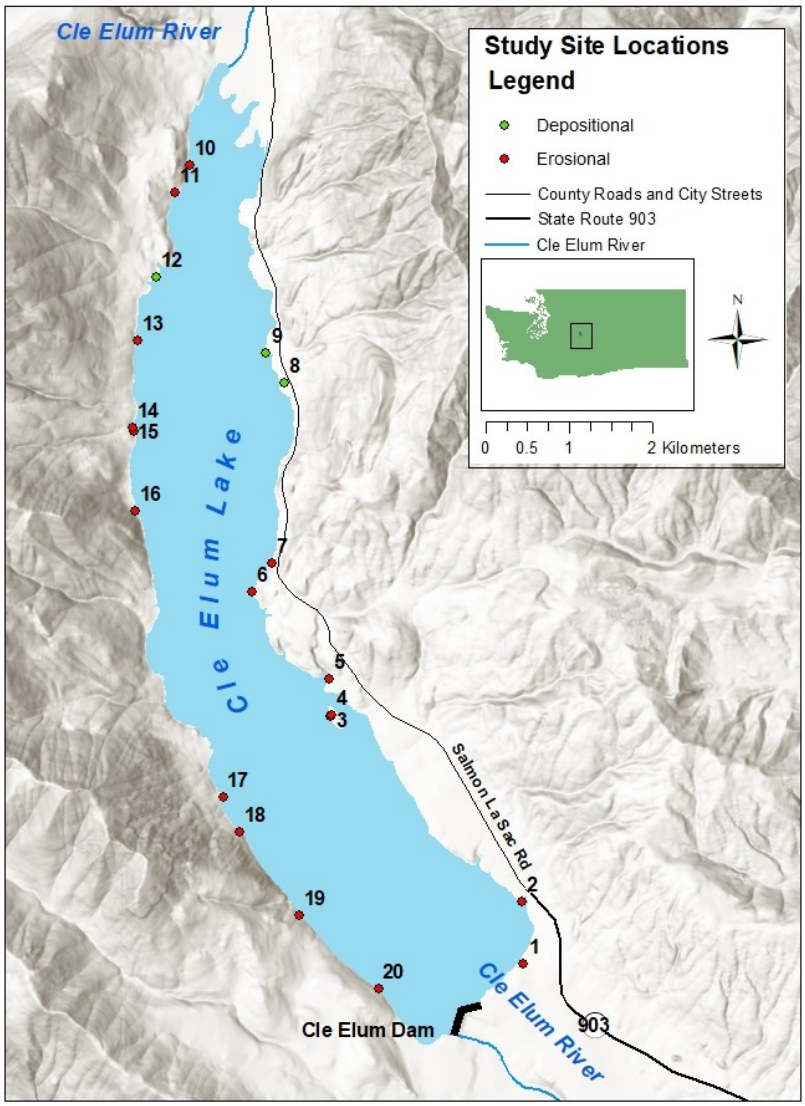

Figure 17: Study site locations (ESRI 2006; USGS 2016; ESRI 2015; WADOT 2020).

includes concave (one), convex (seven), and straight (twelve) shorelines. Slope intervals include moderate slopes (nine) and intermediate (eleven) shorelines (WADNR 2014). Vegetation coverage includes sites with low (four), moderate (twelve), and intermediate

(four) density (USDA 2013). The dominant land cover includes sites with temperate and boreal forest and woodland (nine), shrub and herb wetlands (eight), developed and urban (one), and barren (two) (USGS 2011). Shoreline composition includes the Evans Creek alpine glacial drift (four), the basalt Teanaway Formation (two), intrusive tonalite rocks (two), the sandstone-dominated Swauk Formation (three), the sandstone Roslyn Formation (two), mass-wasting deposits (one), and six with Quaternary alluvium (six) substrates. They were distributed around the lake with nine on the eastern shoreline and eleven on the western shoreline.

I began by noting the date as well as verifying and documenting the location of each site using latitude and longitude from the GPS device. Next, I examined exposures to determine whether they are bluffs composed of unconsolidated sediment prone to rapid failure or slowly eroding bedrock cliffs (Komar and Shih 1993; Knodel, Lange, and Voigt 2008; Davidson-Arnott 2010; Earle 2015). I described landforms and noted any discrepancies with the results of the airphoto interpretation on the data sheet (Boualla et al. 2017). Later, these were reconciled. I also documented landforms photographically and georeferenced them by recording a waypoint with the GPS device (Boualla et al. 2017).

Where outside data on erosion factors was unavailable, I took measurements in the field and noted them on the field checklist. The drawdown of the reservoir beginning at the start of July exposes the shoreline. Therefore, I performed almost all of the field measurements after this time.

First, I supplemented the available geologic data by describing and analyzing shoreline substrates. GIS data was available for geologic units. During fieldwork and

later using photographs taken of each site, I described the sorting and bedding of sedimentary bluffs. In order to describe the composition of bluffs including sediment size and texture, I took a sediment sample for subsequent analysis. I extracted sediment samples as close to the middle of each bluff's height as possible after scraping the outer layer of sediment with a trowel. Once the analysis was complete on each sample, the information on shoreline substrates was used to describe exposure-types such as alluvium, glacial till, lacustrine sediment, and bedrock.

Second, I documented shoreline relief and morphodynamics. Since sediment size characterizes reflective and dissipative shorelines, I performed a Wolman pebble count (Lorang et al. 1993; Miller, Warrick, and Morgan 2011; West Virginia DEO 2019). Next, I used a Trupulse 360 Laser Rangefinder to record the following parameters. First, I measured nearshore width and foreshore slope. This is because narrow nearshore zones and steep foreshores characterize reflective shorelines while dissipative shorelines have broad nearshores (Lorang et al. 1993; Lorang, Komar, and Stanford 1993). In the field, I visually distinguished the nearshore using sediment size and slope angle. Finer sediment marked the outer limit of the nearshore while increasingly coarse sediment and gentler slopes marked the foreshore (Currey and Sack 2009). Second, since waves begin breaking in the nearshore zone and shoreline slope determines breaking wave type, I also measured nearshore slope (Komar 1976; Huggett 2007). Finally, I measured bluff and cliff height as this may affect erosion rates (Amin and Davidson-Arnott 1997).

Third, I characterized vegetation conditions at each site. This included the dominant vegetation coverage, characterized as barren, grassland, shrubs, or forest since this influences erosion. It also included the undercutting of forests atop bluffs as a

prelude to further erosion (Lorang and Stanford 1993). I also photographed plants for later identification and use in interpretation (Lounsbury and Aldrich 1979).

Describing and Mapping Field Measurements

After completing the fieldwork and acquiring external GIS data in step three, I described these findings statistically and cartographically. Since fieldwork was conducted at seventeen confirmed erosional segments, a small sample size was obtained for measurements (n = 17). Therefore, I analyzed field data for normality (Ghasemi and Zahediasl 2012). Outliers influence the mean statistic, making it more appropriate for normally distributed data. In contrast, the median statistic best describes the central tendency of non-normalized field measurements since outliers in their distribution would influence the mean (Minitab 2019). Therefore, the choice of statistics that best describe the central tendency of the field measurements was based on their distribution (Spatz 1993). I categorized the field measurements using natural breaks with only four classes due to the small sample size. These were mapped in order to visualize their spatial distribution.

Acquiring and Synthesizing Data on Shoreline Erosion Variables

Next, I developed a geodatabase using ArcGIS software including each of the erosion risk factors identified in the literature review. This included GIS data from outside source and the field measurements. During this step, the GIS data was pre-processed to obtain variables including fetch, planimetric shape, slope angle, vegetation coverage and type, and geologic units.

Fetch

I incorporated geometric characteristics of shorelines including fetch, planimetric shape, slope angle, and bluff height into the geodatabase. To represent fetch, the mean annual wind direction at Cle Elum Lake was first derived using data from the Yakima Project Hydromet system (Vogiatzis et al. 2004; USBOR 2018). Directional statistics were used to convert azimuths recorded at Cle Elum Dam every fifteen minutes from 2013-2016 into Cartesian coordinates to calculate mean wind angle. This was converted into the four cardinal directions, the four ordinal directions, and the eight secondary-intercardinal directions, resulting in a mean wind angle of 280° (z = 10,361.8, n = 140,041), representing mean westerly winds (Dempsey 2013; USBOR 2018; Marr 2019).

This data is the basis of a GIS layer representing fetch distance along the lakeshore. First, I extracted a shapefile of Cle Elum Lake in ArcGIS using data from the Yakima Project Hydromet system (USBOR 2018). Next, this shapefile was rotated according to the mean wind angle previously calculated. Then, ArcGIS was used to create a grid over the shapefile with a centroid in each cell. I clipped this grid to the lake extent and joined the lake shapefile with the grid shapefile to produce a count of points in each row of the grid (Hyslop 2012; ESRI 2019). This quantifies fetch distance in five foot increments. Finally, I categorized fetch distances for each point as maximum, medium, and minimum using Jenks natural breaks, a method used to assign values to user categories with minimal squared deviations between their means (ESRI 2016).

While the primary purpose of calculating mean wind directions was to determine fetch sizes for further analysis, this was also used to produce additional descriptive wind statistics for illustrative purposes. I also calculated this statistic by season and month.

This indicates the variability of wind patterns here. Wind direction determines the angle at which wind transfers energy to water, making it useful in determining where lakeshore erosion occurs (Gracia 1995). It is important to understand that while Cle Elum Lake's prevailing wind direction is westerly, erosion can occur throughout the lake basin depending on changing wind patterns throughout the year.

Planimetric Shape

I classified the reservoir shoreline's planimetric shape using the shoreline segments shapefile previously drawn as the basis for this layer. QGIS generated a version of the shoreline shapefile with fewer vertices. By comparing this layer to the original shoreline segments layer, I identified segments of the shoreline that protrude lakeward, protrude landward, or are straight and categorized these in a new layer as convex, concave, and straight segments respectively.

Slope Angle

To provide topography data, I downloaded a digital terrain model (DTM) for the Yakima River Basin at a resolution of one foot from the Washington LIDAR Portal (Boualla et al. 2017; Jiménez-Perálvarez et al. 2009; Quantum Spatial 2014; WADNR 2014). This was clipped to the Cle Elum Lake extent using QGIS software, converted to a slope raster, and reclassed into slope angle intervals. These categories include low (0° - 10°), intermediate (11° - 36°), steep (37° - 49°), and very steep (> 50°) slopes based on relevant angles determining breaking wave type (Figure 7) (Davies 1977; O'Halloran and Spennemann 2002; Huggett 2007). Lastly, the reclassed slope raster was converted to a polygon shapefile using the ArcGIS for inclusion in the geodatabase.

Vegetation Coverage

I derived vegetation coverage data from high resolution, four-band 2013 National Agriculture Imagery Program (NAIP) raster files with a resolution of one meter (USDA 2013). Next, ERDAS was used to perform the Normalized Difference Vegetation Index (NDVI) method to create a vegetation coverage raster (GISGeography 2017). This raster layer was clipped to a buffer around Cle Elum Lake using ArcGIS. I used natural breaks to rank the clipped raster into four groups of vegetation coverage ranging from one representing sparse vegetation to four representing the most thickly vegetated areas (Figure 15). Finally, the reclassified raster layer was converted to a polygon shapefile for inclusion in the geodatabase.

Vegetation Type

Vegetation type was characterized using land cover data from the USGS GAP/LANDFIRE National Terrestrial Ecosystems project (USGS 2011). I downloaded raster data with a resolution of 30 m x 30 m and clipped it to the Cle Elum Lake buffer using ArcGIS. The clipped raster was converted into a polygon shapefile using ArcGIS. Finally, I classified this based on the GAP/LANDFIRE National Vegetation Classification system reflecting predominant land cover (Figure 14).

Shoreline Substrates

Geologic data was available from the Washington State Department of Natural Resources including geologic units and landslides (Figure 8) (Frizzell et al. 1984; WADNR 2000; Jiménez-Perálvarez et al. 2009). Two additional variables measured during the fieldwork included average sediment size from the Wolman pebble count and sediment texture. The average of each pebble count was calculated.

Sediment samples were analyzed in the CWU Department of Geography hydrology laboratory using sieve analysis to sort the sediments by grain size and prepare a sample of the smallest sediment for sediment texture analysis. To perform the sieve analysis, I first dried each sample in drying oven for four hours at 83° C. Then, each dried sediment sample was weighed. Next, these were placed in stacked U.S. Standard test sieves. A W.S. Tyler Ro-Tap shaker separated sediment sizes by range including those above 4 mm (fine pebbles and larger), 2 mm to 4 mm (very fine pebbles), 1 mm to 2 mm (very coarse sand), and below 1mm (coarse sand and below) (Earle 2015). I recorded the weight of each of these sediment size ranges and calculated the percentage of the total sample size represented by each range. The fraction sized below 1 mm was set aside for sediment texture analysis.

I conducted further sediment size analysis in the CWU Department of Geology sample preparation laboratory using a Mastersizer 3000 particle size analyzer to determine sediment texture. A 10 g sample was taken from the fraction sized 1 mm and below. This excluded very coarse sand since sediments 1.8 mm and larger exceed the Mastersizer's capacity (Earle 2015; Central Washington University Department of Geology 2019). These were deflocculated in beakers filled with a solution of deionized water and sodium hexametaphosphate for more than twenty-four hours. During this time they were periodically stirred to disperse the grains. Following this, I analyzed each sample using the Mastersizer (Dashtgard 2016). This analyzed each sample 3 times and produced an average of the results. I used the average result to determine sediment texture according to the Udden-Wentworth scale (Wentworth 1922; Earle 2015). To do

this, the percentages of sand, silt and clay were entered into the USDA's online sediment texture calculator to determine sediment texture (USDA 2019).

Step 3: Determining Variables in Shoreline Erosion

I performed statistical analysis to determine which shoreline erosion variables from the GIS data should be included in the erosion susceptibility models (Table 4). First, ArcGIS was used to find the intersections between erosional and depositional segments in both versions of the shoreline inventory within each level of the GIS variables in order to find their total lengths. Next, I used the chi-square ($\chi 2$) test for independence within the Statistix software package to determine if there is a relationship between the GIS variables and shoreline segment type.

Table 4. Variables analyzed using chi-square test.

Fetch	*Geologic Unit*	*Slope Interval*	*Vegetation Cover*	*Vegetation Type*
Minimum	Ec(1s) - continental sedimentary rocks (Swauk Formation)	Low	Low	Agricultural & Developed Vegetation
Medium	Ec(2rl) - continental sedimentary rocks (Roslyn Formation, lower member)	Intermediate	Moderate	Developed & Other Human Use
Maxium	Ec(2rm) - continental sedimentary rocks (Roslyn Formation, middle member)	Steep	High	Forest & Woodland
	Ec(2ru) - continental sedimentary rocks (Roslyn Formation, upper member)	Very Steep	Very High	Nonvascular & Sparse Vascular Rock Vegetation
	Eib - basic intrusive rocks			Open Rock Vegetation
	Eva(ss) – andesite flows (Swauk Formation, Silver Pass Member (Dacite))			Open Water
	Evb(t) – basalt flows (Teanaway Basalt)			Recently Disturbed or Modified
	Jph(d) - phyllite, low grade (Darrington Phyllite)			Shrub & Herb Vegetation
	Mit – tonalite			
	Mva(h) – andesite flows (Howson Andesite)			
	Oir(d) - intrusive rhyolite (Mount Daniel, volcanic rocks of)			
	Qa - alluvium			
	Qad(e) - alpine glacial drift, Fraser-age (Evans Creek Drift)			
	Qf – artificial fill			
	Qls - Mass-wasting Deposits, mostly landslides			
	Qls(m) - Mass-wasting Deposits, other than landslides			
	Qp - peat deposits (and bog deposits)			
	Wtr – water			

This test arranges all of the combinations of the observed frequencies of one variable's classes within each class of a second variable in the cells of a contingency table. Then it calculates the expected frequencies of each combination if there is no relationship between the variables. From this, it calculates the value of $\chi 2$ for each cell based on the difference between the observed frequencies and the expected frequencies. The overall sum of $\chi 2$ is calculated for the entire contingency table (Spatz 1993). Since this test is based on frequencies, I divided the length of each shoreline type within each GIS variable level by one hundred to arrive at a count of 100 m shoreline segments. The overall values of $\chi 2$ were compared to critical values of $\chi 2$ found in a chi-square distribution table based on the degrees of freedom. When the overall $\chi 2$ exceeded the critical value of $\chi 2$, I concluded that there was a relationship between shoreline types and GIS variables. The significance of any relationships were determined based on the *p-value* calculated (GraphPad 2020).

I conducted further analysis of the chi-square results to determine which of the observed classes of GIS variables are responsible for their statistical significance in shoreline erosion. I determined which of the observed classes of significant GIS variables exceeded their expected frequency if there is no relationship between the variables and shoreline erosion. I calculated the proportion of the overall $\chi 2$ value represented by the $\chi 2$ value in each cell of the contingency table containing the cross-tabulation of each geologic unit and slope interval with shoreline type. For geologic unit, I discarded intersections with units classified as "water" in the dataset. This provided a more detailed understanding of the relevant factors in shoreline erosion.

Although the chi-square test for independence established relationships between some of the proposed shoreline erosion variables and shoreline type, the Cramér's V statistic established their strength (Van Den Berg 2020). Cramér's V indicates covariance between two variables (Statistics How To 2020). I used SPSS to calculate Cramér's V between shoreline type and the statistically related variables in the near-term and long-term shoreline inventories. These values were compared to a table of values for the interpretation of Cramér's V values (Cohen 1988).

Step 4: Modelling Erosion Susceptibility and Creating Hazard Maps

Modelling Erosion Susceptibility

For each erosional shoreline segment identified in step 1, I used GIS statistical analysis to identify areas susceptible to future erosion. Significant risk factors were analyzed using the GIS Matrix Method (GMM) (Irigaray 1995). Irigaray developed the GMM with a conceptual basis in previous non-GIS methods to assess landslide vulnerability (DeGraff and Romesburg 1980; Irigaray 1995). Bivariate analysis identifies the association between risk factors and the incidence of specific hazards (Jiménez-Perálvarez et al. 2009). This bivariate method relies on the experience of past hazards to assess the relative risk of future landslides and other natural hazards (Jiménez-Perálvarez et al. 2009; Boualla, Mehdi, and Zourarah 2016; Tošić 2018). This method is appropriate for determining shoreline erosion risk since past shoreline evolution is an indicator of future erosion (Adamo et al. 2014). Bivariate statistical methods such as the GMM are appropriate for medium-scale susceptibility analysis (Jiménez-Perálvarez et al. 2009).

This method involves the creation of three matrices within GIS. The erosion matrix (EM) is the spatial extent of past shoreline erosion within the areas representing

each possible combination of risk factors, calculated on a cell-by-cell basis (Jiménez-Perálvarez et al. 2009; Costanzo et al. 2012). The model derives the EM from two data types. The first is a vector layer representing erosional segments, with values coded as "1" for depositional segments or "2" for erosional segments. The second are vector layers representing erosion variables, with nominal attributes assigned integer values. The total surface of the study area matrix (TSM) is the total area within these risk factor combinations. The susceptibility matrix (SM) is the quotient of the EM divided by the TSM on a cell-by-cell basis to quantify relative hazard as the proportion of mapped erosional segments within each combination of risk factors (Jiménez-Perálvarez et al. 2009). Users then categorize these results into levels of risk using the natural breaks method in GIS (Jiménez-Perálvarez et al. 2010). This assessment assumes that future erosion is more likely in zones that share features with areas subject to past shoreline recession (Jiménez-Perálvarez et al. 2009).

Jiménez-Perálvarez et al. (2009) developed an automatic susceptibility GIS model based on the GMM method and made it available online. I adapted this model to evaluate the significance of the association between erosional landforms and their associated risk factors (Appendix D). The shoreline segment layers were recoded with integer values, assigning "1" to depositional segments and "2" to erosional segments. I also added the GIS data developed during Step 3 representing erosion risk factors. Nominal attributes such as geologic units and data categorized using natural breaks were assigned integer values.

In addition to the shoreline erosion inventory, the model requires at least two variables (Jiménez-Perálvarez et al. 2009). Based on the results of the chi-square test,

geologic unit and slope interval were chosen for inclusion in the models. The models were run using both versions of the shoreline erosion inventory with and without bedrock cliffs included. This resulted in GIS models using the statistical associations between erosion risk and erosion incidence to predict near-term and long-term shoreline retreat for locations within the newly expanded inundation zone sharing characteristics with the previously eroded shoreline.

I further analyzed the proportion of mapped erosional segments within each combination of risk factors found in the susceptibility matrices, which is the main result of GMM. This analysis used both the near-term and long-term shoreline inventory. First, the susceptibility levels representing the greatest proportion of the study area as well as the spatial distribution of highly susceptible areas were determined. Then, the combinations of risk factors within the high (4) and very high (5) susceptibility levels were identified. Finally, the individual risk factors with the most statistically significant relationships to the risk of future erosion were analyzed.

Creating Hazard Maps

Using the results of the GIS model, I created hazard maps of shoreline segments vulnerable to erosion and made management recommendations based on these (Boualla et al. 2017). In order to characterize areas of the lakeshore prone to erosion, the lake was divided into four quadrants representing the four ordinal directions in order to describe the spatial distribution of shoreline segments and susceptibility (Figure 18). I drew lines between the lake's northern-and southernmost points to divide the western and eastern shorelines. The north and south halves of the lake were divided at the point at which it tends towards the southeast.

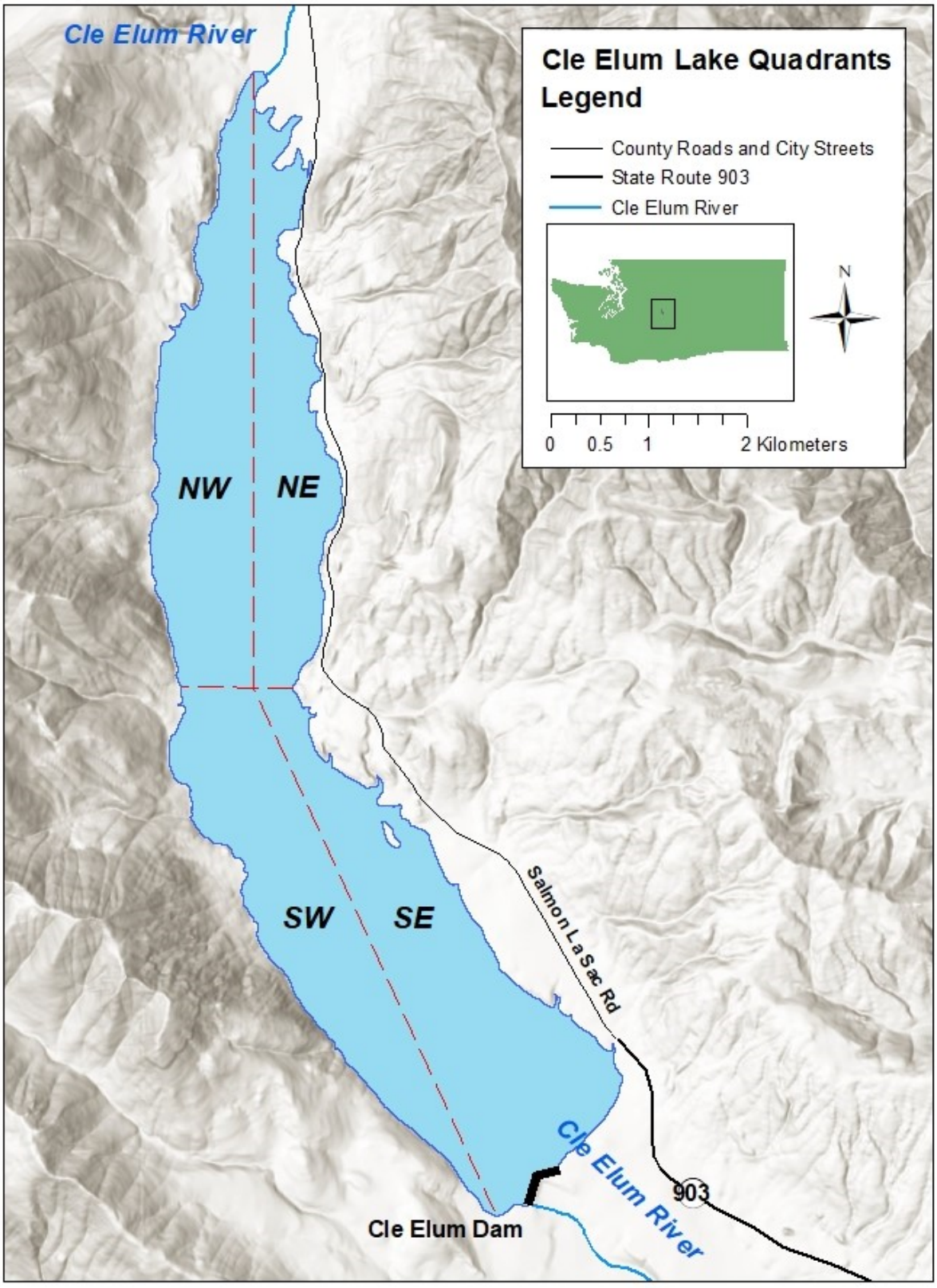

Figure 18: Cle Elum Lake Quadrants (ESRI 2006; USGS 2016; ESRI 2015; WADOT 2020).

Step 5: Management Recommendations

By combining the erosion risk data with the spatial distribution of archaeological sites, cultural resource managers will be able to identify which are most vulnerable to erosion. I also made recommendations for managing cultural resources vulnerable to erosion based on the shoreline inventory and model results.

CHAPTER V

RESULTS AND DISCUSSION

Erosional and Depositional Shoreline Segments

Based on the airphoto interpretation and video survey, I mapped 35.73 km of landforms along the Cle Elum Lake shoreline including the dam area and delta (Figure 19). Of this, 80 erosional and 92 depositional shoreline segments comprise 31.06 km of

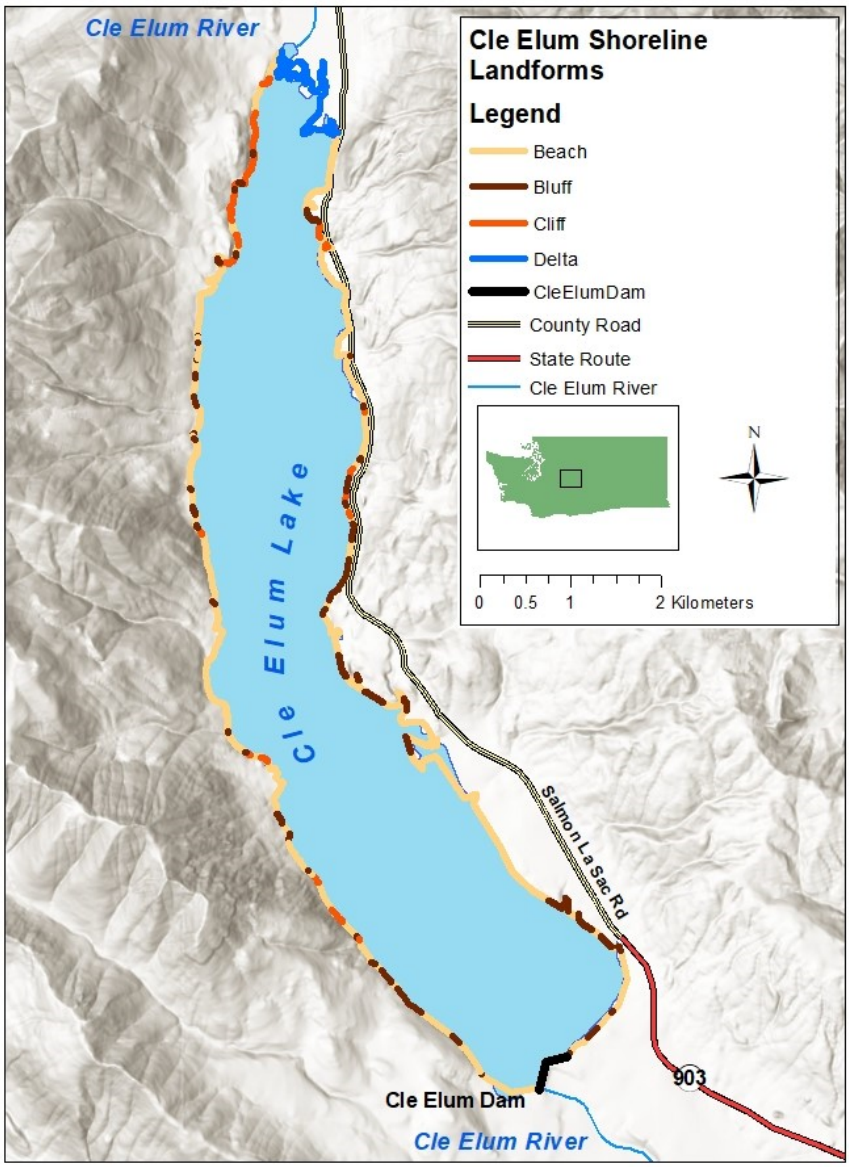

Figure 19: Cle Elum shoreline landforms (ESRI 2006, 2015; USGS 2016; WADOT 2020).

the shoreline. The mean length of these segments is 205.3 m, with mean lengths of 88.5 m for erosional segments, and 260.7 m for depositional segments. Beach sediments mark both transportational and depositional zones (Jacobsen and Schwartz 1981; Chrzastowski, Thompson, and Trask 1994). I mapped all beaches as depositional segments for the purposes of this study.

The spatial distribution of erosional segments depends on their classification in order to create the near-term and long-term erosion models. In the near-term shoreline inventory, erosional shoreline segments were limited to bluffs, which comprise 4.5 km or 14.6 percent of the mapped shoreline segments. They range in length from 0.5 m to 0.5 km. As anticipated, erosion is most evident on the lake's southeastern shoreline, followed by the northeastern, southwestern, and northwestern shorelines (Table 5). This shoreline erosion inventory (Figure 20) forms the basis of the near-term erosion model.

Table 5: Distribution of erosional segments: near-term shoreline erosion.

Quadrant	Proportion of Depositional Segments	Total Bluff Length (km)
SE	44.2%	2
NE	24.3%	1.11
SW	19.5%	0.9
NW	11.9%	0.54

In addition, fifty-six bluffs and twenty-four cliffs were identified as erosional segments representing 22.8 percent or 7.1 km of the shoreline segments. Under this definition of erosional shoreline segments, the northwest shoreline accounts for the greatest share of erosional segments, followed by the southeast, the northeast, and the

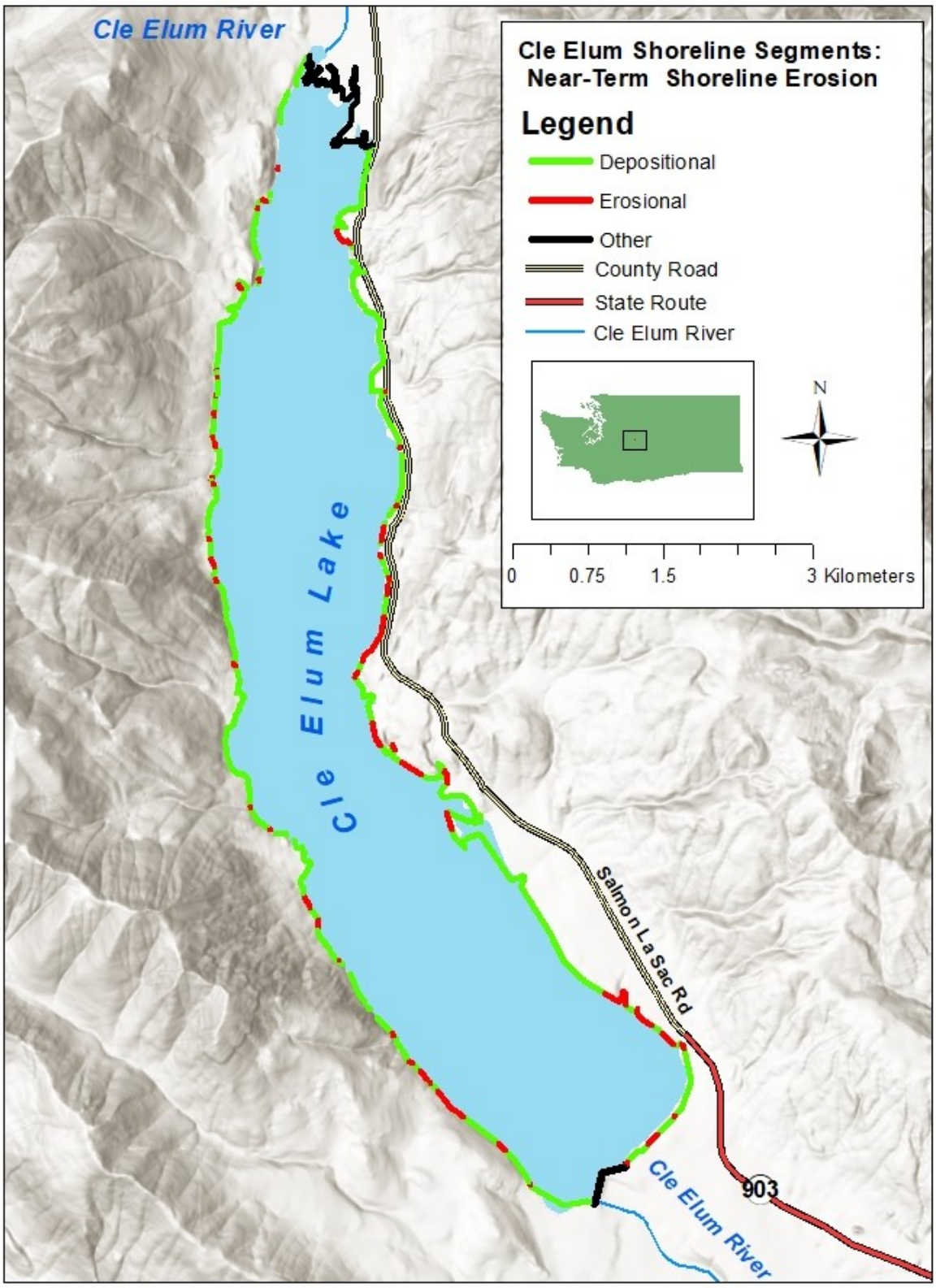

Figure 20: Cle Elum shoreline segments: near-term shoreline erosion (ESRI 2006, 2015; USGS 2016; WADOT 2020).

southwest shorelines (Table 6). The long-term erosion model used this inventory (Figure 21) to analyze erosion susceptibility.

Table 6: Distribution of erosional segments: long-term shoreline erosion.

Quadrant	Proportion of Depositional Segments	Total Bluff Length (km)
NW	30.6%	2.2
SE	28.4%	2
NE	22.9%	1.6
SW	18.1%	1.3

Both inventories include the same set of depositional segments. The beach segments include 24 km or 77.2 percent of the total shoreline segments. They range from 2.7 m to 2.7 km in length. The greatest concentration of beaches in descending order are on the southwest, southeast, northwest, and northeast shorelines (Table 7).

Table 7: Distribution of depositional segments.

Quadrant	Proportion of Depositional Segments	Total Bluff Length (km)
SW	49.6%	17.6
SE	20.4%	7.2
NW	16.0%	5.7
NE	14.0%	5

The finding that depositional segments are both more numerous and more extensive than erosional segments in both shoreline inventories differs from other studies. For example, studies of paleolakes conducted over the last century and a half determined that preserved erosional shorelines dominate lake basins (Russell 1885; Tackman 1993; Lillquist 1995).

One possible explanation for this difference is Cle Elum Lake's long-standing history as storage reservoir with the current dam completed in 1907 (Dick 1993). Impoundment may have led to an increased amplitude and duration of elevated lake

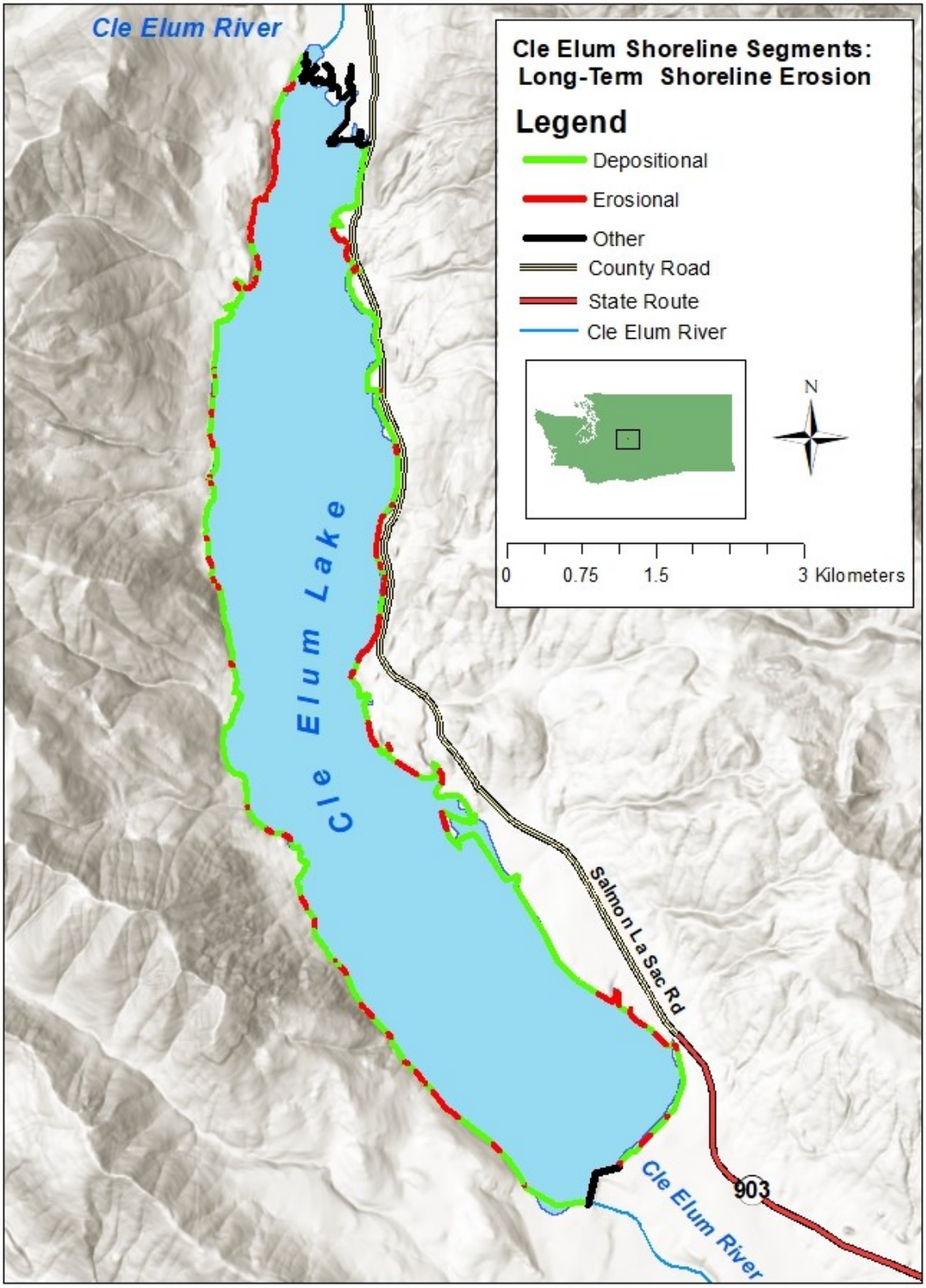

Figure 21: Cle Elum shoreline segments: long-term shoreline erosion (ESRI 2006, 2015; USGS 2016; WADOT 2020).

levels seasonally. This could have extended the annual period when the backshore was subject to wave attack, leading to increased erosion (Figures 22 and 23) (Lorang, Komar, and Stanford 1993). However, erosion rates may have begun slowing in the first decade

Figure 22: Bluff erosion near Sandelin Lane, Cle Elum Lake. Bluff eroded in Quaternary Evans Creek alpine glacial drift. Varial zone in the foreground. View towards the east. Photograph by Michael Horner, June 2019.

of reservoir regulation (Bao et al. 2018). This is because erosion leads to the deposition of fine sediments creating beaches with low gradients that dissipate wave energy (Figure 24) (Lorang et al. 1993; Lorang, Komar, and Stanford 1993). The shoreline reaches an equilibrium profile after a period of several decades. The results of this study reflect a possible decrease in the rate of erosion in the century since the regulation of lake levels began (Lorang, Komar, and Stanford 1993).

A number of other possible explanations relate to Cle Elum Lake's physical characteristics. The first is that Cle Elum Lake has relatively narrow maximum fetch distances of 2.7 km, minimizing wave energy (Gracia 1995; Google Maps 2018). It has

Figure 23: Bluff erosion near Bell Creek, Cle Elum Lake. Bluff eroded in Quaternary alluvium. Lake sediments and driftwood to the right. View towards the south. Photography by Michael Horner, August 2019.

Figure 24: Beach near Morgan creek, Cle Elum Lake. Quaternary alluvium deposits. View towards the south. Photography by Michael Horner, August 2019.

relatively few headlands that are susceptible to erosion (Lakhan 1997). Forest vegetation prevents the erosion of upper shorelines and Cle Elum Lake features mature coniferous forests (Lorang and Stanford 1993; USBOR and WADOE 2015). Steep cliffs and bluffs are most likely to erode in substrates with uniform or well developed stratigraphy (Bird 2001). At almost all of the erosional sites I visited, there is little sorting or bedding and most of the bluffs are composed of very or extremely gravelly sediments. These characteristics may explain the lack of a statistical relationship between most of the shoreline erosion variables considered and the incidence of cliff and bluff erosion.

Physical Characteristics of Erosional Sites

Descriptive Statistics of Field Measurements

The physical characteristics of the shoreline were documented during fieldwork to refine both shoreline inventories. Here, I use these results to describe erosional sites at a more detailed scale than the GIS data affords. As can be seen in the histograms below, foreshore slope was the only measurement with a normal distribution, ranging from 4.6 percent (site 1) to 60 percent (site 17), encompassing all slope interval categories (Figure 25). The mean foreshore slope of erosional sites is intermediate ($\bar{x}$ = 27.4% or 15.32°, SE = 13%).

Non-normalized fieldwork measurements (Table 8) included sediment size, nearshore width, nearshore slope, and bluff height. The median sediment size is 59.2 mm

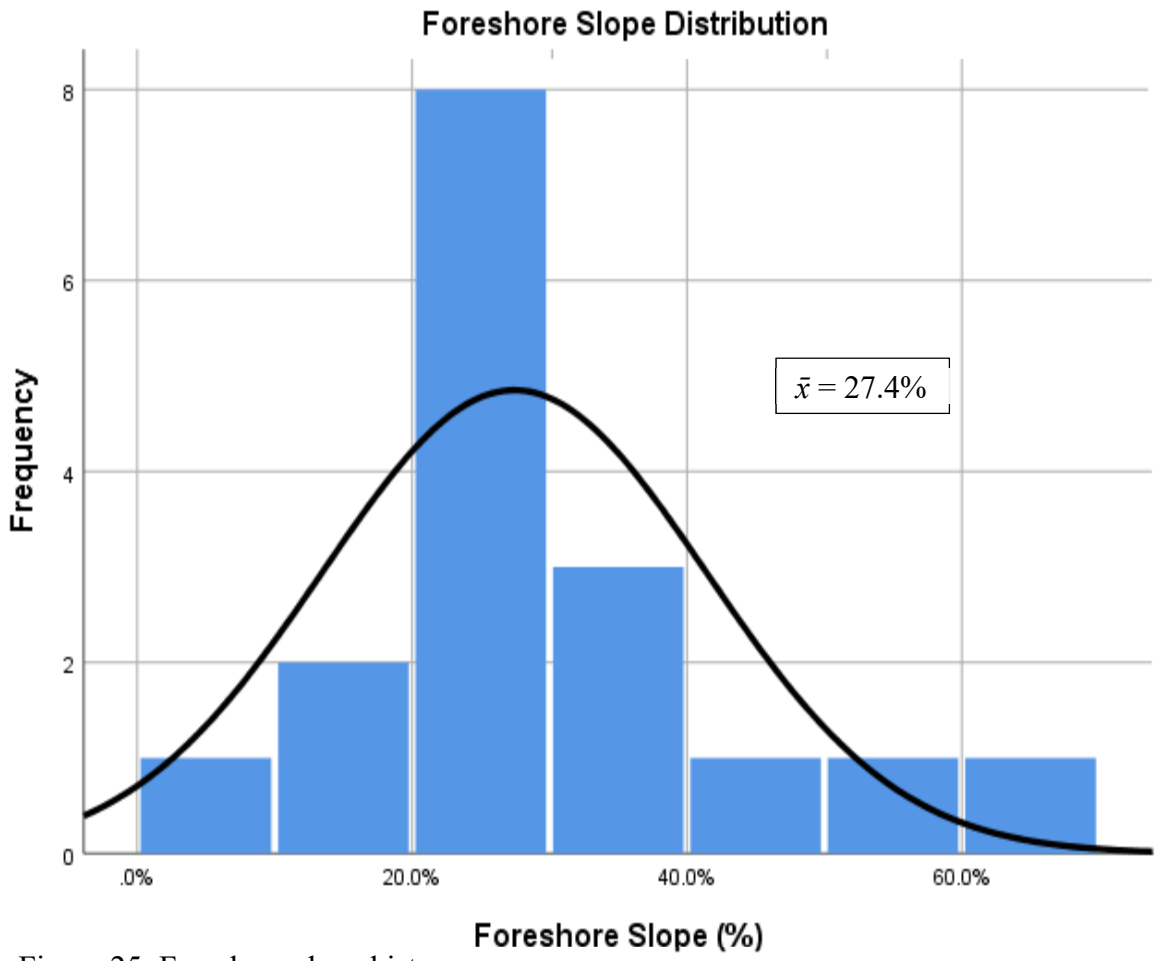

Figure 25: Foreshore slope histogram.

Table 8: Non-normalized field data table.

Field Measurement	*R*	*Min*	*IQR*	*Med*	*Max*
Sediment Size (mm)	104	28	43.9	59.2	132
Nearshore Width (m)	216	2	35.2	20	218
Nearshore Slope (%)	56.6%	0.6%	14.40%	15%	57.2%
Bluff Height (m)	9.7	2	2.2	4.3	11.7

R Range; *Min* Minimum; *IQR* Interquartile Range; *Med* Median; *Max* Maximum; N = 17

(very coarse pebbles) (Figure 26) (Earle 2015). The median nearshore width measured is 20 m (Figure 27). The median nearshore slope measures is low (15% or 8.53°) (Figure 28). Finally, the median bluff height is 4.3 m, with an interquartile range of 2.2 m, and a

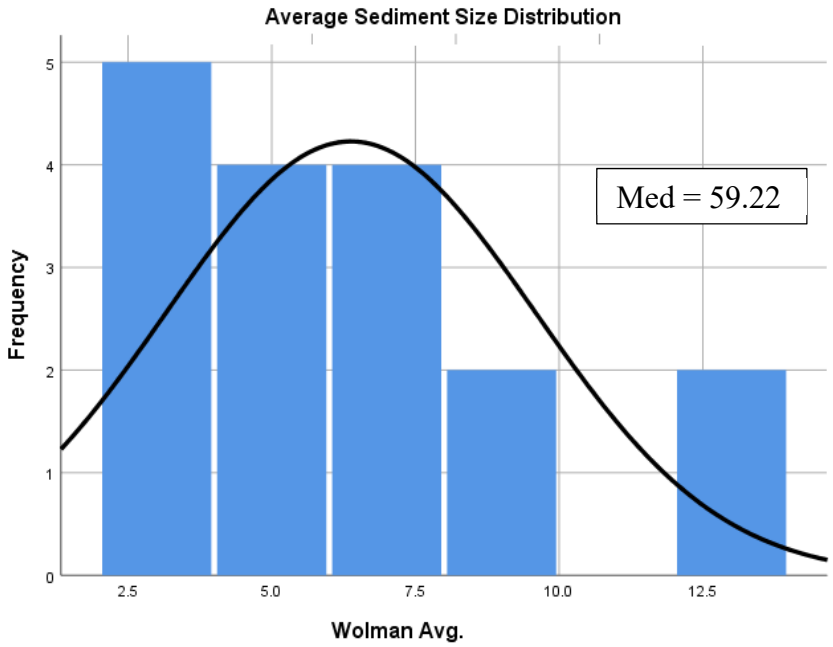

Figure 26: Sediment size histogram.

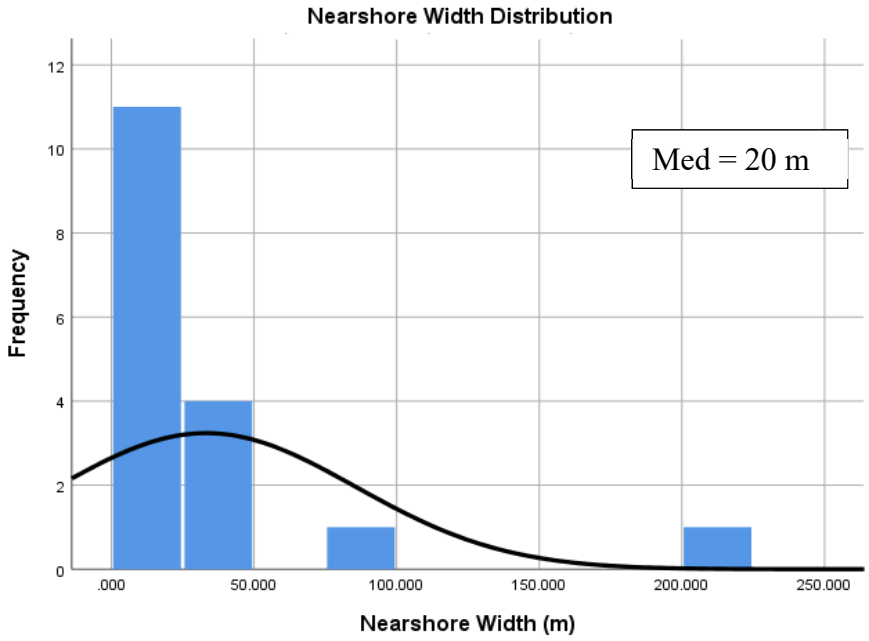

Figure 27: Nearshore width histogram.

range of 2 m to 11.7 m (Figure 29). Given the wide range of bluff heights observed at erosional sites, it is not possible to verify that higher shoreline bluffs are more prone to erosion.

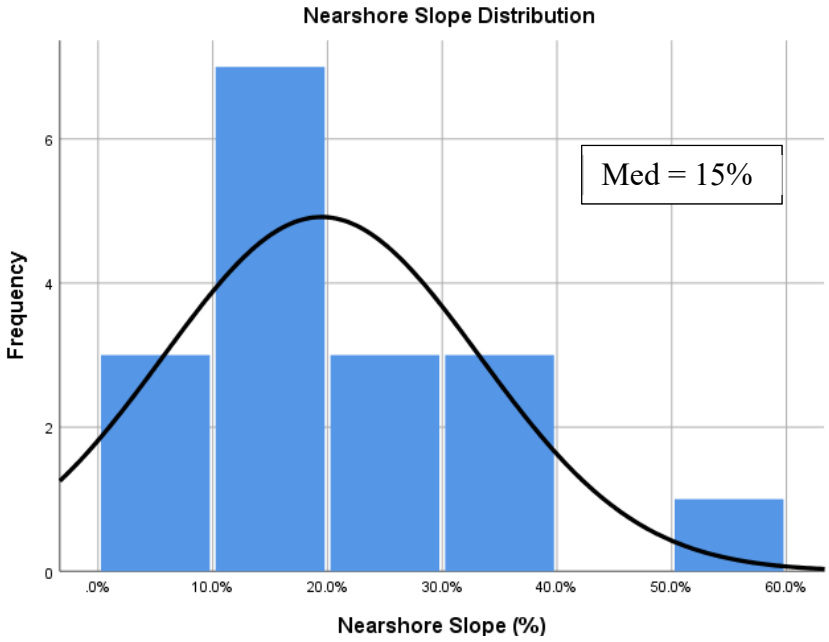

Figure 28: Nearshore slope histogram.

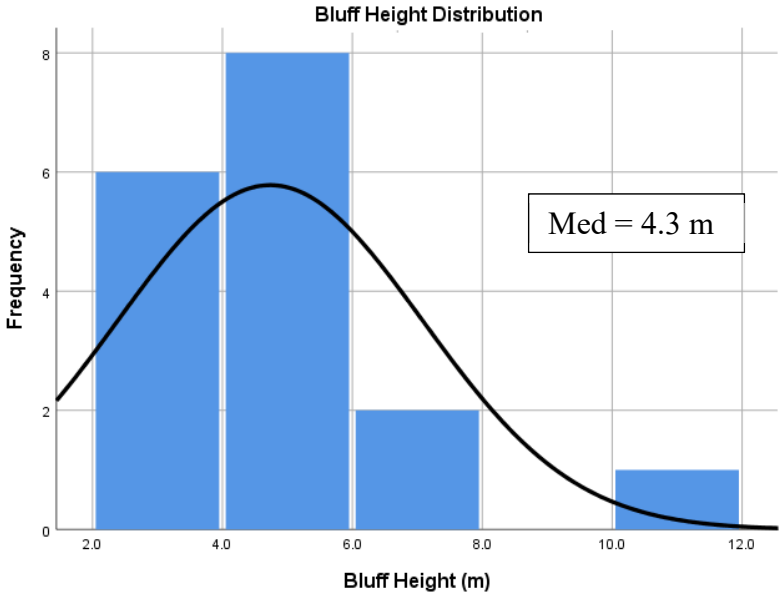

Figure 29: Bluff height histogram.

Taken together, the physical characteristics of these sites reflect conditions expected of erosional shorelines in large storage reservoirs. At Cle Elum Lake, the mean foreshore slope of 27.4 percent compares to beach faces on reflective shorelines at Flathead Lake, Montana with mean slopes of 25 percent. However, the former's median nearshore slope of 15 percent is gentler than the latter. The median sediment size of 59.2 mm (very coarse pebbles) was also similar to the fine gravel and pebbles seen at Flathead Lake (Lorang et al. 1993). Using natural breaks, I classed nearshore widths at Cle Elum Lake (Figure 31). The median nearshore width of 20 m places it in the second smallest class. Relatively small nearshore widths reflect erosion as nearshore zones lose sediment volume (Lorang et al. 1993; Lorang, Komar, and Stanford 1993).

Mapping Field Measurements

Based on the maps of the field measurements, a qualitative assessment of their spatial distribution follows for potential use as field indicators of erosion. Sites with similar sediment sizes appear clustered in pairs in several locations (Figure 30). Sites with the smallest average sediment sizes between 28 mm (coarse pebble) and 41.25 mm (very coarse pebble) exist in the northeastern, northwestern, and southeastern corners of the lake. Along the central part of the western shoreline are five sites with sediment sizes between 41.25 mm and 64.9 mm (small cobble). Sites with sediment sizes between 64.9 mm and 93.4 mm (small cobble) are on the southwestern and eastern shorelines. The largest average sediment sizes between 93.4 mm and 132.4 mm (large cobble) are at one location, which is Picnic Island, located at Wish Poosh (Wentworth 1922; Earle 2015).

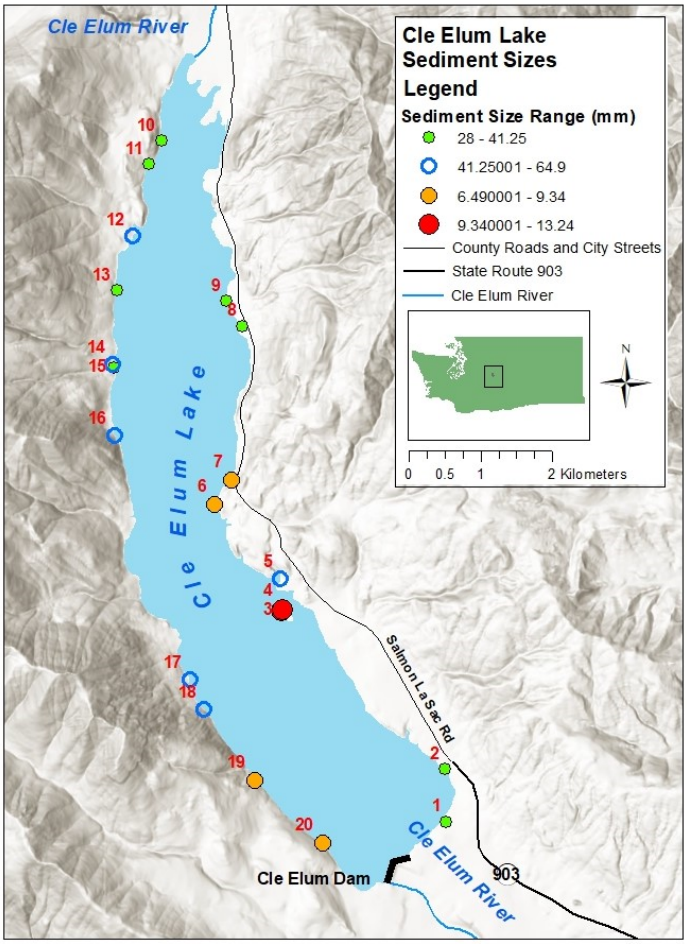

Figure 30: Cle Elum Lake sediment sizes (ESRI 2006, 2015; USGS 2016; WADOT 2020).

Study sites overwhelmingly feature relatively narrow nearshore widths (Figure 31). Nearshore widths below 43 m exist at all but two of the study sites. The continual drawdown of the reservoir over the course of the summer when I performed field work, and frequent difficulty visually distinguishing the nearshore, suggested that these measures simply reflect the continual lowering of the lake's elevation. However, the distribution of narrow nearshore zones in the parts of the lake that I visited after the reservoir was drawndown indicate that these measurements may be more accurate than initially anticipated.

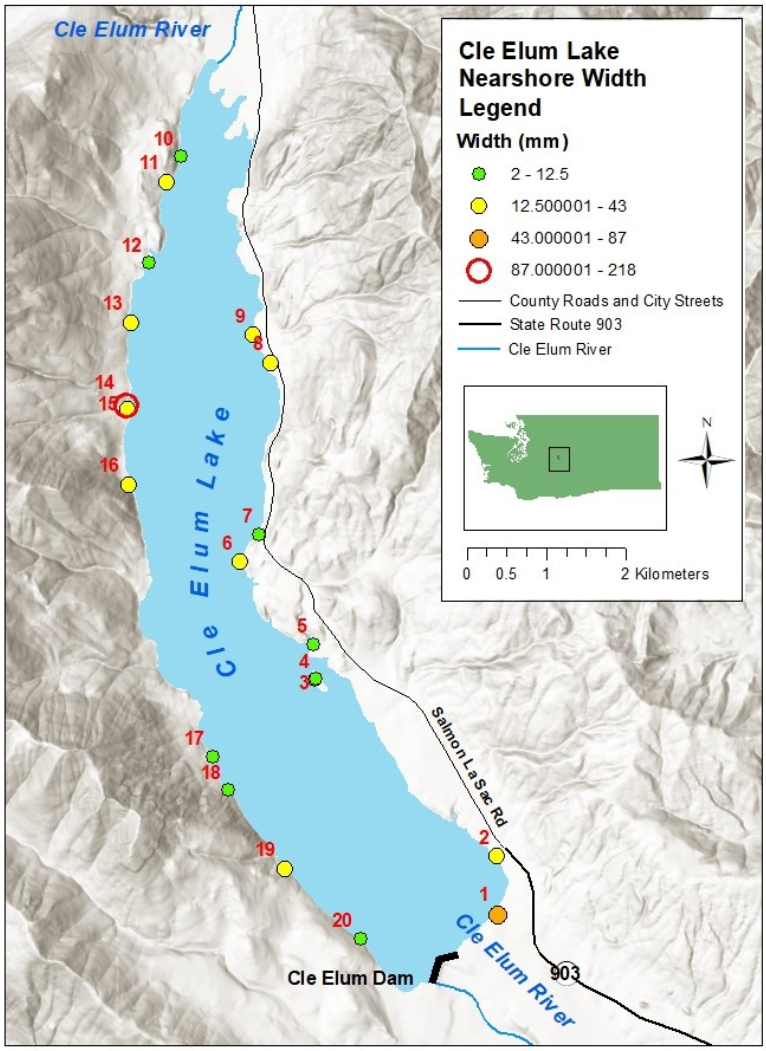

Figure 31: Cle Elum Lake nearshore widths (ESRI 2006, 2015; USGS 2016; WADOT 2020).

Foreshore slopes measured at the study slopes are primarily intermediate followed by low (Figure 32). Seventeen sites around the lakeshore have intermediate foreshore slopes between 11° and 36°. They are distributed around the lakeshore. Three sites along the eastern and southeastern shoreline have low foreshore slopes between 0° and 10°. These field measurements reflect the slope intervals mapped in the lake basin as a whole, which are overwhelmingly low or intermediate.

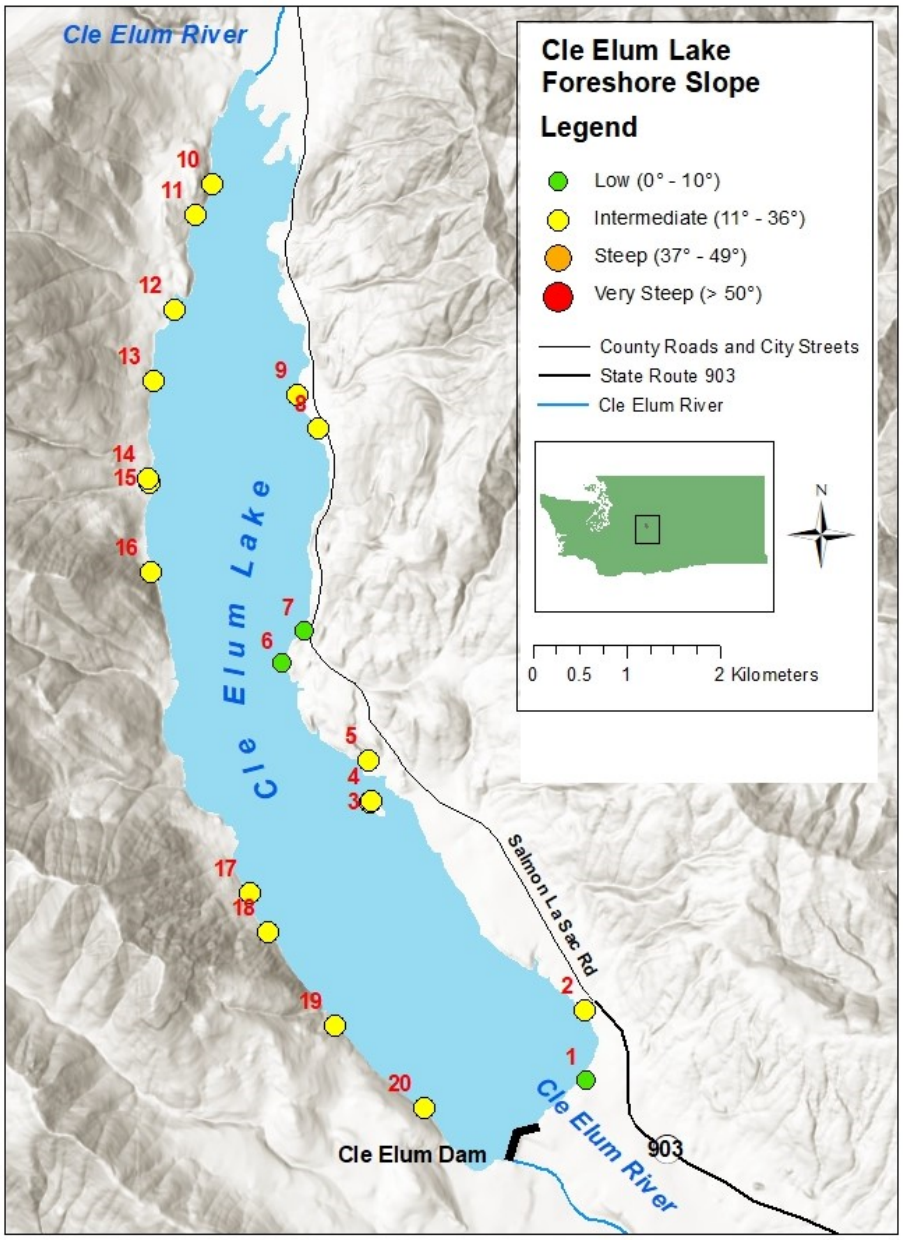

Figure 32: Cle Elum Lake foreshore slopes (ESRI 2006, 2015; USGS 2016; WADOT 2020).

Low and intermediate slopes also characterize study site nearshore zones (Figure 33). Twelve study sites around the lake have low nearshore slopes between 0° and 10. Six of these are clustered in the northwestern corner of the lake while two are found in the southeastern corner of the lake. Eight sites, which are largely in the southwestern corner

of the lake and along the eastern shoreline, have intermediate nearshore slopes between 11° and 36°.

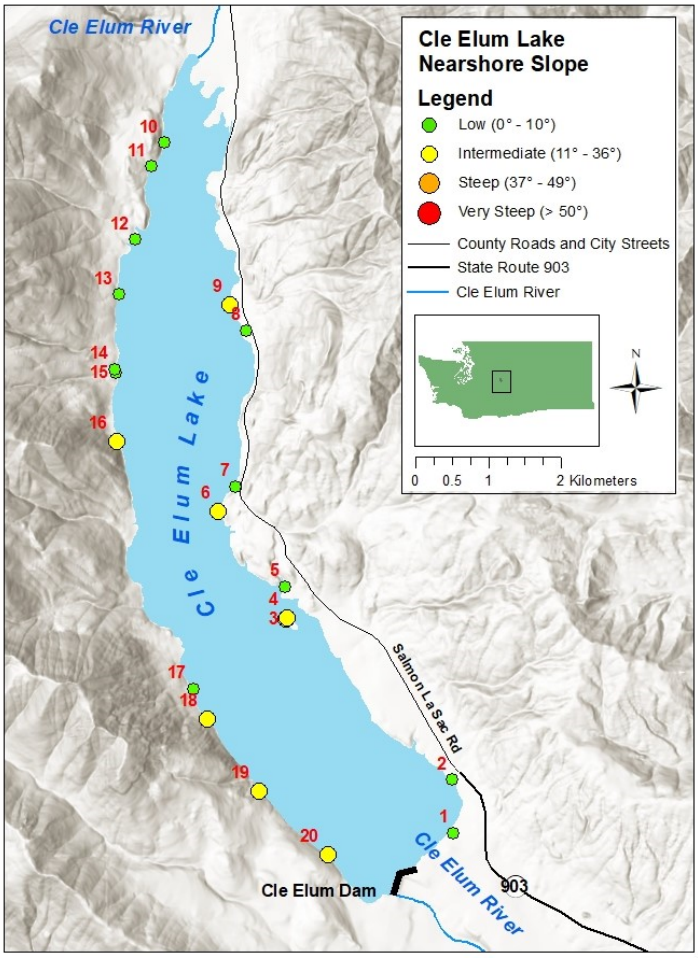

Figure 33: Cle Elum Lake nearshore slopes (ESRI 2006, 2015; USGS 2016; WADOT 2020).

Study site sediment textures (Appendix E) are most commonly silt loam interspersed with gravel, reflecting a lack of sorting or bedding (Figure 34). The sieve and Mastersizer analysis indicated that silt loam interspersed with gravel characterized twelve of the study sites around the lakeshore. Of the remainder of the sites, six were also interspersed with gravel. Many of these sites were interpreted to be mantled in glacial drift and Quaternary alluvium. These may erode less quickly than sandy bluffs (Davis, Fingleton, and Pritchett 1975; Buckler and Winters 1983).

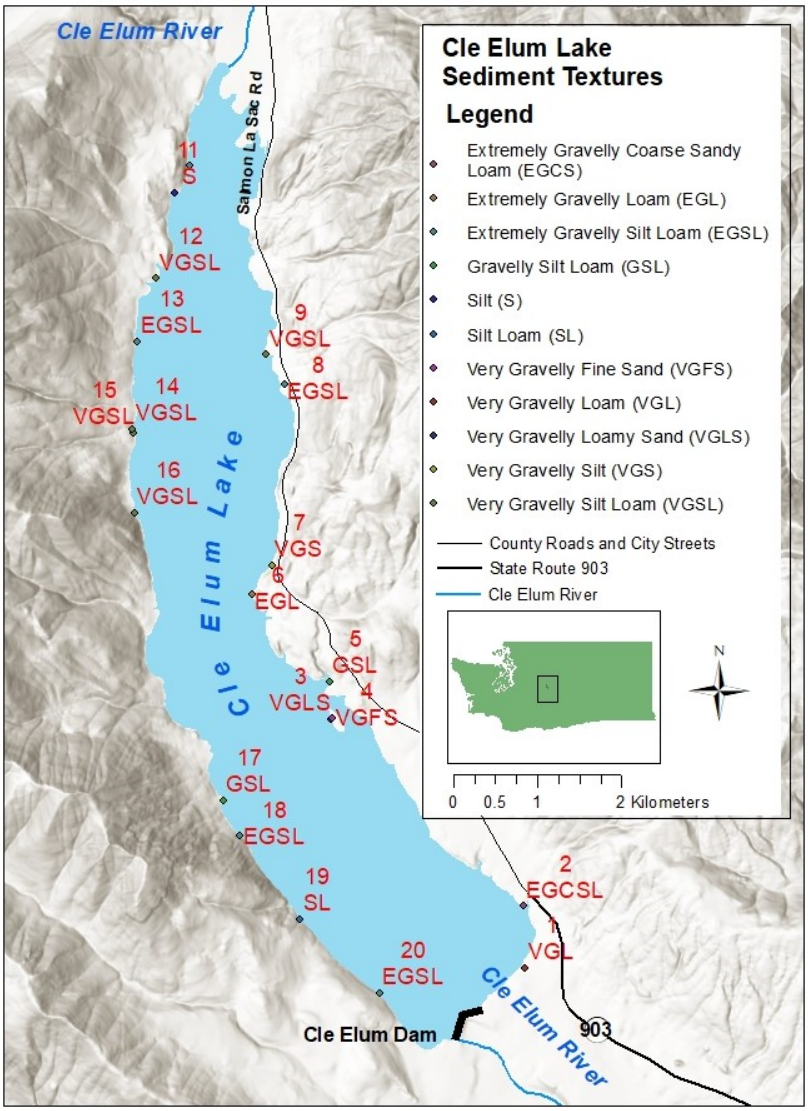

Figure 34: Cle Elum Lake sediment textures (ESRI 2006, 2015; USGS 2016; WADOT 2020).

Bluff heights at the study sites are generally low (Figure 35). Relatively low bluff heights between 3.6 m and 6.4 m are found around much of the basin, particularly along the southern half of the lakeshore. Six study sites around the lakeshore have bluffs heights 3.6 m or lower, while ten have bluff heights between 3.600001 m and 6.4 m. Just two sites had bluffs higher than 6.4 m. Two sites lack bluffs. The frequency of lower bluffs among these erosional sites suggests that a lack of talus may render them more susceptible to erosion (Sunamura 1983).

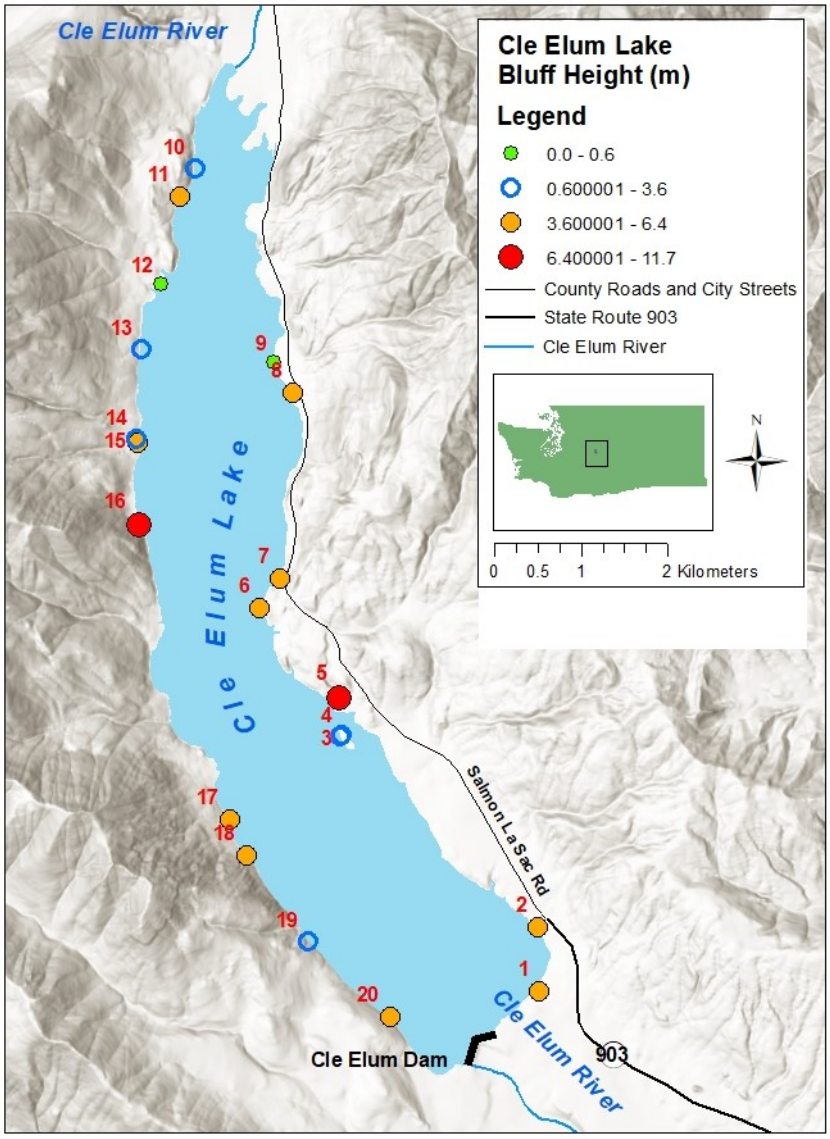

Figure 35: Cle Elum Lake bluff heights (ESRI 2006, 2015; USGS 2016; WADOT 2020).

Variables in Shoreline Erosion

For the near-term shoreline inventory that excludes cliffs from the erosional shoreline segments, a statistically significant relationship of small strength exists between geologic unit and shoreline type**,** $\chi 2$ (DF=8, n = 286) = 22.95, P = 0.0034, ϕ_{Cramer} = 0.283 (Table 9). In this inventory, a statistically significant relationship of small strength exists between slope interval and shoreline type, $\chi 2$ (DF=3, n = 268) = 10.58, P = 0.0142,

ϕ_{Cramer} = 0.199**.** For the second shoreline inventory that included cliffs as erosional segments, significant relationships were also seen between the potential erosion variables and shoreline type. A significant relationship of medium strength exists between geologic unit and shoreline type, $\chi 2$ (DF=8, n = 311) = 41.06, P < 0.0001, ϕ_{Cramer} = 0.365 (Table 10). When cliffs are included as erosion indicators, there is a significant relationship of small strength between slope interval and shoreline type, $\chi 2$ (DF=3, n = 292) = 14.18, P = .0027 ϕ_{Cramer} = 0.220 (Cohen 1988). The results of this test between all of the other variables and shoreline type in both inventories produced overall $\chi 2$ values less than the critical values of $\chi 2$ with the relevant degrees of freedom. This indicated that fetch, planimetric shape, vegetation cover, and vegetation type are not related to erosional and depositional shorelines. Based on these results, I performed additional analysis of the chi-square ($\chi 2$) results to identify which geologic units and slope intervals contribute the most to the relationship between these variables and erosion in the near-term and long-term shoreline inventories.

Table 9: Significant Factors: near-term shoreline erosion.

Factor	*N*	$\chi 2$	*DF*	*P*	*V*
Fetch	47	2.78	2	0.2487	-
Geologic Unit	46	22.95*	8	0.0034	0.283
Planimetric Shape	49	2.36	2	0.3068	-
Slope Interval	43	10.58*	3	0.0142	0.199
Vegetation Cover	46	1.46	3	0.6925	-
Vegetation Type	46	2.56	5	0.7670	-

Note. *indicates significant results. *N* Total observed cases of erosional segments; $\chi 2$ Chi-Square; *P = 0.05*; *DF* Degrees of freedom; *P* Chi-Square probability; *V* Cramer's V

Table 10: Significant Factors: long-term shoreline erosion.

Factor	*N*	*χ2*	*DF*	*P*	*V*
Fetch	73	4.97	2	0.0833	0.126
Geologic Unit	71	41.06*	8	< 0.0001	0.365
Planimetric Shape	73	0.40	2	0.8187	0.036
Slope Interval	67	14.18*	3	0.0027	0.220
Vegetation Cover	71	3.35	3	0.3408	0.104
Vegetation Type	71	1.60	5	0.9015	0.072

Note. *indicates significant results. *N* Total observed cases of erosional segments; *χ2* Chi-Square; *P = 0.05*; *DF* Degrees of freedom; *P* Chi-Square probability; *V* Cramer's V

Variables in Near-Term Erosion

In the near-term shoreline inventory (Tables 11 and 12), the middle member of the Roslyn Formation sandstone (Ec(2rm)) is the most significant geologic unit associated with bluff erosion. It contributes the largest share of the total *χ2* value (30.2 percent). In addition, the observed number of bluffs composed of this unit compared to the expected frequency is the greatest according to the chi-square analysis. This is likely due to the presence of this unit along the southwest lakeshore where there are a number of bluffs (Tabor et al. 2000). The chi-square analysis found that there were fewer bluffs composed of the other units than expected.

Table 11: Intersections of shoreline segments and geologic units: near-term shoreline erosion.

Geologic Unit	Shoreline Segment	Length (m)	Count	Percentage
Ec(1s)	Erosional	331.9	3	7.2%
Ec(2rm)	Erosional	568.6	6	12.4%
Eib	Erosional	90.5	1	2.0%
Eva(ss)	Erosional	13.1	0	0.3%
Evb(t)	Erosional	316	3	6.9%
Qa	Erosional	188.7	2	4.1%
Qad(e)	Erosional	381.7	4	8.3%
Qls(m)	Erosional	25.7	0	0.6%
wtr	Erosional	2667.9	27	58.2%

Table 12: Geologic units associated with erosion: near-term shoreline erosion.

Factor	*O*	*E*	*Class %*	*χ2*
Ec(1s)	3	7.72	19.1%	2.89
Ec(2rm)	6	2.57	30.2%	4.56
Eib	1	0.97	0.0%	0.00
Eva(ss)	0	1.13	7.5%	1.13
Evb(t)	3	5.47	7.3%	1.11
Qa	2	4.02	6.7%	1.02
Qad(e)	4	6.59	6.7%	1.02
Qls(m)	0	0.97	6.4%	0.97

Note. O Observed count of 100 m erosional shoreline segments. *E* Expected count.

In the near-term erosion inventory, intermediate slopes (11° - 36°) appear to be the most important slope interval related to bluff erosion. They contribute 15.6 percent of the overall *χ2* value (Tables 13 and 14). Although this is only the third highest contribution, intermediate slopes are the class with the greatest number of observed erosional bluffs compared to their expected frequency. Intermediate slopes are the most prominent slope interval around the lake basin with the exception of the southeastern shoreline. After this, steep slopes (37° - 49°) contribute 15.9 percent of the overall *χ2* value. However, there were only slightly more erosional bluffs than expected along steep shoreline segments. Steep slopes coincide with bluffs on the southwestern shoreline and to a smaller extent on the other parts of the lakeshore.

Table 13: Intersections of shoreline segments and slope intervals: near-term shoreline erosion.

Slope Interval	Shoreline Segment	Length (m)	Count	Percentage
Low	Erosional	909.2	9	20.8%
Intermediate	Erosional	3048.2	30	69.9%
Steep	Erosional	327.7	3	7.5%
Very Steep	Erosional	75.9	1	1.7%

Table 14: Slope intervals associated with erosion: near-term shoreline erosion.

Factor	*O*	*E*	*Class %*	*χ2*
Low	9	17.49	38.9%	4.12
Intermediate	30	23.75	15.6%	1.65
Steep	3	1.44	15.9%	1.68
Very Steep	1	0.32	13.6%	1.44

Note. O Observed count of 100 m erosional shoreline segments. *E* Expected count.

Variables in Long-Term Erosion

In the long-term shoreline erosion inventory, the relationship between geologic unit and erosional shorelines is largely due to a strong overlap between erosional shorelines and intrusive diabase, gabbro, and basalt (Eib). This contributes 45.1 percent of the total *χ2* value excluding intersections between shoreline segments and units coded as open water in the geologic unit layer (Tables 15 and 16). This is more than five times the contribution of any other geologic unit. Again, more cliffs and bluffs were observed within this geologic unit than expected statistically. These coincide with an occurrence of these intrusive igneous rocks along the northwest corner of the lake, which is the longest bedrock cliff mapped in the shoreline inventory (Huggett 2007). Next, the Roslyn

Table 15: Intersections of shoreline segments and geologic units: long-term shoreline erosion.

Geologic Unit	Shoreline Segment	Length (m)	Count	Percentage
Ec(1s)	Erosional	817.6	8	21.6%
Ec(2rm)	Erosional	568.6	6	15.0%
Eib	Erosional	1177.3	12	31.1%
Eva(ss)	Erosional	13.1	0	0.3%
Evb(t)	Erosional	585.6	6	15.5%
Qa	Erosional	188.7	2	5.0%
Qad(e)	Erosional	409.7	4	10.8%
Qls(m)	Erosional	25.7	0	0.7%
wtr	Erosional	3336.5	33	88.1%

Table 16: Geologic units associated with erosion: long-term shoreline erosion.

Factor	*O*	*E*	*Class %*	$\chi 2$
Ec(1s)	8	12.1	3.7%	1.39
Ec(2rm)	6	3.65	4.0%	1.51
Eib	12	3.88	45.1%	16.98
Eva(ss)	0	1.60	4.3%	1.60
Evb(t)	6	8.45	1.9%	0.71
Qa	2	5.71	6.4%	2.41
Qad(e)	4	9.36	8.2%	3.07
Qls(m)	0	1.37	3.6%	1.37

Note. O Observed count of 100 m erosional shoreline segments. *E* Expected count.

Formation sandstone (Ec(2rm)) contributes 4 % of the total $\chi 2$ value. This is the fourth highest share. However, it is the only other unit with more observed bluffs than expected.

In the long-term shoreline inventory, intermediate slopes again have the most important relationship with shoreline erosion. They make the third highest contribution to the $\chi 2$ value (10.9 percent) but their observed frequency relative to the expected amount was the greatest (Tables 17 and 18). Steep slopes are the class making the greatest contribution to the overall $\chi 2$ value (27 percent), although their incidence compared to their expected frequency in erosional areas was less than intermediate slopes.

Table 17: Intersections of shoreline segments and slope intervals: long-term shoreline erosion.

Slope Interval	Shoreline Segment	Length (m)	Count	Percentage
Low	Erosional	1534.6	15	22.6%
Intermediate	Erosional	4473.2	45	65.9%
Steep	Erosional	638.6	6	9.4%
Very Steep	Erosional	139.5	1	2.1%

Table 18: Slope intervals associated with erosion: long-term shoreline erosion.

Factor	*O*	*E*	*Class %*	$\chi 2$
Low	15	26.39	34.6%	4.91
Intermediate	45	37.4	10.9%	1.54
Steep	6	2.75	27.0%	3.83
Very Steep	1	0.46	4.5%	0.64

Note. O Observed count of 100 m erosional shoreline segments. *E* Expected count.

Relationships Between Significant Variables and the Spatial Distribution of Shoreline Erosion

Based on several factors, I initially anticipated that the greatest degree of bluff erosion is on the eastern and southeastern shoreline. The factors first considered included the importance of fetch as a predictor of wave energy in lakes, wave energy dispersal due to planimetric shape, and slope interval (Yasso 1965; Gracia 1995; O'Halloran and Spennemann 2002). The maximum fetch distance is in the southern part of the lake (Figure 36). A prominent headland potentially subject to higher wave energy is located near Bell Creek on the eastern shoreline (Figure 37) (Yasso 1965). Finally, parts of the eastern shoreline have intermediate slopes that may generate plunging waves causing erosion (O'Halloran and Spennemann 2002; Lieberman and Grabowski 2007).

After mapping shoreline erosion, I determined that a high degree of near-term bluff erosion is in the southeastern quadrant and at the intersection between the southeastern and northeastern quadrants. A correspondingly high concentration of depositional segments are located along the southwestern shoreline. I also found that most of the long-term erosional segments are on the northwestern shoreline. Although not initially anticipated, this result makes sense given the high concentration of cliffs in the northwest part of the lake and bluffs in the southeast quadrant.

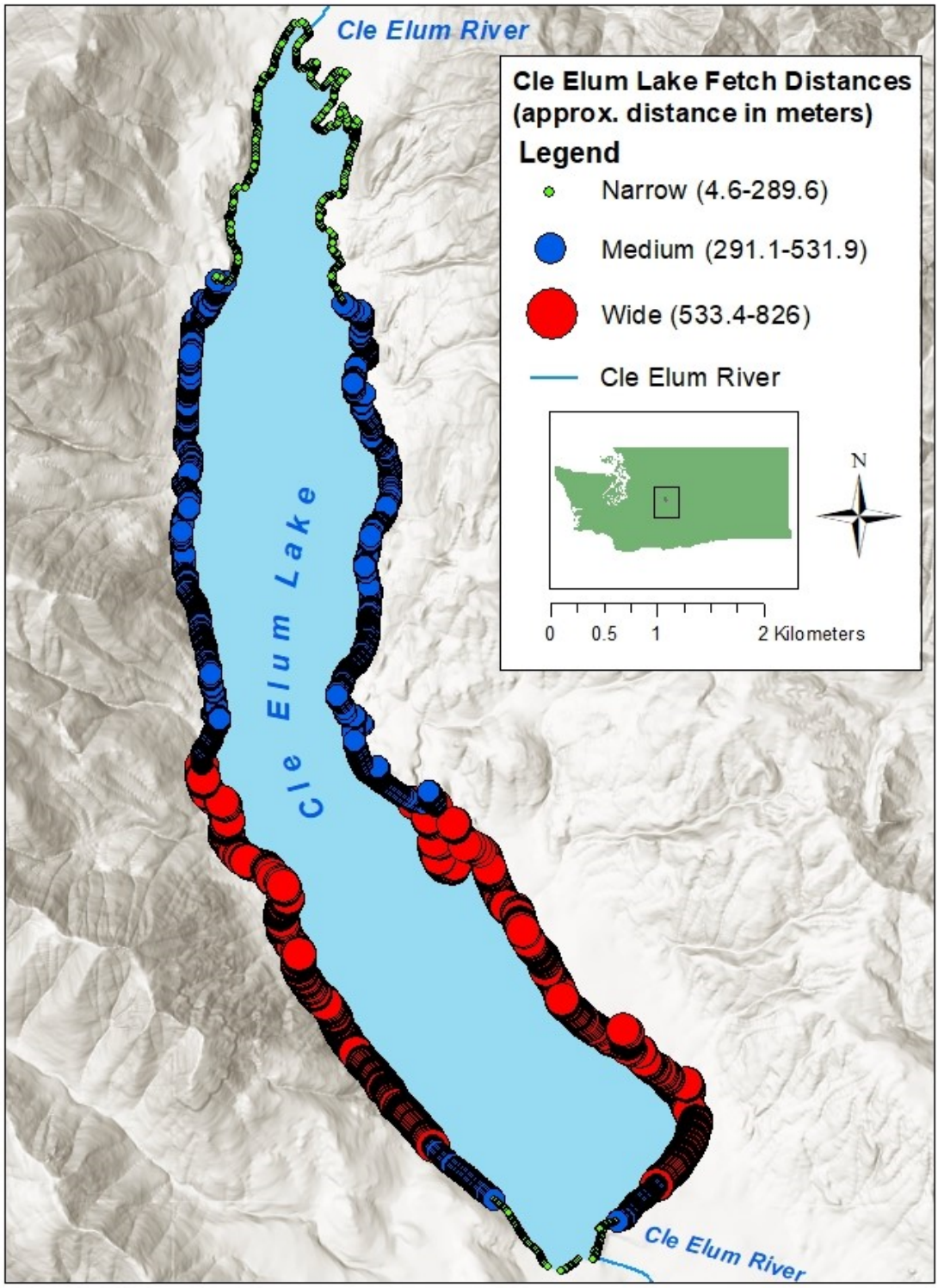

Figure 36: Cle Elum Lake fetch distances (ESRI 2006, 2015; USGS 2016).

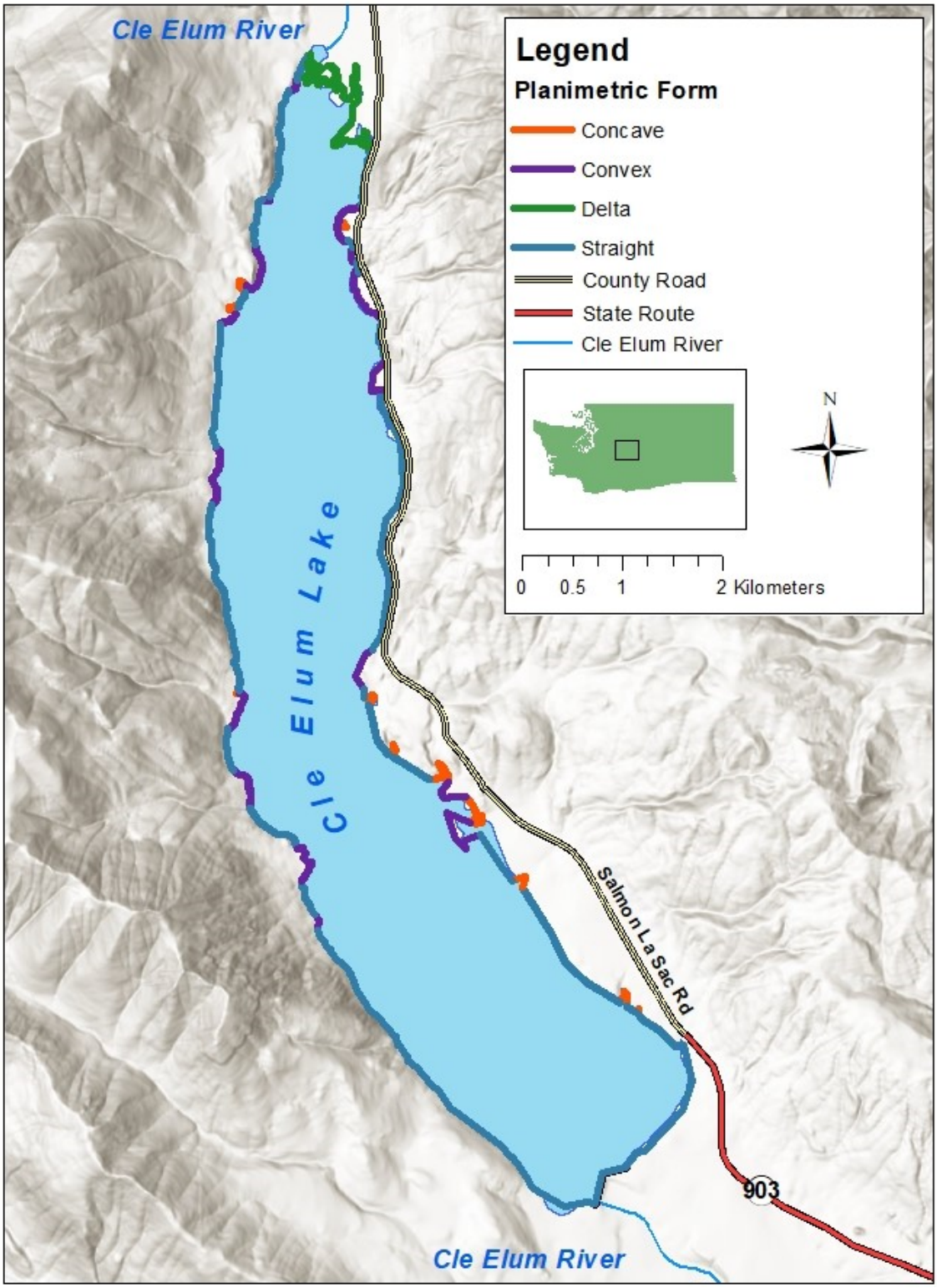

Figure 37: Cle Elum Lake Shoreline planimetric form (ESRI 2006; USGS 2016; ESRI 2015; WADOT 2020).

However, the statistical analysis of the relationships between the proposed risk factors and shoreline type belies the expectation that this spatial distribution is due to the factors I first considered. The importance of lithology in shoreline erosion is due to different geologic units in the two inventories. In the near-term shoreline inventory, extensive sandstone substrates appear to be responsible for the largest share of the relationship between geologic unit and shoreline erosion. This is a surprising result since I anticipated that even weakly lithified sandstone would be more resistant to erosion than unconsolidated sediment (Stanford and Hauer 1992; USGS 2004; Davidson-Arnott 2010). In contrast, the intrusive igneous cliffs along the northwestern shoreline contribute the most to the relationship between shoreline erosion and geologic units when cliffs are included as erosional segments in the long-term erosion layer (Huggett 2007). This is a less surprising result given the length of this unit relative to the total shoreline.

In both inventories, intermediate and steep slopes also appear to have the strongest relationship with shoreline erosion. This is not surprising since the literature review identified intermediate slopes as promoting plunging waves leading to high erosion rates (O'Halloran and Spennemann 2002). Fetch, planimetric shape, vegetation cover, and vegetation type do not appear to be causal factors for bluff erosion at Cle Elum Lake. Overall, the consistent role of geologic units in shoreline erosion for both the near-term and long-term shoreline inventories matches the results of some other studies that emphasize the importance of shoreline substrates in determining the spatial distribution of shoreline erosion (USGS 2004).

Erosion Susceptibility and Hazard Maps

From the results of the GIS model, I produced hazard maps and further analyzed the results. To visualize shoreline erosion susceptibility and query the results for meaningful relationships, I classed the GMM output. Natural breaks rounded to the nearest whole number formed five levels of susceptibility based on the percentage of area within each combination of variables susceptible to erosion (Tables 19 and 20) (Jiménez-Perálvarez et al. 2009). This made it possible to determine the spatial distribution of erosion susceptibility levels.

Table 19: Susceptibility levels: near-term shoreline erosion

Susceptibility Level	Percentage Susceptible to Erosion
Very Low (1)	0% to 3%.
Low (2)	3% to 13%.
Moderate (3)	13% to 30%.
High (4)	30% to 61%.
Very High (5)	61% to 100%.

Table 20: Susceptibility levels: long-term shoreline erosion

Susceptibility Level	Percentage Susceptible to Erosion
Very Low (1)	0% to 9%.
Low (2)	9% to 25%.
Moderate (3)	25% to 48%.
High (4)	48% to 75%.
Very High (5)	75% to 100%.

Near-Term Erosion Susceptibility

For the near-term shoreline model, the areas with the highest erosion susceptibility are limited to a relatively small portion of the lakeshore (Figure 38). Areas with very low and low erosion susceptibility represent 87.3 percent of the study area matrix, which also includes areas adjacent to the shoreline. When I added moderately

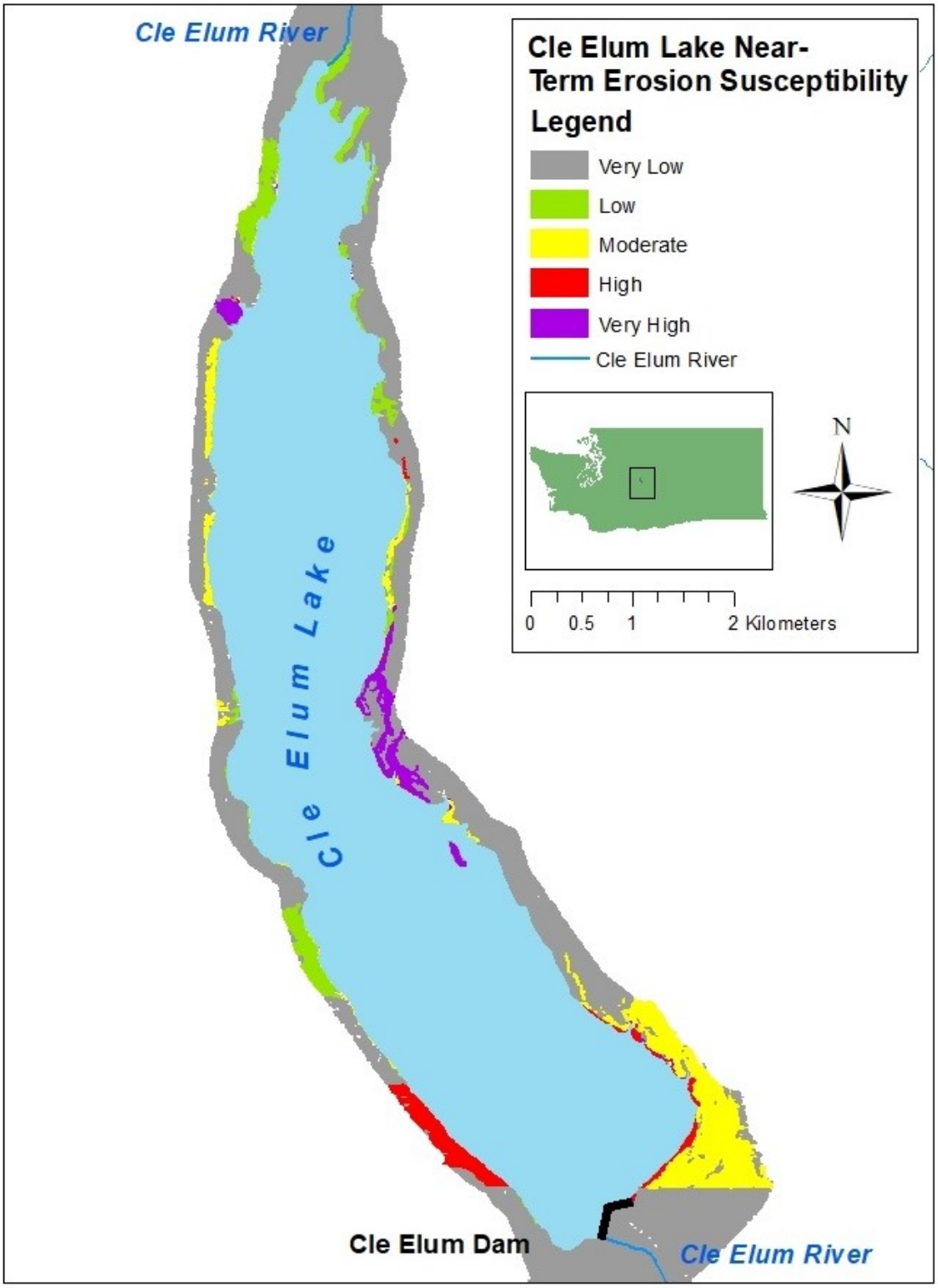

Figure 38: Cle Elum Lake near-term erosion susceptibility (ESRI 2006; USGS 2016; ESRI 2015; WADOT 2020).

areas to this, the parts of the lakeshore that are not highly susceptible to erosion rises to 94.7 percent. The areas classified as within the two highest susceptibility classes covered 5.3 percent of the area analyzed.

As with the spatial distribution of erosional segments, I anticipated that the GIS erosion susceptibility analysis would determine that the eastern and southeastern shorelines are at the greatest risk of future erosion since past erosion indicates the course of future shoreline recession (Adamo et al. 2014). Again, the results of both susceptibility models confirmed initial expectations. In the near-term erosion susceptibility analysis, highly susceptible areas are particularly prevalent along the southeastern shoreline, where 59.58 percent of the areas in the top two susceptibility classes are located. The second highest concentration of highly susceptible areas is the southwestern shoreline with 32.46 percent of the high or very high-risk areas. Although the highest two susceptibility levels represent a relatively small part of the lakeshore, the area at high risk was almost twice as large as the area at very high risk, at 3.5 percent and 1.8 percent respectively.

Within the two highest susceptibility levels, were a variety of geologic units in combination (Table 21) with the slope intervals previously identified with shoreline

Table 21: High susceptibility level variable combinations: near-term shoreline erosion.

Susceptibility	Geologic Unit	Slope
High	Ec(1s) - continental sedimentary rocks (Swauk Formation)	Low
High	Ec(2rm) - continental sedimentary rocks (Roslyn Formation, middle	Intermediate
High	Evb(t) – basalt flows (Teanaway Basalt)	Steep
High	Qad(e) - alpine glacial drift, Fraser-age (Evans Creek Drift)	Intermediate
High	Wtr – water	Intermediate
High	Wtr – water	Low
Very High	Ec(1s) - continental sedimentary rocks (Swauk Formation)	Low
Very High	Eib - basic intrusive rocks	Intermediate
Very High	Qa - alluvium	Intermediate
Very High	Qad(e) - alpine glacial drift, Fraser-age (Evans Creek Drift)	Intermediate
Very High	Qad(e) - alpine glacial drift, Fraser-age (Evans Creek Drift)	Low
Very High	Wtr – water	Intermediate
Very High	Wtr – water	Low
Very High	Wtr – water	Steep

erosion. In the highly susceptible areas, low slopes coincide with the Swauk Formation. Intermediate slopes are associated with intrusive igneous rocks (diabase, gabbro, and basalt), the middle member of the Roslyn Formation, Quaternary alluvium, and Evans Creek alpine glacial. Quaternary alluvium coincides with a highly susceptible area between Bell and Morgan creeks. These are among the geologic units most susceptible to shoreline erosion (USGS 2004). Finally, there is a tie between steep slopes and the Teanaway Formation in terms of erosion susceptibility.

Long-Term Erosion Susceptibility

Areas at the highest risk of shoreline erosion are even more limited according to the long-term erosion model (Figure 39). The areas at the two lowest susceptibility levels include 91.3 percent of the study area matrix and 97.2 percent including moderately susceptible areas. The two highest susceptibility classes only account for 2.8 percent of the study area. Again, the part of the lakeshore with the greatest concentration of highly and very highly susceptible areas is the southeastern shoreline with 54.5 percent of the area in the top two risk categories. In this model, however, the second most susceptible area is the northwestern shoreline with 20.1 percent at high risk of erosion. Again, this is likely attributable to the extensive tonalite exposure in the northwestern corner of the lake. In this case, the area at high risk is more than three times the size of the area at very high risk.

There are some similarities and differences with the near-term erosion model regarding the combinations of geologic units and slope intervals associated with high erosion susceptibility. Both models identify the Swauk Formation combined with low

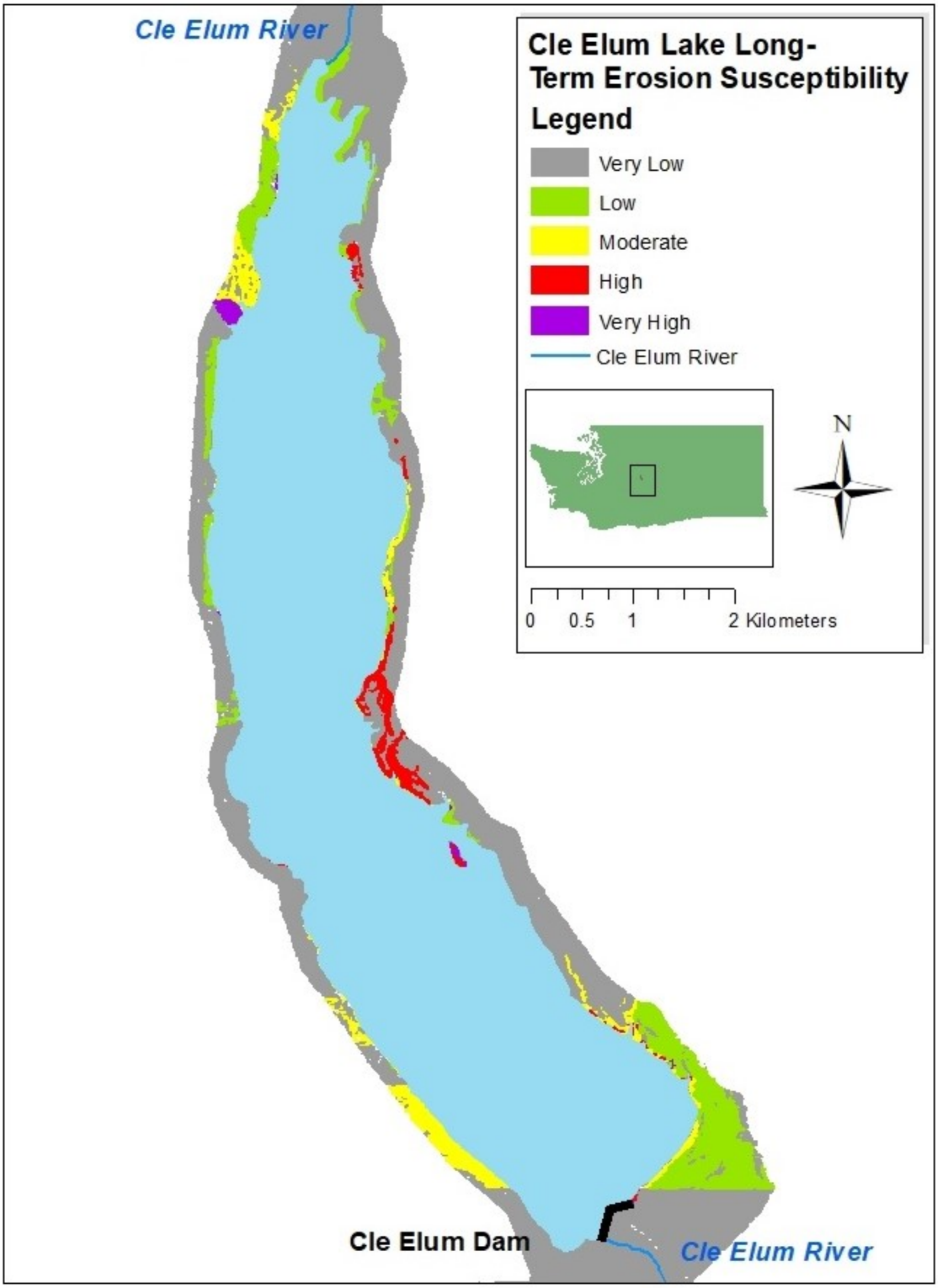

Figure 39: Cle Elum Lake long-term erosion susceptibility (ESRI 2006; USGS 2016; ESRI 2015; WADOT 2020).

slopes (Table 22). They also identify intrusive igneous rocks (diabase, gabbro, and basalt), Quaternary alluvium, and Evans Creek alpine glacial drift combined with intermediate slopes as highly susceptible to erosion. However, this model determined that highly susceptible areas including the Teanaway Formation in combination with low rather than steep slopes, the Swauk Formation with intermediate rather than low slopes, and diabase, gabbro, and basalt with low rather than intermediate slopes. It also classes the Evans Creek drift and low slopes as highly susceptible to erosion.

Table 22: High susceptibility level variable combinations: long-term shoreline erosion.

Susceptibility	Geologic Unit	Slope
High	Evb(t) – basalt flows (Teanaway Basalt)	Low
High	Qa - alluvium	Intermediate
High	Qad(e) - alpine glacial drift, Fraser-age (Evans Creek Drift)	Intermediate
High	Qad(e) - alpine glacial drift, Fraser-age (Evans Creek Drift)	Low
High	Wtr – water	Intermediate
High	Wtr – water	Low
Very High	Ec(1s) - continental sedimentary rocks (Swauk Formation)	Intermediate
Very High	Ec(1s) - continental sedimentary rocks (Swauk Formation)	Low
Very High	Eib - basic intrusive rocks	Intermediate
Very High	Eib - basic intrusive rocks	Low
Very High	Qad(e) - alpine glacial drift, Fraser-age (Evans Creek Drift)	Intermediate
Very High	Qad(e) - alpine glacial drift, Fraser-age (Evans Creek Drift)	Low
Very High	Wtr – water	Intermediate
Very High	Wtr – water	Steep

Risk Factors Associated with Erosion Susceptibility

Additional chi-square and Cramér's V analysis of the GMM output revealed unexpected relationships between the initial set of proposed risk factors and erosion susceptibility. Although the initial statistical analysis only found relationships between geologic unit, slope, and shoreline type, this analysis found a relationship between five of the proposed erosion variables and the susceptibility levels determined by the near-term and long-term erosion models. For the near- term erosion inventory, a statistically

significant relationship appears between the susceptibility levels and fetch, geologic unit, slope interval, vegetation cover, and vegetation type (Table 23). Again, geologic units stood out with a large relationship to erosion susceptibility. Medium relationships were detected between susceptibility level, fetch, and vegetation type. A small relationship was determined for slope interval and vegetation cover. Because the planimetric shape layer was a polyline and the susceptibility matrix output were polygons, I was not able to perform the retrospective analysis for this variable.

Table 23: Relationship between variables and erosion susceptibility: near-term shoreline erosion.

Factor	*N*	*χ2*	*DF*	*P*	*V*
Fetch	89875	8891.45*	8	< 0.0001	0.222
Geologic Unit	189618	80337.87*	44	< 0.0001	0.325
Slope Interval	180632	13559.582*	12	< 0.0001	0.155
Vegetation Cover	138541	10846.49*	12	< 0.0001	0.162
Vegetation Type	189625	15526.5*	20	< 0.0001	0.143

Note. *indicates significant results. *N* Total observed cases of 100 m^2 area represented by each variable with each susceptibility class; *χ2* Chi-Square; *P = 0.5*; *DF* Degrees of freedom; *P* Chi-Square probability; *V* Cramer's V

Additionally, this analysis revealed four relationships of at least medium strength between the shoreline erosion factors and the long-term erosion susceptibility results (Table 24). Again, there was a significant relationship detected between susceptibility level and all of the GIS variables (except planimetric form). Of these, it detected a medium relationship for geologic unit, fetch, slope interval, and vegetation type. Only vegetation cover had a small relationship to susceptibility level.

I re-ran the near-term erosion GMM model with all of the variables and examined the results. Many combinations of variable classes are associated with the top two highest susceptibility levels. It appears that while there are not individual statistical relationships

Table 24: Relationship between variables and erosion susceptibility: long-term shoreline erosion.

Factor	*N*	*χ2*	*DF*	*P*	*V*
Fetch	89876	14825.13*	8	< 0.0001	0.287
Geologic Unit	189619	53706.73*	44	< 0.0001	0.266
Slope Interval	187884	16773.336*	12	< 0.0001	0.172
Vegetation Cover	138539	11679.07*	12	< 0.0001	0.168
Vegetation Type	189625	15695.68*	20	< 0.0001	0.144

Note. *indicates significant results. *N* Total observed cases of 100 m^2 area represented by each variable with each susceptibility class; *χ2* Chi-Square; *P = 0.5*; *DF* Degrees of freedom; *P* Chi-Square probability; *V* Cramer's V

between shoreline type and fetch, vegetation cover, and vegetation type, there are relationships between various combinations of these factors along with geologic units and slope interval. One possible explanation for this is that these conditions reflect erosion. Therefore, they may not be causal factors but are useful as indicators of future erosion.

GIS Matrix Model Efficacy and Applicability

In general, the GIS Matrix Model restricts the areas at high susceptibility for adverse events to those areas existing within the combinations of variables associated with them (Jiménez-Perálvarez et al. 2009). This was also the case in this study as both models limited the area in the highest two susceptibility classes to less than 6 percent of the study area matrix. However, the near-term shoreline inventory only included a total of 28.5 km of erosional shoreline segments while the long-term layer included 31.1 km. As a result, the long-term erosion model calculated a larger spatial extent of past shoreline erosion within the areas representing each possible combination of risk factors. This produced a larger numerator when the susceptibility matrix was calculated.

There are two practical implications for the use of this model for erosion susceptibility analysis. First, resource managers may only be interested in erosion

occurring over a few years as opposed to a period of centuries. Second, they may be interested in an estimate of future erosion that is less conservative than that produced by the long-term erosion model.

Implications for Management Recommendations

Based on these all of these results, it is possible to characterize near-term erosion in those areas most susceptible to shoreline recession. Erosional segments around the lakeshore are likely to have an underlying sandstone lithology, making them moderately resistant to erosion. Sediment sizes are relatively large (median = 59.2 mm), which is typical of erosional portions of littoral cells (Jacobsen and Schwartz 1981). Sites along the southeastern shoreline feature grain sizes between about 28 mm and 41 mm (ranging between coarse and very coarse pebbles) while sites along the southwestern shoreline feature grain sizes ranging between about 93 mm and 132 mm (ranging between small and large cobbles). Sediment textures are largely gravelly silt loams, although silt loams, gravelly loams and sands, and sandy loams occur along the southeastern and southwestern shorelines. Silts are subject to wave erosion (Stanford and Hauer 1992). Nearshore widths (median = 20 m) including those along the southeastern and southwestern nearshores are mainly under 43 m. This, along with large median grain sizes are typical of reflective shorelines (Lorang et al. 1993).

As a glacial lake, Cle Elum Lake's shoreline topography is gentle with most slopes below 36° (mean = 27.4% or 15.32°) (USBOR and WADOE 2015). Intermediate slopes appear to make the greatest contribution to the relationship between slope angle and shoreline erosion followed by steep slopes. Unsurprisingly, intermediate foreshore slopes characterize all but one erosional site along the southeastern and southwestern

shorelines. Erosional sites have low and intermediate nearshore slopes (median = 15% or 8.53°) in the southeastern and southwestern corners of the lake. Erosion at these sites may result from plunging waves, promoted by intermediate slope angles (O'Halloran and Spennemann 2002; Huggett 2007). Relatively low bluffs characterize most of the erosional sites and are mainly below 6.4 m in the southern half of the lake. These may be subject to additional erosion as they lack talus (Sunamura 1983).

The frequency and extensiveness of depositional segments and the presence of wetlands in this century-old reservoir may indicate that erosion rates have slowed over time, however, new high water levels following enlargement may increase the erosion rate once again (Lorang and Stanford 1993; Lorang, Komar, and Stanford 1993; USBOR and WADOE 2011; USBOR and WADOE 2015). Both near-term and long-term erosion is likely to be the most prevalent in the southeastern part of the lake. Due to this expected risk, I anticipate that there a number of archaeological sites vulnerable to erosion due to reservoir enlargement. On Cle Elum's eastern and southeastern shorelines, lithic caches at the greatest risk for erosion include isolated sites found in the varial zone near Speelyi Beach and Morgan Creek (Steinkraus et al. 2014). Another is a site spread across a headland and extending into the varial zone at Anna Bell North that includes multiple artifacts (Steinkraus et al. 2014; Google 2017).

The Bureau of Reclamation has installed shoreline protection structures at Speelyi Beach and rip-rap has been constructed along other parts of the shoreline such as Wish Poosh (USBOR and WADOE 2015). Rip-rap has also been constructed by homeowners (Figure 40) (Steinkraus et al. 2014). Managers should pay particular attention to parts of the eastern shoreline where rip-rap (Figure 41) does not exist (Forest 41) and shoreline

protection is not planned (Figure 42).

Figure 40: Rip-Rap near Speelyi Beach, Cle Elum Lake. Photograph by Michael Horner.

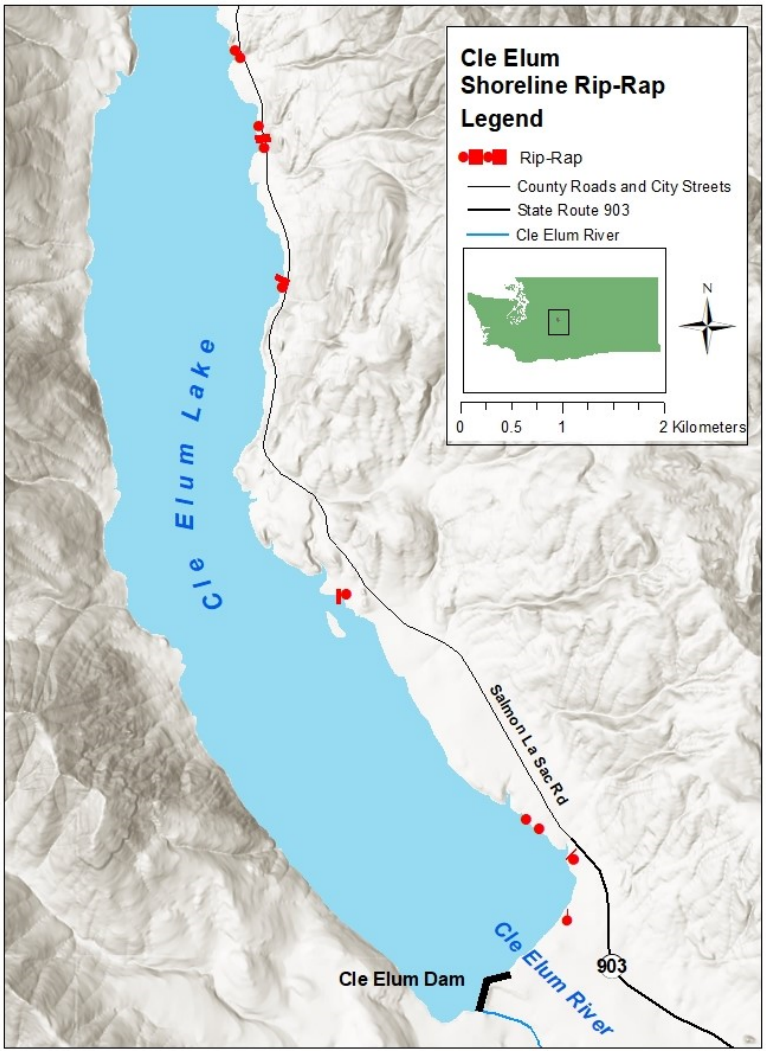

Figure 41: Cle Elum shoreline rip-rap (ESRI 2006, 2015; USGS 2016; WADOT 2020).

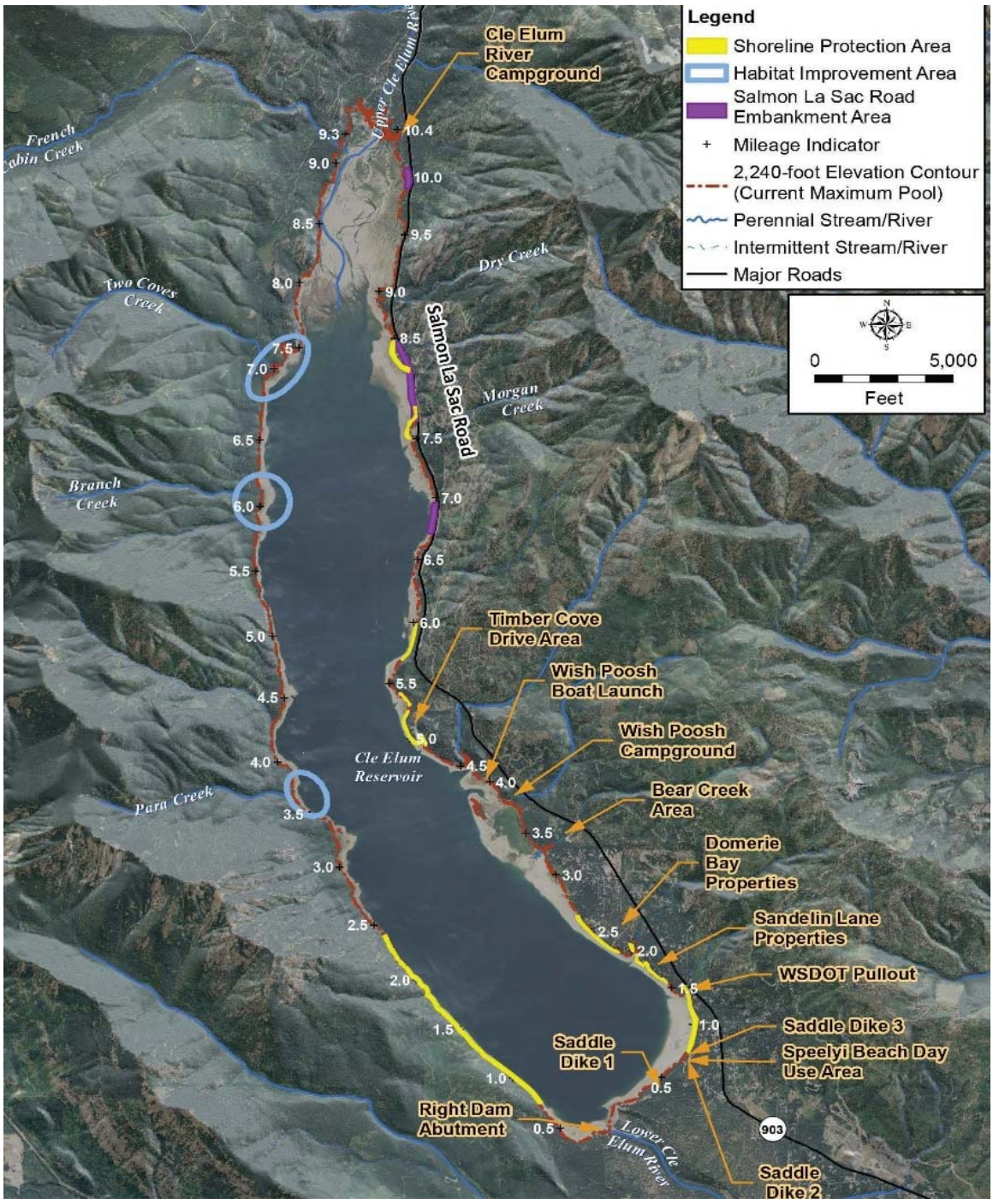

Figure 42: Cle Elum Lake reservoir expansion shoreline protection. Includes rockery walls, anchored logs, and perched beaches (BOR and WADOE 2015).

CHAPTER VI

CONCLUSIONS AND FURTHER RESEARCH

Conclusions

In this study, I determined potential risk to archaeological resources posed by shoreline erosion resulting from the expansion of Cle Elum Lake. Eighty erosional segments were mapped. The more rapidly occurring bluff erosion is concentrated along the eastern shoreline, particularly in the southeastern quadrant of the lake. Field measurements indicate that erosional sites reflect the morphodynamics of reflective shorelines. The sandstone-dominated middle member of the Roslyn Formation contributes the most to the association between geologic unit and near-term erosion. Intermediate and steep slopes make the greatest contribution to the tie between slope interval and erosion. These findings were used to model future erosion susceptibility, which indicates that the highest risk of bluff erosion largely exists along the southeastern and southwestern shorelines. Further analysis of the GMM results indicates that bluff erosion risk is tied to various combinations of all of the risk factors examined. Based on the shoreline segment mapping, statistical and GIS analysis, as well as fieldwork, it was possible to typify erosional areas along the Cle Elum lakeshore.

Near-term bluff erosion is likely to be the greatest concern to cultural and natural resource managers. The most important aspect of bluff erosion for their consideration is the spatial distribution of both past erosion and areas susceptible to future shoreline recession. Although bluff erosion occurs in all four quadrants of the lake basin, resource managers may be most interested in the eastern shoreline since it accounts for 68.5 percent of the total shoreline erosion, and in the southeastern shoreline in particular since

it accounts for the largest area susceptible to erosion. At the same time, this is the most developed part of the basin with access via Salmon La Sac Road and residential areas including Speelyi Beach, Sandelin Lane, Domerie Bay Road, and Timber Cove Drive (USBOR and WADOE 2015).

Management Recommendations

Background

To address the erosion of cultural resources in the margin of Cle Elum Lake, Reclamation requires a wide variety of management recommendations. One reason for this is that key stakeholders including the Yakama Nation may prefer inundation to the possible disturbance of archaeologic sites resulting from efforts to protect them (Lenihan et al. 1981; Ferri 2015). In addition, engineering solutions are costly (Brandt and Hassan 2000). Reclamation's plans for mitigating ongoing impacts to cultural resources will be announced in a Cultural Resources Management Plan (CRMP) no later than five years following the Record of Decision regarding the Cle Elum Pool Raise Project, which was issued 25 June 2015 (USBOR and WADOE 2015). Therefore, the CRMP is anticipated by June 2020. These management recommendations are intended to broaden the suite of engineering and non-engineering approaches included in the CRMP for managers to mitigate the impacts of shoreline erosion on cultural resources.

Reclamation's Preferred Alternative for Controlling Shoreline Erosion

The environmental impact statement (EIS) for the Cle Elum Pool Raise Project included four alternatives for increasing storage capacity and protecting the lakeshore from increased erosion (USBOR and WADOE 2015). The Record of Decision announced Reclamation's choice of its preferred alternative: "Additional Storage Capacity for

Instream Flow with Hybrid Shoreline Protection". As part of this alternative, general shoreline protection includes a variety of engineered approaches to control erosion (USBOR and WADOE 2015). Shoreline protection is intended for shoreline segments subject to additional recession due to the Cle Elum Pool Raise Project (USBOR and WADOE 2015).

Reclamation's Plans for Protecting Cultural Resources

In addition to these structural means to mitigate shoreline erosion are non-engineering measures to address the impact of reservoir enlargement on cultural resources (USBOR and WADOE 2015). Prior to the Pool Raise Project, Central Washington Anthropological Survey completed a survey of the Cle Elum Pool Raise Project's area of potential effect (Steinkraus et al. 2014; USBOR and WADOE 2015). Reclamation also performed additional surveys of the entire lakeshore to locate and record specific archaeological sites. This will inform mitigation steps included in the CRMP (USBOR and WADOE 2015).

In addition to the mitigation steps under development, Reclamation has already determined a number of measures for inclusion in the CRMP. Reclamation plans to survey the varial zone to study the impacts of fluctuations on sediment transport and subsequent impacts on cultural resources. This survey will improve Reclamation's knowledge of previously identified sites and add new sites to its inventory. From this, Reclamation plans to assess the eligibility of sites for inclusion in the National Register of Historic Places and for designation as traditional cultural properties. It will also consult with the Yakama Nation as well as the Umatilla and Colville tribes regarding Native

American sacred sites. Additional mitigation steps will be based on the survey and consultations (USBOR and WADOE 2015).

Management Recommendations: Engineering Approaches

The following are recommendations for potential inclusion in the CRMP to protect the expanded reservoir shoreline from erosion and stabilize archaeological sites. They build on and expand the options discussed in the EIS. The first engineering recommendation is to consider additional shoreline protection in addition to the areas proposed for erosion mitigation in the EIS, based on the shoreline survey and the near-term erosion susceptibility analysis. The EIS plans shoreline protection mainly along the southwestern shoreline followed by the southeastern and northeastern shorelines. In several instances, this expands upon existing rip-rap found along the southeastern and northeastern shorelines. However, 59.58 percent of the area classified in the highest two susceptibility categories is found on the southeastern shoreline, which has also has the highest concentration of erosional bluffs (44.2 percent). Here, 6.2 km of shoreline coincides with the areas assessed at the two highest erosion susceptibility levels. However, 0.7 km of rip-rap has already been constructed here. Therefore, a total of 5.5 km of shoreline protection should be planned along the southeastern shoreline.

In the southeastern portion of the lake, shoreline protection is planned for some areas at the highest risk of erosion while other locations require additional shoreline protection. In the far southeastern corner of the lake at Speelyi Beach, Sandelin Lane, and Domerie Bay Road, planned shoreline protection areas coincide with areas assessed as being in the highest two susceptibility categories. Residential development is notable in these areas. However, the largest area at the highest risk of future erosion is near Wish

Poosh campground and boat launch. Here, measures are planned to protect the parking lot and access road. However, this location does not appear as a shoreline protection area and no steps are planned to protect the areas most susceptible erosion particularly Picnic Island (Figure 43), the mouth of Newport Creek, and along the shoreline just north of this (USBOR and WADOE 2015).

The second recommendation is to apply bioengineered methods in additional areas subject to erosion. The EIS already includes the use of organic materials such as anchored logs and perched beaches. It notes that this would promote vegetation and improve littoral habitats by allowing for more natural hydrologic and geomorphic processes (USBOR and WADOE 2015). The east side of Picnic Island is one location where such approaches would be appropriate since it is on the leeward side of the island and may experience lower wave energy than other areas where rock barriers would be more suitable (Michigan Natural Shoreline Partnership 2018).

The third recommendation is for Reclamation to include measures in the CRMP to protect cultural resources specifically. The previous steps are intended to stabilize the shoreline generally and not cultural resources in particular. Additional measures may be appropriate to protect shorelines and preserve archaeological sites. Reclamation should consider the use of fast growing vegetation to prevent the erosion of archaeological sites (O'Halloran and Spennemann 2002). If the disturbance of sites from the construction of shoreline protection structures is unacceptable to key stakeholders, protecting them with sealants or concrete may be preferable (Lenihan et al. 1981; Ferri 2015). These measures should be used where there are known cultural resources in locations such as Ann Bell North, Speelyi Beach, Morgan Creek, and Wish Poosh (Steinkraus et al. 2014).

Figure 43: Wish Poosh Beach and Picnic Island, Cle Elum Lake. View towards the southeast. Photography by Michael Horner, May 2020.

Management Recommendations: Non-Engineering Approaches

In addition to these, the CRMP should include a process for managing the long-term impacts of reservoir expansion on cultural resources at Cle Elum and Bumping lakes. Increased water storage for offstream use under the Yakima Plan use may take 13 years to complete (Anchor QEA 2017). Resource managers should implement a plan for continual monitoring of archaeological sites during this period and beyond (Brandt and Hassan 2000). This should be considered for inclusion in the Cle Elum Pool Raise Project and Bumping Lake Enlargement CRMPs since these are meant to address ongoing, long-term impacts to cultural resources due to increased reservoir elevations (USBOR and WADOE 2015). This is particularly crucial for Bumping Lake since its expansion will be even larger, raising the elevation of the lake almost 20 m, from 1043.9 m to 1063.8 m. An additional 7.69 km^3 (1,900 acres) will be submerged (USBOR and WADOE 2012). Here,

three archaeological sites have already been identified including lithic scatters, stone tools, projectile points, debitage, and possibly a pit house and fishing camp (Draper and Washington State University 1991; USBOR and Yakima Indian Nation 1999). Impacts to cultural resources will arise from these projects and it will be necessary to detect and mitigate them over many decades.

A community group involving a broad array of stakeholders should be brought together to manage cultural resources in Yakima Basin reservoirs collaboratively. Interested stakeholders include the Bureau of Reclamation, the Washington State Department of Ecology ("Ecology"), the Yakama Nation, and others (USBOR and WADOE 2012). Reclamation and Ecology are the joint lead agencies for the Yakima Plan. They are conducting the National Environmental Policy Act (NEPA) review for the Cle Elum Pool Raise Project in conjunction with the requirements of Section 106 of the NHPA (USBOR and WADOE 2012, 2015). Section 106 will determine eventual steps to mitigate impacts to cultural resources. It requires consultation with stakeholders including the Yakama Nation, the Colville Confederated tribes, and cooperating agencies including the U.S. Forest Service (USBOR and WADOE 2015). Cooperation will be required among this group for a number of reasons. Community engagement will be required to protect cultural resources over an extended timeframe and with uncertain financial resources. In addition, stakeholders must overcome a contentious history of competition over water resources in the Yakima Basin to support agriculture and fisheries (Colman 2016). Therefore, a framework for the collaborative management of cultural resources in Yakima Basin reservoirs is needed.

To guide the protection of cultural resources, I propose a facilitated process

incorporating adaptive management. To ensure commitment by all interested parties to the process, this process will seek to encourage interaction between stakeholders and create a community of committed individuals and groups equipped to manage impacts on cultural resources arising from reservoir expansion. This will be accomplished by encouraging frequent interactions, through both meetings and community events, to create relationships and build a sense of community (Wondolleck and Yaffee 2000). This will allow the stakeholder group to work creatively to solve these problems, taking into account compatible interests, and using the best scientific information available.

Therefore, the framework for collaborative cultural resource management includes the following steps. First, interested stakeholders and a facilitator should convene as a group to initiate the collaborative management process. The group should establish a routine meeting schedule that is mutually acceptable to all. A meeting place and time should be chosen to maximize involvement. The venue should be a neutral place such as a community center and not an agency headquarters (Weeks 1992). Meetings should be facilitated to level the playing field and prevent established policies and procedures of agencies from negating the contributions of all participants (Wondolleck and Yaffee 2000). The stakeholders and facilitator should also discuss the proposed framework for collaboration. They should make suggestions about the framework and incorporate any changes. After this, the group should take a final decision on adopting the amended collaborative framework for managing cultural resources.

Second, interested stakeholders will need to make a commitment to managing cultural resources in Yakima Basin reservoirs over a period of decades (Wondolleck and Yaffee 2000; Anchor QEA 2017). Therefore, the initial stakeholder meetings should be

used to build a common vision based on compatible interests. In addition to the previously mentioned steps to maximize stakeholder inclusion, it may be necessary to address conflicting beliefs and values that may be compounded by mistrust (Wondolleck and Yaffee 2000). The Values Orientation Theory suggests that groups holding different value systems still face common problems (Hill 2002). Stakeholders should identify shared problems to help overcome mistrust (Wondolleck and Yaffee 2000). From this, they can articulate a shared vision based on common needs (Weeks 1992).

Third, routine meetings should be initiated as a forum for distributing relevant technical information and responding to problems and disputes arising from impacts to cultural resources. Throughout this process, members of the group with technical expertise should be tasked with gathering technical information and disseminating it to the stakeholder group on a frequent basis. There are two reasons for this. If there is a perception that agencies are not sharing information, this may become a barrier to cooperation. Additionally, disseminating information about progress will allow the stakeholder group to take action more proactively to prevent or address problems. It will be incumbent upon those with the means to gather and analyze this information to present it in a way that is clear to all participants in order to promote science-based decision-making (Wondolleck and Yaffee 2000). The stakeholder group should engage with the public through outreach and enjoyable events that help create a sense of community while also disseminating important information about cultural resources in Yakima Basin reservoirs.

An agile approach is needed to addressing these issues. Due to the lengthy timeline for implementation during which unanticipated problems can arise, the Yakima

Plan's Framework for Implementation Report recommends that an adaptive management approach be used in implementing the plan (Anchor QEA 2017). This approach should be extended to managing cultural resources in reservoirs. The ongoing monitoring of cultural resources will reveal impacts to cultural resources and provide a basis for addressing them (Wondolleck and Yaffee 2000). An adaptive management approach will allow the stakeholder group to respond to new information concerning cultural resources.

Further Research

Since shoreline erosion due to accelerating reservoir construction and expansion is a complex research problem requiring a multidisciplinary approach, numerous opportunities exist for further research. Worldwide, the construction of 50,000 major reservoirs over the last century increased water storage from less than 100 km^3 in 1900 to 8,300 km^3 in 2000 (Biemans 2011; International Rivers 2020). In 2006, the Three Gorges Reservoir was completed, adding 1,080 km^3 to this capacity (Bao et al. 2018). Given the world's growing dependence on artificial water storage, there is every reason to expect the trend towards reservoir expansion to continue (Barnett, Adam, and Lettenmaier 2005). Therefore, the significance of this research can be expanded by examining additional environmental, economic, and cultural implications of reservoir building globally. Although science is always an iterative process, results can be refined and expanded through a closer examination of shoreline erosion variables. Based on the experience gained in the process of completing this study, methods can be improved and expanded upon. Further research can improve our understanding of the costs and benefits of reservoir expansion on natural and human systems.

Expanded Significance

The significance of this research can be expanded by examining additional implications of reservoir expansion. Sociocultural implications for cultural resources in the Yakima Basin can be examined by comparing the economic and social benefits of provisioning water for fisheries and agriculture versus the costs to cultural resources. Reclamation estimated that the present value of the benefits of the Yakima Plan for agriculture and municipal water supplies over 100 years ranged from $2.2 billion to $3.8 billion (ECONorthwest 2011). Little is known about the economic and social value of cultural resources in the Yakima Basin, however. Here, cultural resources can be defined as both archaeological resources and the broader aesthetics of the natural landscape and traditional cultural properties (Brandt and Hassan 2000). Contingent valuation methods involve interviewing key stakeholders to determine the use, nonuse, and total willingness to pay for cultural resources. This would provide additional context for management recommendations (Kim, Wong and Cho 2005).

Moving beyond cultural resources, another area for research is to examine the physical effects of reservoir expansion on natural systems. The geomorphic effects of erosion on biotic and abiotic systems has important implications for water quality and ecosystem services (Bao et al. 2018). Following reservoir construction and expansion, increased erosion and sedimentation may continue for several decades, offsetting increases to storage capacity over the life of the reservoir (Lorang, Komar, and Stanford 1993; USBOR and WADOE 2015; Sadeghian et al. 2017).

Finally, the significance of this research can be enhanced by increasing its geographic scope. Two-thirds of the world's rivers are already dammed (International

Rivers 2020). The methods developed in this study are applicable to assessing erosion susceptibility in reservoirs throughout the world.

Additional Factors for Consideration

This study can also be improved through the consideration of additional erosion variables and processes. Although landforms were considered as indicators of erosion or deposition, using these to map drift cells would provide additional context for understanding the role of sediment budgets (Jacobsen and Schwartz 1981; Davidson-Arnott 2010). With a shoreline development ratio of 2.21 before the completion of the Pool Raise project, Cle Elum Lake features few pronounced headlands and bays (USGS 2016). This makes drift cells difficult to distinguish along this shoreline. Annual mean fetch does not appear to be a statistically significant factor in erosion at Cle Elum Lake. However, this study did not examine the impact of changes in mean seasonal wind direction on fetch, the role of wind duration by direction, or reservoir fluctuations in combination with these wind conditions. Ice shove driven by wind is another important cause of erosion in large fluctuating reservoirs, particularly in temperate regions (Gatto 1982; Krumbein 2010). I examined airphotos for erosional features related to ice shove such as straight and cellular marks including grooves and scrapes, bowls, cusps, ice-thrust and ice-push ridges, and ice ramparts as well as damaged vegetation without success (Gatto 1982). These may not have been evident since ice shove is more frequent where fetch is more than 4 km, exceeding Cle Elum Lake's maximum fetch distance (Gatto 1982). However, this factor may be relevant when studying reservoir erosion in other contexts. A potential gap in the literature not fully examined in this study is the role of bluff height (Quigley et al. 1976; Buckler and Winters 1983; Rashid et al. 1989; Amin and

Davidson-Arnott 1997). As previously noted, it was difficult to draw conclusions about the relationship between bluff height and erosion at Cle Elum Lake given the interquartile range of 2.2 m in the bluffs measured.

Finally, the results of this study indicate a future research direction distinguishing causal factors from the results of erosion. Geologic unit and slope interval were the only variables with statistically significant relationships to past shoreline erosion. However, significant relationships were found between erosion susceptibility and fetch, slope interval, vegetation cover, vegetation type, and geologic unit. I previously hypothesized that these are indicators of erosion rather than causal factors. For example, varial zones are left devegetated by wave action or thinly vegetated by flood tolerant species (O'Halloran and Spennemann 2002; USBOR and WADOE 2015). Additional research is required to determine if these non-significant variables indicate shoreline erosion rather than cause it.

Enhanced Methods

The final avenue for further research are improved and expanded methods. The first is performing fieldwork at additional depositional sites for a better point of comparison with erosional sites. This would allow a meaningful comparison of the means and medians of field measurements. Second, future research might involve combining the results of this study with confidential data from the Washington State Department of Archaeology and Historic Preservation's Washington Information System for Architectural and Archaeological Records Data (WISAARD) (WADAHP 2020). From this, generalized hazard maps for archaeological resources can be created.

REFERENCES

Adamo, F., C. De Capua, P. Filianoti, A.M.L. Lanzolla and R. Morello. 2014. A coastal erosion model to predict shoreline changes. *Measurement* 47:734-740. http://dx.doi.org/10.1016/j.measurement.2013.09.048.

Amin, S.M.N, and R.G.D. Davidson-Arnott. 1995. Toe erosion of glacial till bluffs: Lake Erie south shore. *Canadian Journal of Earth Sciences* 32(7):829-837. doi: 10.1139/e95-069.

——— 1997. A statistical analysis of the controls on shoreline erosion rates, Lake Ontario. *Journal of Coastal Research* 13(4):1093-1101. https://www.jstor.org/stable/4298717.

Anchor QEA. 2017. Yakima River Basin integrated water resource management plan framework for implementation report. Contract No. 08CA10677A ID/IQ, U.S. Department of the Interior. Bureau of Reclamation, Yakima, WA and State of Washington Department of Ecology, Union Gap, WA.; https://www.usbr.gov/pn/programs/yrbwep/2011integratedplan/plan/framework.pdf.

ArcGIS, version 10.8, Esri, Redlands, CA.

Archaeological Resources Protection Act of 1979, 16 U.S.C. § 470aa et seq (1979).

Bao, Y., X. He, A. Wen, P. Gao, Q. Tang, D. Yan, and Y. Long. 2018. Dynamic changes of soil erosion in a typical disturbance zone of China's Three Gorges Reservoir. *CATENA* 169: 128-139. doi: 10.1016/j.catena.2018.05.032.

Barnett, T. P., J.C. Adam, and D.P. Lettenmaier. 2005. Potential impacts of a warming climate on water availability in snow-dominated regions. *Nature* 438(7066):303-09. doi: 10.1038/nature04141.

Battjes, J.A. 1974. Surf similarity. *Coastal Engineering Proceedings* 1(14):466-480. doi: http://dx.doi.org/10.9753/icce.v14.26.

Benson, R.D. 2012. Federal water law and the "double whammy": how the Bureau of Reclamation can help the West adapt to drought and climate change. *Ecology Law Quarterly* 39(4):1049-083. https://digitalrepository.unm.edu/cgi/viewcontent.cgi?article=1332&context=law_facultyscholarship.

Biemans, H., I. Haddeland, P. Kabat, F. Ludwig, R. W. A. Hutjes, J. Heinke, W. von Bloh, and D. Gerten. 2011. Impact of reservoirs on river discharge and irrigation water supply during the 20th century. *Water Resources Research* 47(3):1-15. doi: 10.1029/2009WR008929.

Bird, E. 2001. *Coastal geomorphology: an introduction*. New York, NY: John Wiley & Sons.

Boualla, O., K. Mehdi, A. Fadili, A. Makan, and B. Zourarah. 2017. GIS-based landslide susceptibility mapping in the Safi region, West Morocco. *Bulletin of Engineering Geology and the Environment* 78(3). doi: 10.1007/s10064-017-1217-y.

Boualla, O., K. Mehdi, and B. Zourarah. 2016, Collapse dolines susceptibility mapping in Doukkala Abda (Western Morocco) by using GIS matrix method (GMM). *Modeling Earth Systems and Environment* 2(1):1-18. doi: 10.1007/s40808-015-0064-8.

Brandt, S.A. and F. Hassan. 2000. Dams and cultural heritage management. World Commission on Dams, Cape Town, South Africa. https://www.researchgate.net/profile/Steven_Brandt2/publication/23778272_WCD_Working_Papers_Dams_and_Cultural_Heritage_Manaagement/links/5739f30408ae9ace840dbabc.pdf.

Buckler, W.R. and H.A. Winters. 1983. Lake Michigan bluff recession. *Annals of the Association of American Geographers* 73(1):89-110. doi: 10.1111/j.1467-8306.1983.tb01398.x.

Caltopo. 2020. Cle Elum Lake. https://caltopo.com/map.html#ll=47.29611,-121.09749&z=12&b=t&o=r&n=0.25&a=cfabbcc89:0x7c5a2536811827a2!8m2!3d47.2796369!4d-121.1040505 (accessed 28 March 2020).

Castañeda, C., F. Javier Gracia., E. Luna., and R. Rodríguez-Ochoa. 2015. Edaphic and geomorphic evidences of water level fluctuations in Gallocanta Lake, NE Spain. *Geoderma,* 239:265-279. doi: 10.1016/j.geoderma.2014.11.005.

Central Washington Department of Geology. 2016. *Mastersizer 3000 standard operating procedure.* Murdock Charitable Trust Multidisciplinary Research Laboratory. http://www.sfu.ca/arise/publications/Mastersizer%20procedure-for%20web.pdf (accessed 30 December 2019).

Chesterman, C. W., and K. E. Lowe. 2018. *National Audubon Society field guide to rocks and minerals: North Americ*a. New York, NY: Alfred A. Knopf.

Chrzastowski, M.J., T.A. Thompson., and C.B. Trask. 1994. Coastal geomorphology and littoral cell divisions along the Illinois-Indiana coast of Lake Michigan. *Journal of Great Lakes Research* 20(1): 27-43. doi: 10.1016/S0380-1330(94)71130-8.

Cibicki, M. Email to Michael Horner. Personal communication. Wenatchee, WA, July 24, 2017.

Cohen, J. 1988. *Statistical power analysis for the behavioral sciences*. 2nd ed. New York, NY: Routledge. doi.org/10.1111/1467-8721.ep10768783.

Cohen, S.B. *The Columbia Gazetteer of the World*. New York: Columbia University Press, 1998.

Colman, Z. 2016. How the western water wars may end. *Christian Science Monitor* 16 October.

Costanzo, D., E. Rotigliano, C. Irigaray, J. Jiménez-Perálvarez, and J. Chacón. 2012. Factors selection in landslide susceptibility modelling on large scale following the GIS matrix method: application to the river Beiro basin (Spain). *Natural Hazards and Earth System Sciences* 12(12): 327-340. doi:10.5194/nhess-12-327-2012.

Cronin, A. and D.M. Ostergren. 2007. Tribal watershed management: culture, science, capacity, and collaboration. *American Indian Quarterly* 31 (1):87-214. https://muse.jhu.edu/article/211008/pdf.

Currey, Donald R., and Dorothy Sack. 2009. Hemiarid lake basins: geomorphic patterns. In *Geomorphology of desert environments*, ed. A.D. Abrahams and A.J. Parsons, 471-487. Dordrecht, Netherlands: Springer. doi: 10.1007/978-1-4020-5719-9_15.

Dashtgard, S. 2016. Mastersizer procedure. Simon Fraser University. Applied Research in Ichnology and Sedimentology (ARISE). http://www.sfu.ca/arise/publications/. Mastersizer%20procedure-for%20web.pdf (accessed 30 December 2019).

Davidson-Arnott, R. 2010. *Introduction to Coastal Processes and Geomorphology*. Cambridge, UK: Cambridge University Press. Doi: 10.2112/1551-5036(2006)22[1589:BR]2.0.CO;2

Davidson-Arnott, R. G. D., and B. Greenwood. 1999. Waves and sediment transport in the nearshore zone In *Coastal Zones and Estuaries*, ed. F.I. Isla, 43-60. Oxford, UK: EOLSS. https://www.eolss.net/Sample-Chapters/C09/E2-06-01-02.pdf

Davies, J.L. 1977. *Geographical Variation in Coastal Development*. London: Longman Publishing Group.

Davis, R. A. Jr. 1996. *Coasts.* Upper Saddle River, NJ: Prentice Hall.

Davis, R. A. Jr., W. G. Fingleton, and P. C. Pritchett. 1975. Beach profile changes east coast of Lake Michigan, 1970-72. Miscellaneous Paper No. 10-75, U.S. Army Corps of Engineers Coastal Engineering Research Center, Fort Belvoir, VA. http://hdl.handle.net/11681/25588

DeGraff, J. V., and C. Romesburg. 1980. Regional landslide susceptibility assessment for wildland management: a matrix approach. In *Thresholds in Geomorphology, vol. 19*, ed. D.R. Coates, and J.D. Vitek, 401-414. Boston: Alien & Unwin.

Dempsey, C. 2013. Cardinal directions and ordinal directions. Geo Lounge. https://www.geolounge.com/cardinal-directions-ordinal-directions/ (accessed 30 December 2019).

Dey, D.B. 1988. Cle Elum Lake: productivity and fertilization potential. Northwest Fisheries Center, National Marine Fisheries Service, National Oceanic and Atmospheric Administration, Seattle, WA.

Dick, T.A. 1993. The Yakima Project. Bureau of Reclamation History Program, Denver, CO.

Draper, J.A. and Washington State University Center for Northwest Anthropology. 1991. Results of an archaeological survey and test excavations at Bumping Lake Reservoir, Yakima County, Washington. Contributions in Cultural Resource Management 37. Pullman, WA.

Dreamflows River Flow Reports. 2020. Cle Elum - inflow Cle Elum Lake. https://www.dreamflows.com/reports.php (accessed 19 January 2020).

Earle, S. 2015. *Physical Geology*. Vancouver, BC: BCCampus OpenEd.

ECONorthwest. 2011. Yakima River basin study: economic effects of Yakima Basin integrated water resource management plan technical memorandum. U.S. Department of the Interior. Bureau of Reclamation (BOR) and Washington State Department of Ecology (WADOE), Yakima, WA.

Elsner, M., M. Cuo, L. Voisin, N. Deems, J. Hamlet A., Vano, J.. Mickelson K.E.B, Lee, S., Lettenmaier, D. P.2010. Implications of 21st century climate change for the hydrology of Washington State. *Climatic Change* 102(1): 225-60. doi: 10.1007/s10584-010-9855-0.

ERDAS, version 10.3, Hexagon Geospatial, Madison, AL, USA.

ESRI. *U.S. States*. Redlands, CA: ESRI, 2006. https://www.arcgis.com/home/item.html?id=1a6cae723af14f9cae228b133aebc620.

———. *World Hillshade*. Redlands, California, USA: ESRI, 2015. https://www.arcgis.com/home/item.html?id=1b243539f4514b6ba35e7d995890db1d.

———. 2016. FAQ: What is the Jenks optimization method? https://support.esri.com/en/technical-article/000006743 (accessed 30 December 2019).

———. 2019. How to: Count the number of point features within a polygon. https://support.esri.com/en/technical-article/000008599 (accessed 30 December 2019).

Ferri, R. Interview by Michael Horner and Brian Straniti. Personal interview. Ellensburg, WA, November 14, 2015.

Fisher G.B., C.B. Amos, B. Bookhagen, D.W. Burbank, V. Godard. 2012. Channel widths, landslides, faults, and beyond: The new world order of high-spatial resolution Google Earth imagery in the study of earth surface processes. *Geological Society of America Special Papers* 492(01): 1-22. doi: 10.1130/2012.2492(01).

Fookes, P. G., S. G. Dale, and J. M. Land. 1991. Some observations on a comparative aerial photography interpretation of a landslipped area. *Quarterly Journal of Engineering Geology and Hydrogeology* 24(3): 249-265. doi: https://doi.org/10.1144/ GSL.QJEG.1991.024.03.01

Franklin, J.F., and C.T. Dyrness. 1973. Natural vegetation of Oregon and Washington. Corvalis, OR: Oregon State University Press.

Frizzell, V.A. Jr., R.W. Tabor, D.B. Booth, K.M. Ort, and R.B. Waitt. *Preliminary geologic map of the Snoqualmie Pass 1:100,000 quadrangle, Washington*. Map. Reston, VA: United States Geologic Survey, 1984.

Garmin. 2019. *eTrex 10/20/20X/30/30X Owner's Manual*. Olathe, KS.

Garrett, B.L. 2007. History submerged: a legacy of modernity. MMA thesis, James Cook University.

Gatto, L.W. 1982. Reservoir bank erosion caused and influenced by ice cover. Special Report 82-31, U.S. Army Cold Regions Research and Engineering Laboratory, Hanover, NH.

Gendaszek, A.S., D.M. Ely, SR. Hinkle, S.C. Kahle and W.B. Welch. 2014. Hydrogeologic framework and groundwater/surface-water interactions of the Upper Yakima River Basin, Kittitas County, Central Washington. Scientific Investigations Report 2014-5119, U.S. Department of the Interior. U.S. Geological Survey (USGS), Reston, VA.
Ghasemi, A. and S. Zahediasl. 2012. Normality tests for statistical analysis: a guide for non-statisticians. *International Journal of Endocrinology and*

Metabolism 10 (2):486-489. https://www.ncbi.nlm.nih.gov/pmc/articles/PMC3693611/.

Gilbert, G.K. 1885. The topographic features of lake shores. Fifth Annual Report of the Director, 1883-84, U.S. Department of the Interior. U.S. Geological Survey (USGS). U.S. Government Printing Office. Washington, DC.

GISGeography. How to create NDVI maps in ArcGIS. http://gisgeography.com/how-to-ndvi-maps-arcgis/ (accessed 24 June 2017).

Google Earth, version 7.3.2.5776 (64-bit), Google, Mountain View, CA, USA.

Google Maps. 2018. Cle Elum Lake. https://www.google.com/maps/place/Cle+Elum+Lake/@47.2779493,-121.1308515,15.75z/data=!4m5!3m4!1s0x549a0d52fabbcc89:0x7c5a2536811827a2!8m2!3d47.2796369!4d-121.1040505 (accessed 21 March 2018).

Gracia Prieto, F.J., 1995. Shoreline forms and deposits in Gallocanta Lake (NE Spain). *Geomorphology* 11 (4):323-335. doi: 10.1016/0169-555X(94)00080-B.

GraphPad. 2020. P Value Calculator. https://www.graphpad.com/quickcalcs/pvalue1.cfm (accessed 15 February 2020).

Griggs, G.B., and K.W. Fulton-Bennett. 1988. Rip rap revetments and seawalls and their effectiveness along the central California coast. *Shore and Beach* 56(2):3-11. https://www.researchgate.net/profile/Gary_Griggs/publication/293625216_RIP_RAP_REVETMENTS_AND_SEAWALLS_AND_THEIR_EFFECTIVENESS_ALONG_THE_CENTRAL_CALIFORNIA_COAST/links/571e34b908aead26e71a83c5.pdf.

Gyssels, G., J. Poesen, E. Bochet, and Y. Li. 2005. Impact of plant roots on the resistance of soils to erosion by water: a review. *Progress in Physical Geography* 29(2): 189-217. doi: 10.1191/0309133305pp443ra.

Hall, N.D., B.B. Stuntz, and R.H. Abrams. 2008. Climate change and freshwater resources. *Natural Resources & Environment* 22(3): 30-35. http://www.jstor.org/stable/40924924.

Harjo, S.S. 2004. American Indian Religious Freedom Act after twenty-five years: an introduction. *Wicazo Sa Review* 19(2): 129-136. http://www.jstor.org/stable/1409502.

Highland, L. and P.T. Bobrowsky. 2008. The landslide handbook: a guide to understanding landslides. Reston, VA: U.S. Geological Survey.

Huggett, R.J. 2007. *Fundamentals of geomorphology. 3rd ed*. New York, NY: Routledge.

Hungr, O., S. Leroueil, and L. Picarelli. 2014. The Varnes classification of landslide types, an update. *Landslides* 11(2): 167-194. doi: 10.1007/s10346-013-0436-y.

Hyslop, M.D. 2012. Tutorial – Creating a regular grid for point sampling. Michigan Technological University. http://gis.mtu.edu/wp-content/uploads/2012/06/Regular_Sampling_Tutorial.pdf (accessed 30 December 2019).

International Rivers. 2020. Where we work. https://www.internationalrivers.org/our-work (accessed 29 March 2020).

Irigaray, C. 1995. Movimientos de ladera: Inventario, análisis y cartografía de susceptibilidad mediante un sistema de información geográfica (SIG). Aplicación a las zonas de Colmenar (Ma), Rute (Co) y Montefrío (Gr). (Hillside movements: Inventory, analysis and susceptibility cartography through a geographic information system (GIS). Application to the areas of Colmenar (Ma), Rute (Co) and Montefrío (Gr).). PhD dissertation, University of Granada.

Irigaray, C., T. Fernandez, and J. Chacon. 1996. Metodologìa de anàlisis de factores determinantes de movimientos de ladera mediante un S.I.G. aplicaciòn al Sector de Rute (Còrdoba, España). (Methodology of analysis of determinants of slope movements through a G.I.S. application to the Rute Sector (Córdoba, Spain)). Paper presented at *VI Congreso Nacional y Conferencia Internacional de Geologia Ambiental y Ordenaciòn del Territorio (VI Congress National and International Conference on Environmental Geology and Land Use Planning*), ed. Chacon, J. and Irigaray, C. https://www.researchgate.net/profile/C_Irigaray/publication/267211758_Methodology_for_the_analysis_of_landslide_determinant_factors_by_means_of_a_GIS_Aplication_to_the_Colmenar_area_Malaga_Spain/links/574c1b2508ae538af6a50c01/Methodology-for-the-analysis-of-landslide-determinant-factors-by-means-of-a-GIS-Aplication-to-the-Colmenar-area-Malaga-Spain.pdf

Irigaray, C., T. Fernandez, R. El Hamdouni, and J. Chacon. 2007. Evaluation and validation of landslide-susceptibility maps obtained by a GIS matrix method: examples from the Betic Cordillera (southern Spain). *Natural Hazards* 41: 61-79. doi: 10.1007/s11069-006-9027-8.

Jackson, N.L., K.F. Nordstrom, I. Eliot, and G. Masselink. 2002. 'Low energy' sandy beaches in marine and estuarine environments: a review. *Geomorphology* 48(1-3): 147-162. doi: 10.1016/S0169-555X(02)00179-4.

Jacobsen, E.E., and M.L. Schwartz. 1981. The use of geomorphic indicators to determine the direction of net shore-drift. *Shore and Beach* 49(4): 38-43.

Jewell, P. W. 2016. Quantitative identification of erosional Lake Bonneville shorelines, Utah. *Geomorphology* 253: 135-145. doi: 10.1016/j.geomorph.2015.09.022.

Jiménez-Perálvarez, J. D., C. Irigaray, R. El Hamdouni, and J. Chacón. 2009. Building models for automatic landslide-susceptibility analysis, mapping and validation in ArcGIS. *Natural Hazards* 50(3): 571-590. doi: 10.1007/s11069-008-9305-8.

Jiménez-Perálvarez, J. D., C. Irigaray, R. El Hamdouni, and J. Chacón. 2010. Landslide-susceptibility mapping in a semi-arid mountain environment: an example from the southern slopes of Sierra Nevada (Granada, Spain). *Bulletin of Engineering Geology and the Environment* 70(2): 265-277. doi: 10.1007/s10064-010-0332-9.

Joyce, A.T. 1978. Procedures for ground truth information for a supervised approach to a computer-implemented land cover classification of landsat-acquired multispectral scanner data. NASA Reference Publication 1015, National Aeronautics and Space Administration, Houston, TX.

Kamphuis, J.W. 1987. Recession rate of glacial till bluffs. *Journal of Waterway, Port, Coastal, and Ocean Engineering* 113(1): 60-73. doi: 10.1061/(ASCE)0733-950X(1987)113:1(60).

Keil, A., Berking, J., Mügler, I., Schütt, B., Schwalb, A., and Steeb, P. 2010. Hydrological and geomorphological basin and catchment characteristics of Lake Nam Co, South-Central Tibet. *Quaternary International* 218(1): 118-130. doi: 10.1016/j.quaint.2009.02.022.

Kim, S.S., K.K.F. Wong, and M. Cho. 2007. Assessing the economic value of a World Heritage Site and willingness-to-pay determinants: a case of Changdeok Palace. *Tourism Management* 28(1): 317-22. https://doi.org/10.1016/ j.tourman.2005.12.024.

King, T.F. 2013. *Cultural resource laws and practice*, 4th ed. Lanham, MD: Altamira Press.

Kirillin, G., M.S. Lorang, T.C. Lippmann, C.C. Gotschalk, and S. Schimmelpfennig. 2015. Surface seiches in Flathead Lake. *Hydrology and Earth System Sciences* 19(6): 2605-2615. doi: 10.5194/hess-19-2605-2015.

Knodel, K., G. Lange and H.J. Voigt. 2008. *Environmental geology: handbook of field methods and case studies*. Berlin: Springer.

Komar, P.D. 1976. *Beach processes and sedimentation.* Englewood Cliffs, NJ: Prentice-Hall.

Komar, P.D., and S. Shih. 1993. Cliff erosion along the Oregon coast: A tectonic-sea level imprint plus local controls by beach processes. *Journal of Coastal Research* 9(3): 747-765. www.jstor.org/stable/4298127.

Krumbein, W.C. 2010. Littoral processes in lakes. *Coastal Engineering Proceedings* 1(1): 155-160. doi: 10.1.1.871.9456.

Lakhan, V.C., and D.A. Pepper. 1997. Relationship between concavity and convexity of a coast and erosion and accretion patterns. *Journal of Coastal Research* 13(1): 226-232. http://www.jstor.org/stable/4298609.

Lenihan, D. T.L. Carrell, S. Fosberg, L. Murphy, S.L. Rayl, and J. A. Ware. 1981. The final report of the national reservoir inundation study. Volume 1, United States Department of the Interior, National Park Service, Southwest Cultural Resources Center, Santa Fe, NM.

Lewis, C.F.M., D.K. Rea, J.B. Hubeny, T.A. Thompson, S.M. Blasco, J.W. King, M. Reddin, and T.C. Moore Jr. 2010. Using geological history of the Laurentian Great Lakes to better understand their future. *Aquatic Ecosystem Health & Management Society* 13(2): 118-126. doi: 10.1080/14634981003799950.

Lewis, P., S. Fotheringham, and A. Winstanley. 2011. Spatial video and GIS. *International Journal of Geographical Information Science* 25(5): 697-716. doi: 10.1080/13658816.2010.505196.

Leyva, S. 2020. Coastal processes lesson. The Geophile Pages. http://geophile.net/Lessons/coasts/coasts_01.html# (accessed 16 March 2020).

Lieberman, D.M. and Grabowski. 2007. Physical, chemical, and biological characteristics of Cle Elum and Bumping lakes in the Upper Yakima River Basin: storage dam fish passage study Yakima Project Washington. Technical Series No. PN-Y*DF*P-005, U.S. Department of the Interior. Bureau of Reclamation. Boise, ID.

Lillquist, K.D. 1995. Late Quaternary Lake Franklin: lacustrine chronology, coastal geomorphology, and hydro-isostatic deflection in Ruby Valley and northern Butte Valley, Nevada. PhD. diss., University of Utah.

Lorang, M.S., and J.A. Stanford. 1993. Variability of shoreline erosion and accretion within a beach compartment of Flathead Lake, Montana. *Limnology and Oceanography* 38(8): 1783-1795. doi: 10.4319/lo.1993.38.8.1783.

Lorang, M.S., J.A. Stanford, F.R. Hauer, and J.H. Jourdonnais. 1993. Dissipative and reflective beaches in a large lake and the physical effects of lake level regulation. *Ocean & Coastal Management* 19(3): 263-287. doi: 10.1016/0964-5691(93)90045-Z.

Lorang, M.S., P.D. Komar, and J.A. Stanford. 1993. Lake level regulation and shoreline erosion on Flathead Lake, Montana: a response to the redistribution of annual wave energy. *Journal of Coastal Research* 9(2): 494-508. www.jstor.org/stable/4298105.

Lovrić, N., and R. Tošić. 2017. Validation of landslide susceptibility maps (case study: urban area of the municipality of Banja Luka - B&H. *Bulletin of the Serbian Geographical Society* 97(1): 19-34. https://doi.org/10.2298/GSGD1701019L.

Manning, C. 2016. Email to Michael Horner, Personal communication. Ellensburg, WA, April 28, 2016. *Cle Elum Lake bathymetry.*

Markell, J. 2017. Year in Review: Progress on Yakima Basin plan, steelhead back in Manastash. *Daily Record*. 23 December.

Marr, P. "Directional (Circular) Statistics". Lecture, Quantitative Methods from Shippensburg University, Shippensburg, PA, April 17, 2019.

Michigan Natural Shoreline Partnership. 2018. Understanding Erosion at the Shoreline. http://www.mishorelinepartnership.org/erosion-at-the-shoreline.html (accessed 20 November 2018).

Miller, I.M., J.A. Warrick, and C. Morgan. 2011. Observations of coarse sediment movements on the mixed beach of the Elwha Delta, Washington. *Marine Geology* 282(3-4): 201-214. doi: 10.1016/j.margeo.2011.02.012.

Minitab. 2019. Interpret all Statistics and Graphs for Descriptive Statistics. https://support.minitab.com/en-us/minitab-express/1/help-and-how-to/basic-statistics/summary-statistics/descriptive-statistics/interpret-the-results/all-statistics-and-graphs/#mean (accessed 29 February 2020).

Mires, P.B. 2004. Teaching geographic field methods to cultural resource management technicians. *Journal of Geography* 103(1): 8-15. https://doi.org/10.1080/00221340408978567.

Mosisch, T.D., and A.H. Arthington. 1998. The impacts of power boating and water skiing on lakes and reservoirs. *Lakes & Reservoirs: Research & Management* 3(1): 1-17. doi: 10.1111/j.1440-1770.1998.tb00028.x.

Mote, P.W., A.F. Hamlet, M.P. Clark, and D.P. Lettenmaier. 2005. Declining mountain snowpack in western North America. *Bulletin of the American meteorological Society* 86(1): 39-49. https://doi.org/10.1175/BAMS-86-1-39.

National Centers for Environmental Information (NCEI). *1981-2010 U.S. Climate Normals. Cle Elum, WA US.* Asheville, NC: National Oceanic and Atmospheric

Administration (NOAA), 2018. https://www.ncdc.noaa.gov/cdo-web/datatools/normals.

Niu, R.Q., B. Du, Y. Wang, L.P. Zhang, and T. Chen. 2014. Impact of fractional vegetation cover change on soil erosion in Miyun reservoir basin, China. *Environmental earth sciences* 72(8): 2741-2749. doi: 10.1007/s12665-014-3179-8.

O'Halloran, C., and D.H.R. Spennemann. 2002. Wave action impact on archaeological sites in a freshwater reservoir: the case of Lake Hume, New South Wales. *Australian Archaeology* (54): 6-12. https://doi.org/10.1080/03122417.2002.11681735.

Osborn, R.P. 2012. Climate change and the Columbia River Treaty. *Washington Journal of Environmental Law & Policy* 2(1): 75–123. https://digitalcommons.law.uw.edu/wjelp/vol2/iss1/2/.

Osgood, R.A. 2005. Shoreline density. *Lake and Reservoir Management* 21(1): 125-126. https://doi.org/10.1080/07438140509354420.

Osterkamp, W.R., C.R. Hupp, and M. Stoffel. 2012. The interactions between vegetation and erosion: new directions for research at the interface of ecology and geomorphology. *Earth Surface Processes and Landforms* 37(1): 23-36. doi: 10.1002/esp.2173.

Porter, S.C. 1976. Pleistocene glaciation in the southern part of the North Cascade Range, Washington. *Geological Society of America Bulletin* 87 (1): 61-75. doi: .1130/0016-7606(1976)87<61:PGITSP>2.0.CO.

Quantum Spatial, Inc. Yakima River Basin, WA LiDAR survey. https://lidarportal.dnr.wa.gov/ (accessed 30 December 2019).

QGIS, version 2.18.11, QGIS.

Quigley, R.M., P.J. Gelinas, W.T. Bou, and R.W. Packer. 1976. Cyclic erosion-instability relationships: Lake Erie north shore bluffs. *Canadian Geotechnical Journal* 14: 310-323. doi: 10.1139/t77-037.

Rasid, H., R.S. Dilley, D. Baker, and P. Otterson. 1989. Coping with the effects of high water levels on property hazards: North shore of Lake Superior. *Journal of Great Lakes Research* 15(2): 205-216. doi: 10.1016/S0380-1330(89)71476-3.

Reid, J.R. 1992. Mechanisms of shoreline erosion along lakes and reservoirs. In Proceedings, U.S. Army Corps of Engineers workshop on reservoir shoreline

erosion: a national problem, ed. H.H. Allen and J.L. Tingle, 18-32. Vicksburg, MS. https://apps.dtic.mil/dtic/tr/fulltext/u2/a27056893.pdf#page=41.

Rich, J.L. 1951. Three critical environments of deposition, and criteria for recognition of rocks deposited in each of them. *Geological Society of America Bulletin* 62(1): 1-20. https://doi.org/10.1130/0016-7606(1951)62[1:TCEODA]2.0.CO;2.

Rinella, J.F., S.W. McKenzie, and G.J. Fuhrer. 1992. *S*urface-water-quality assessment of the Yakima River basin, Washington: analysis of available water-quality data through 1985 water year, Open-file report 91-453. United States Department of the Interior, United States Geological Survey, Portland, OR.

Ritter, D.F., R.C. Kochel, and J. R. Miller. 1995. *Process geomorphology*. Long Grove, IL: Waveland.

Rubensdotter, L., and Rosqvist, G. 2003. The effect of geomorphological setting on Holocene lake sediment variability, northern Swedish Lapland. *Journal of Quaternary Science* 18(8): 757-767. doi: 10.1002/jqs.800.

Russell, I.C. 1885. Geological history of Lake Lahontan: a Quaternary lake of northwestern Nevada. Vol. 11, US Government Printing Office, Washington, DC.

Sadeghian, A., D. de Boer, and K.E. Lindenschmidt. 2017. Sedimentation and erosion in Lake Diefenbaker, Canada: solutions for shoreline retreat monitoring. *Environmental Monitoring and Assessment* 189(10): 507. doi: 10.1007/s10661-017-6217-7.

Schiefer, E., and B. Klinkenberg. 2004. The distribution and morphometry of lakes and reservoirs in British Columbia: a provincial inventory. *The Canadian Geographer* 48 (3): 345-355. doi: 10.1111/j.0008-3658.2004.00064.x.

Shipman, H. 2008. A geomorphic classification of Puget Sound nearshore landforms. Puget Sound Nearshore Partnership Report No. 2008-01, United States Army Corps of Engineers Seattle District, Seattle, WA.

Sierra, J. P., and M. Casas-Prat. 2014. Analysis of potential impacts on coastal areas due to changes in wave conditions. *Climatic Change* 124(4): 861-876. doi: 10.1007/s10584-014-1120-5.

Spatz, C. 1993. *Basic statistics: Tales of distributions*. 5th ed. Belmont, CA: Wadsworth.

SPSS, version 26, IBM Corporation.

Stanford, J.A., and F.R. Hauer. 1992. Mitigating the impacts of stream and lake regulation in the Flathead River catchment, Montana, USA: an ecosystem

perspective. *Aquatic Conservation: Marine and Freshwater Ecosystems* 2(1): 35-63. doi: 10.1002/aqc.3270020104.

Statistics How To. 2020. *V statistics.* https://www.statisticshowto.datasciencecentral.com/v-statistics/ (accessed 16 February 2020).

Statistix, version 10, Analytical Software, Tallahassee, FL.

Steinkraus, S.M.H., J.W. McLean, M.F. Steinkraus, A.R. Taylor, and K.R. Snider. 2014. Pedestrian survey and limited subsurface testing of the Cle Elum 3 foot pool raise supplemental shoreline survey. U.S. Department of the Interior. Bureau of Reclamation, Yakima, WA and Washington State Department of Archaeology and Historic Preservation, Olympia, WA.

Stilson, M.L., D. Meatte, R.G. Whitlam, and Washington Department of Transportation. 2003. *A field guide to Washington state archaeology*. Olympia, WA: Office of Archaeology and Historic Preservation.

Su, X., C. Nilsson, F. Pilotto, S. Liu, S. Shi, and B. Zeng. 2017. Soil erosion and deposition in the new shorelines of the Three Gorges Reservoir. *Science of the Total Environment* 599-600: 1485-1492. doi: 10.1016/j.scitotenv.2017.05.001.

Sunamura, T. 1977: A relationship between wave-induced cliff erosion and erosive force of waves. *The Journal of Geology* 85(5): 613-618. http://www.jstor.org/stable/30059121.

———. 1983. Processes of sea cliff and platform erosion. In *CRC Handbook of Coastal Processes and Erosion,* ed. P. Komar, 233-265. Boca Raton, FL: CRC Press.

Synge, F.M. 1966. The relationship of the raised strandlines and main end-moraines on the Isle of Mull, and in the district of Lorn, Scotland. *Proceedings of the Geologists' Association* 77(3): 315-328. https://doi.org/10.1016/S0016-7878(66)80037-8.

Tabor, R.W., V.A. Frizzell, Jr., D.B. Booth, and R.B. Waitt. *Geologic map of the Snoqualmie Pass 30 x 60 minute quadrangle, Washington*. Map. Reston, VA: United States Geological Survey, 2000.

Tackman, G. 1993. Middle and late Pleistocene hydrologic history of Diamond Valley, Eureka and Elko counties, Nevada, with climatic and isostatic implications. PhD diss., University of Utah.

Taylor, S.A. and C.A. Gazis. 2014. A geochemical study of the impact of irrigation and aquifer lithology on groundwater in the Upper Yakima River Basin, Washington, USA. *Environmental Earth Science* 72: 1569-1587. doi: 10.1007/s12665-014-3062-7.

Thornton, K. W., R. H. Kennedy, J. H. Carroll, W. W. Walker, R. C. Gunkel, and S. Ashby. 1981. Reservoir sedimentation and water quality—an heuristic model. In Proceedings of the symposium on surface water impoundments, vol. 1, pp. 654-661. American Society of Civil Engineers, New York, NY.

Tošić, R., N. Lovrić, S. Dragićević and S. Manojlović. 2018. Assessment of torrential flood susceptibility using GIS matrix method: case study - Vrbas River Basin (B&H). *Carpathian Journal of Earth and Environmental Sciences* 13(2): 369-382. doi: 10.26471/cjees/2018/013/032.

U.S. Department of Agriculture (USDA). Natural Resource Conservation Service. *Washington State, (4-band, 1 meter) 2013 NAIP aerial photography*. Washington, DC: Natural Resource Conservation Service, 2013. http://wagda.lib.washington.edu:6080/arcgis/rest/services/Imagery_services/NAIP2013/ImageServer (accessed 27 March 2019).

———. 2019. Soil texture calculator. https://www.nrcs.usda.gov/wps/portal/nrcs/detail/soils/survey/?cid=nrcs142p2_054167 (accessed 1 January 2020).

———. 2015. Shasta Lake water resources investigation environmental impact statment. United States Department of the Interior. United States Bureau of Reclamation, Sacramento, CA.

———. 2018. Cle Elum Dam. https://www.usbr.gov/projects/index.php?id=306 (accessed 26 January 2018).

———.*Yakima hydromet real-time (15-minute) data access*. Yakima, WA: United States Bureau of Reclamation, 2018. https://www.usbr.gov/pn/hydromet/yakima/yakwebdayread.html.

———.*Yakima hydromet real-time reservoir storage*. Yakima, WA: United States Bureau of Reclamation, 2018. https://www.usbr.gov/pn-bin/yak/dfcgi.pl?sta=CLE.

_____. *Yakima hydromet real-time (15-minute) data access*. Discharge or Flow (cfs) for Cle Elum Reservoir, River and Weather Station. Yakima, WA: United States Bureau of Reclamation, 2020. https://www.usbr.gov/pn/hydromet/yakima/yakwebdayread.html.

_____. *Yakima* Hydromet Real-Time (15-minute) Data Access. Discharge or Flow (cfs) for Yakima River near Umtanum. Yakima, WA: United States Bureau of Reclamation, 2020. https://www.usbr.gov/pn/hydromet/yakima/yakwebdayread.html.

U.S. Department of the Interior. Bureau of Reclamation (USBOR) and State of Idaho Water Resource Board. 2015. Shasta Lake water resources investigation. United States Bureau of Reclamation and Idaho Water Resource Board, Boise, ID.

U.S. Department of the Interior. Bureau of Reclamation (USBOR) and Washington State Department of Ecology (WADOE). 2011. Yakima River Basin study: Bumping Lake enlargement planning design summary update. U.S. Department of the Interior. Bureau of Reclamation and Washington State Department of Ecology, Yakima, WA.

———. 2011. Cle Elum Dam fish passage facilities and fish reintroduction project final environmental impact statement. U.S. Department of the Interior. Bureau of Reclamation and Washington State Department of Ecology, Yakima, WA.

———. 2012. Yakima River Basin integrated water resource management plan: final programmatic environmental impact statement – Benton, Kittitas, Klickitat and Yakima counties. U.S. Department of the Interior. Bureau of Reclamation and Washington State Department of Ecology, Yakima, WA.

———. 2015. Cle Elum pool raise project: final environmental impact statement. U.S. Department of the Interior. Bureau of Reclamation and Washington State Department of Ecology, Yakima, WA.

———. 2015. Record of decision for the Cle Elum pool raise project: final environmental impact statement. U.S. Department of the Interior. Bureau of Reclamation and Washington State Department of Ecology, Yakima, WA.

———. 2004. Formation, evolution, and stability of coastal cliffs: status and trends, ed. M.A. Hampton and G.B. Griggs. Professional Paper, 1693, U.S. Government Printing Office, Washington, DC.

U.S. Department of the Interior. U.S. Geological Survey (USGS). *Drainage Basins; United States, Canada*. Reston, VI: U.S. Geological Survey, 2008. https://www.usgs.gov/core-science-systems/ngp/national-hydrography/watershed-boundary-dataset?qt-science_support_page_related_con=4#qt-science_support_page_related_con.

———. *Washington State GAP/LANDFIRE National Terrestrial Ecosystems*. Reston, VA: U.S. Geological Survey, 2011. https://www.usgs.gov/core-science-systems/science-analytics-and-synthesis/gap.

———. 2020. Water density. https://www.usgs.gov/special-topic/water-science-school/science/water-density?qt-science_center_objects=0#qt-science_center_objects (accessed 27 May 2020).

Utah Division of Water Resources. 2016. Utah State water plan. Utah Department of Natural Resources, Salt Lake City, UT.

Valley Air Photos. *Bumping and Cle Elum Lakes Airphotos*. 2012. In Okanogan/Wenatchee National Forest. Salt Lake City, UT: U.S. Department of Agriculture. Farm Service Agency.

Van Den Berg, R.G. 2020. SPSS Tutorials. Cramér's V – What and Why? https://www.spss-tutorials.com/cramers-v-what-and-why/ (accessed 16 February 2020).

Vano, J.A., M.J. Scott, N. Voisin, C.O. Stöckle, A.F. Hamlet, K.E.B. Mickelson, M. M. Elsner and D.P. Lettenmaier. 2010. Climate change impacts on water management and irrigated agriculture in the Yakima River Basin, Washington, USA. *Climatic Change* 102 (1): 287-317. doi: 10.1007/s10584-010-9856-z.

Vogiatzis, N., K. Kotti, S. Spanomitsios, and M. Stoukides. 2004. Analysis of wind potential and characteristics in North Aegean, Greece. *Renewable energy* 29 (7): 1193-1208. doi: 10.1016/j.renene.2003.11.017.

Vosough, A. 2011. Wave energy. *International Journal of Multidisciplinary Sciences and Engineering* 2 (7): 60-63. http://www.ijmse.org/Volume2/Issue7/paper12.pdf.

Washington State Department of Archaeology and Historic Preservation (WADAHP). 2020. Washington Information System for Architectural and Archaeological Records Data (WISAARD). https://wisaard.dahp.wa.gov/ (accessed 4 April 2020).

Washington State Department of Ecology (WADOE). *City Boundaries and Urban Growth Areas*. Lacey, WA: Washington State Department of Ecology, 2015. http://geo.wa.gov/datasets/washington-state-city-urban-growth-areas-2018.

Washington State. Department of Natural Resources (WADNR). *Washington State Yakima K2K 2014 DTM*. Olympia, WA: Washington State Department of Natural Resources, 2014. https://lidarportal.dnr.wa.gov/.

———.*1:100,000-Scale Digital Geology of Washington State*. Olympia, WA: Washington State Department of Natural Resources, 2000. http://wagda.lib.washington.edu/data/geography/wa_state/wageol/.

Washington State Department of Transportation (WADOT). *County routes (CRAB)*. Olympia, WA: Washington State Department of Transportation, 2020. https://geo.wa.gov/datasets/WSDOT::wsdot-county-road-administration-board-crab-routes.

———. *Washington State Highways LRS (Linear Reference Systems)*. Olympia, WA: Washington State Department of Transportation, 2020. https://www.wsdot.wa.gov/mapsdata/geodatacatalog/maps/NOSCALE/dot_TDO/LRS/WSDOT_LRS.htm.

Weeks, D. 1992. *The eight essential steps to conflict resolution: preserving relationships at work, at home, and in the community*. Los Angeles, CA: Tarcher.

Wentworth, C.K. 1922. A scale of grade and class terms for clastic sediments. *The Journal of Geology* 30(5): 377-392. http://www.journals.uchicago.edu/t-and-c.

West Virginia. Department of Environmental Protection. 2019. Pebble count methods. https://dep.wv.gov/WWE/getinvolved/sos/Documents/SOPs/PebbleCount_Methods.pdf (accessed 21 December 2019).

Wise, E.K. 2012. Hydroclimatology of the US Intermountain West. *Progress in Physical Geography* 36(4): 458-479. doi: 10.1177/0309133312446538.

Wondolleck, J.M., and S.L. Yaffee. 2000. *Making collaboration work: Lessons from innovation in natural resource managment*. Washington, DC: Island Press.

Wright, L. D., and A.D. Short. 1984. Morphodynamic variability of surf zones and beaches: a synthesis. *Marine Geology.* 56(1-4): 93-118. doi: 10.1016/0025-3227(79)90149-X.

Wyskup, D. 2006. Interpreting site formation processes affecting re-emergent cultural sites within reservoirs: a case study of St. Thomas, Nevada. MA thesis, West Virginia University.

Yakama Nation Fisheries. 2015. Sockeye returns to Cle Elum Lake. http://yakamafish-nsn.gov/restore/stories/sockeye-returns-cle-elum-lake (accessed 20 February 2018).

Yakima Subbasin Fish and Wildlife Planning Board. 2004. Yakima subbasin plan. Northwest Power and Conservation Council. Portland, OR.

Yasso, W.E. 1965. Plan geometry of headland-bay beaches. *The Journal of Geology* 73(5): 702-714. http://www.jstor.org/stable/30079652.

Zelo, I., H. Shipman, and J. Brennan. 2000. Alternative bank protection methods for Puget Sound Shorelines. Publication # 00-06-012. Washington State Department of Ecology, Olympia, WA.

APPENDIXES

Appendix A: GPS Tracks

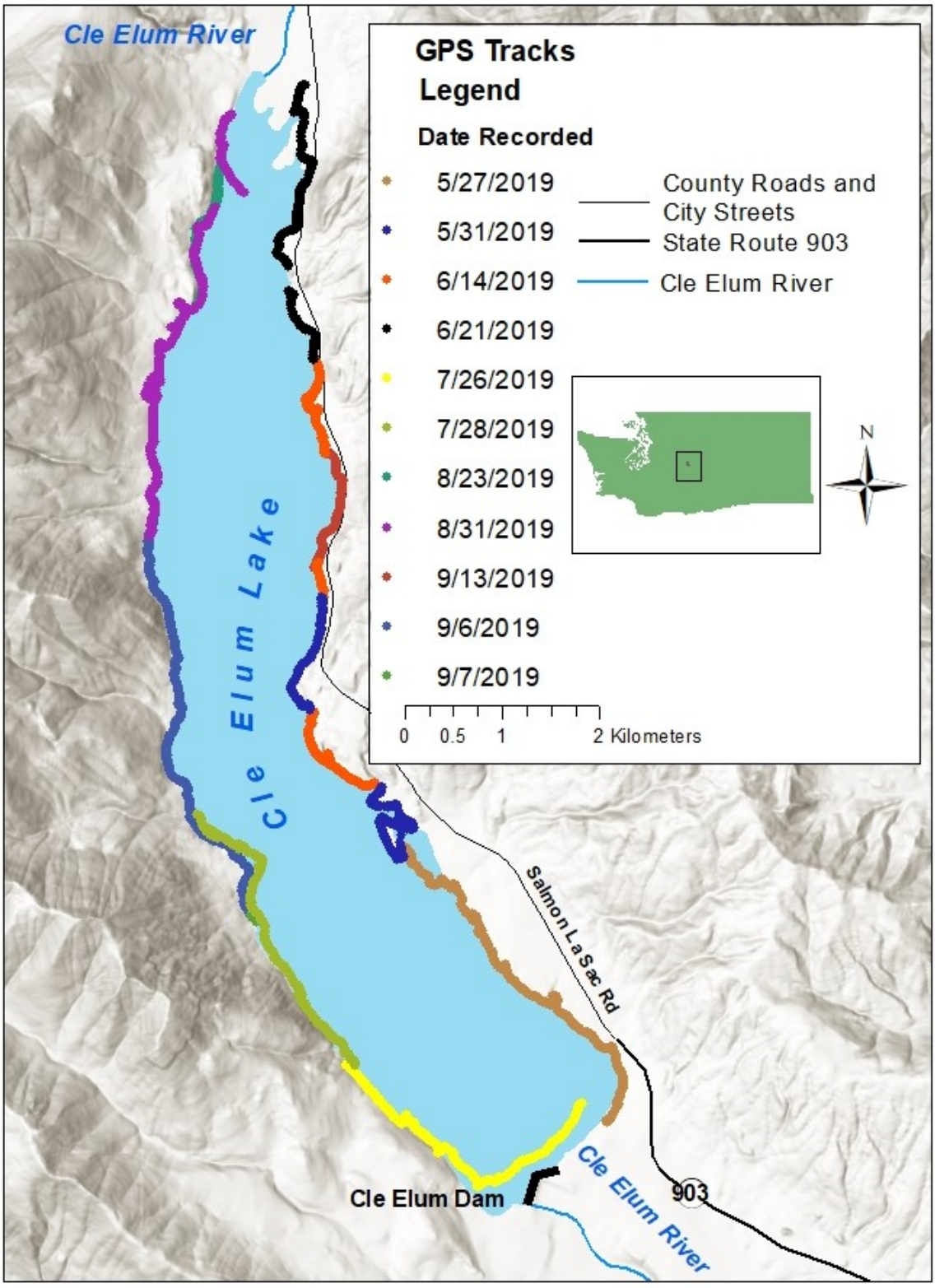

Appendix B: Field Checklist

Shoreline Erosion Ground Truth Data

1) Site Survey Start

Date: _____ **Site #:** _____ **GPS Data:** _____

Waypoint: ( ) Yes ( ) No
Lat, Long; Elev. (h, m, s)

2) Ground Truth Landforms

Erosion Confirmed: ( ) Yes ( ) No **Landform Photographed:** ( ) Yes ( ) No

Landform(s) Present: _____

Description of Site, Landforms, and Comments (note any variation from airphoto interpretation including evidence of erosion):

_____

_____

_____

_____

3) Determine Shoreline Relief and Morphodynamics

Wolman Pebble Count Performed: ( ) Yes ( ) No **Nearshore Width:** _____

Foreshore Slope (%): _____ **Nearshore Slope (%):** _____

_____

_____

_____

4) Characterize Vegetation

Dominant Vegetation: ( ) None ( ) Grassland ( ) Shrub ( ) Forest

Plants Photographed: ( ) Yes ( ) No **Undercutting/slumping:** ( ) Yes ( ) No

Comments (note species present and variation from airphoto interpretation):

_____

_____

_____

5) Describe Physical Shoreline Characteristics

Describe Shoreline Substrates

Exposures are ( ) Bedrock ( ) Quaternary Sed.

Exposures Photographed: ( ) Yes ( ) No

Note texture, sorting, and bedding of sediments.

Soil Sample Taken: ( ) Yes ( ) No

Measure the Height of Slopes and Bluffs and Substrate Thickness

Slope/Bluff Height: _____

Appendix C – Study Sites and Site Photographs.

Site	Location	Erosion (Y/N)	Landform(s)	Sorting	Bedding	Sediment Texture	Wolman Average	Nearshore Width (m)	Foreshore Slope (%)	Nearshore Slope (%)	Bluff Height (m)
1	47° 15' 16.40", -121° 03' 42.60"	Yes	Bluff	None	None	Very Gravelly Loam	3.16	87	4.6%	3.0%	4.60
2	47° 15' 34.69", -121° 03' 48.86"	Yes	Bluff	None	None	Extremely Gravelly Coarse Sandy Loam	2.80	20	21.5%	0.6%	4.5
3	47° 16' 48.76", -121° 05' 23.04"	Yes	Bluff	None	None	Very Gravelly Loamy Sand	13.03	2	55.5%	57.2%	2.50
4	47° 16' 53.98", -121° 05' 27.71"	Yes	Bluff	None	None	Very Gravelly Fine Sand	13.24	2.5	21.5%	35.2%	3.6
5	47° 17' 00.43", -121° 05' 39.31"	Yes	Bluff	None	None	Gravelly Silt Loam	6.21	2.1	34.4%	15.0%	11.70
6	47° 17' 33.46", -121° 06' 23.22"	Yes	Bluff	None	None	Extremely Gravelly Loam	7.46	20	14.0%	20.0%	5.2
7	47° 17' 44.90", -121° 06' 12.40"	Yes	Bluff	None	None	Very Gravelly Silt	8.67	8.672	15.0%	15.0%	5.2
8	47° 18' 54.50", -121° 06' 10.00"	No	Beach and Bedrock	N/A	N/A	Extremely Gravelly Silt Loam	3.56	36	25.0%	5.0%	4.6
9	47° 19' 05.80", -121° 06' 16.40"	No	Beach	None	None	Very Gravelly Silt Loam	2.81	19.4	20.0%	18.4%	0
10	47° 20' 18.36", -12° 10' 70.46"	Yes	Bluff	None	None	Extremely Gravelly Silt Loam	4.125	10	60.0%	14.0%	3
11	47° 20' 07.80", -121° 07' 08.60"	Yes	Bluff	Yes	Yes	Silt	3.3541	40	23.0%	12.7%	4.1
12	47° 19' 34.80", -121° 07' 18.60"	No	Steep Slope	None	None	Very Gravelly Silt Loam	4.915	12.5	18.4%	16.3%	0.6
13	47° 19' 12.80", -121° 07' 30.60"	Yes	Bluff	None	None	Extremely Gravelly Silt Loam	3.99	43	30.0%	16.0%	2
14	47° 18' 35.40", -121° 07' 31.70"	Yes	Bluff	None	None	Very Gravelly Silt Loam	5.11	218	25.0%	7.5%	2.3
15	47° 17' 12.70", -121° 07' 23.70"	Yes	Bluff	None	None	Very Gravelly Silt Loam	3.20	39	40.0%	15.0%	4
16	47° 18' 04.60", -121° 07' 30.10"	Yes	Bluff	None	None	Very Gravelly Silt Loam	5.92	23	30.0%	32.0%	7.9
17	47° 16' 16.08", -121° 06' 36.89"	Yes	Bluff	None	None	Gravelly Silt Loam	4.92	4.892	26.9%	11.6%	5.7
18	47° 16' 00.90", -121° 06' 29.10"	Yes	Bluff	None	None	Extremely Gravelly Silt Loam	6.49	11.7	20.0%	34.7%	6.4
19	47° 15' 28.91", -121° 05' 55.11"	Yes	Bluff	None	None	Silt Loam	9.34	29	23.6%	21.1%	3.50
20	47° 15' 00.90", -121° 05' 08.50"	Yes	Bluff	None	None	Extremely Gravelly Silt Loam	7.37	3.8	21.4%	20.4%	4.3

Appendix C (CONTINUED) – Study Sites and Site Photographs.

Site	Dominant Vegetation	Undercutting (Y/N)	Fetch	Planimetric Form	Slope Angle	Vegetation Cover	Vegetation Type	Geologic Unit	Interpretation	Date
1	Forest	Yes	Narrow	Straight	Low	High	Developed & Urban	Qad(e) - Evans Creek Alpine Glaical Drift	Glacial drift	7/13/2019
2	Forest	Yes	Wide	Straight	Intermediate	Moderate	Shrub & Herb Wetland	Qad(e) - Evans Creek Alpine Glaical Drift	Glacial drift	6/21/2019
3	Forest & shrub	No	Wide	Convex	Low	High	Barren	Qad(e) - Evans Creek Alpine Glaical Drift	Glacial drift	7/13/2019
4	Forest	Yes	Wide	Convex	Low	Moderate	Barren	Qad(e) - Evans Creek Alpine Glaical Drift	Glacial drift	7/13/2019
5	Forest	Yes	Medium	Concave	Intermediate	Moderate	Shrub & Herb Wetland	Qls(m) - Mass-Wasting Deposits, other than landslides	Intersection of mass wasting and basalt flows	7/13/2019
6	Forest	Yes	Medium	Convex	Intermediate	Moderate	Shrub & Herb Wetland	Qa - Quaternary Alluvium	Quaternary alluvium	9/6/2019
7	Forest	Yes	Medium	Straight	Low	Moderate	Temperate & Boreal Forest & Woodland	Qad(e) - Evans Creek Alpine Glaical Drift	Quaternary alluvium	8/30/2019
8	Barren, Grassland, & Shrub	No	Medium	Straight	Low	Moderate	Shrub & Herb Wetland	Qa - Quaternary Alluvium	Continental sedimentary rock and Quaternary alluvium	8/31/2019
9	Grassland & shrub	No	Medium	Convex	Intermediate	Moderate	Shrub & Herb Wetland	Qad(e) - Evans Creek Alpine Glaical Drift	Quaternary alluvium	8/30/2019
10	Forest & shrub	Yes	Narrow	Straight	Low	Moderate	Temperate & Boreal Forest & Woodland	Eib - Diabase, Gabbro, and Basalt	Basic intrusive rock and glacial drift	8/23/2019
11	Forest & shrub	Yes	Narrow	Straight	Intermediate	Moderate	Temperate & Boreal Forest & Woodland	Eib - Diabase, Gabbro, and Basalt	Quatnerary lake sediments	8/23/2019
12	Forest & shrub	Yes	Narrow	Straight	Intermediate	Moderate	Shrub & Herb Wetland	Ec(1s) - Swauk Formation (Sandstone)	Continental sedimentary rock and alluvium	8/23/2019
13	Forest & shrub	Yes	Medium	Straight	Low	Moderate	Temperate & Boreal Forest & Woodland	Ec(1s) - Swauk Formation (Sandstone)	Continental sedimentary rock and glacial drift	8/31/2019
14	Forest & shrub	Yes	Medium	Convex	Low	High	Shrub & Herb Wetland	Qa - Quaternary Alluvium	Quaternary alluvium	9/6/2019
15	Forest	Yes	Medium	Convex	Intermediate	High	Shrub & Herb Wetland	Qa - Quaternary Alluvium	Quaternary alluvium	9/6/2019
16	Forest	Yes	Medium	Straight	Intermediate	Low	Temperate & Boreal Forest & Woodland	Ec(1s) - Swauk Formation (Sandstone)	Glacial till and continental sedimentary rock	8/31/2019
17	Forest	Yes	Wide	Convex	Intermediate	Low	Temperate & Boreal Forest & Woodland	Evb(t) - Teanaway Formation (Basalt)	Glacial drift and basalt flows	7/28/2019
18	Forest	Yes	Wide	Straight	Intermediate	Low	Temperate & Boreal Forest & Woodland	Evb(t) - Teanaway Formation (Basalt)	Glacial drift atop basalt flows	7/28/2019
19	Forest	Yes	Wide	Straight	Low	Low	Temperate & Boreal Forest & Woodland	Ec(2rm) - Roslyn Formation (middle member)	Continental sedimentary rocks and glacial drift	7/26/2019
20	Forest & shrub	Yes	Medium	Straight	Intermediate	Moderate	Temperate & Boreal Forest & Woodland	Ec(2rm) - Roslyn Formation (middle member)	Continental sedimentary rocks and glacial drift	7/26/2019

Appendix C1: Study sites (Wentworth 1922; Earle 2015).

Site 1

Site 2

Site 3

Site 4

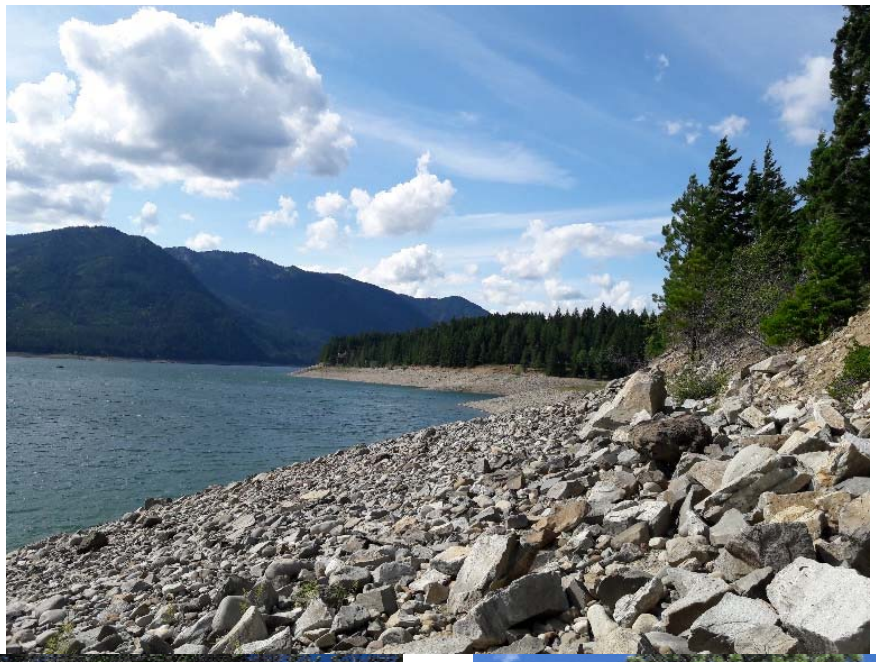

Site 5

Site 6

Site 7

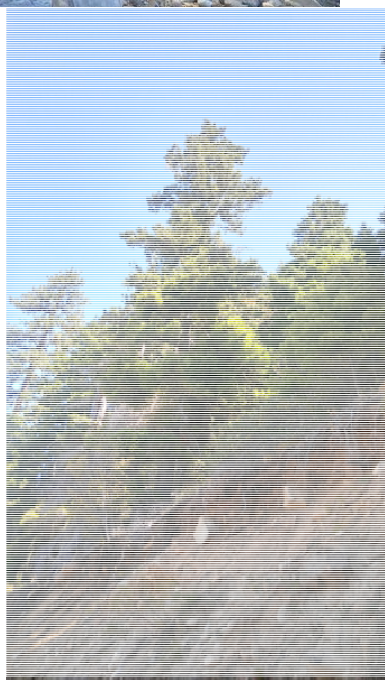

Site 8

Site 9

Site 10

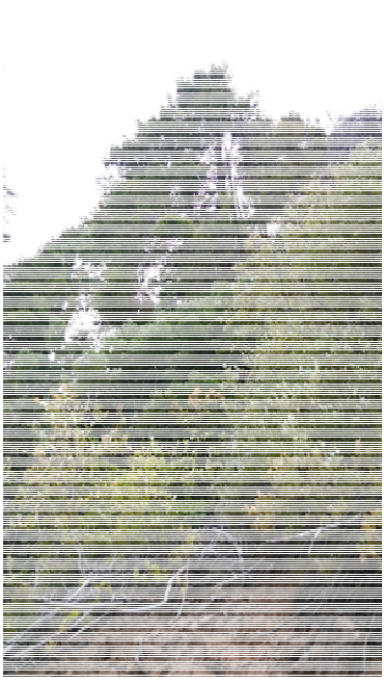

Site 11

Site 12

Site 13

Site 14

Site 15

Site 16

Site 17

Site 18

Site 19

Site 20

Appendix C2: Site Photographs. Photography by Michael Horner, 2018-2019.

Appendix D – GMM Flowchart.

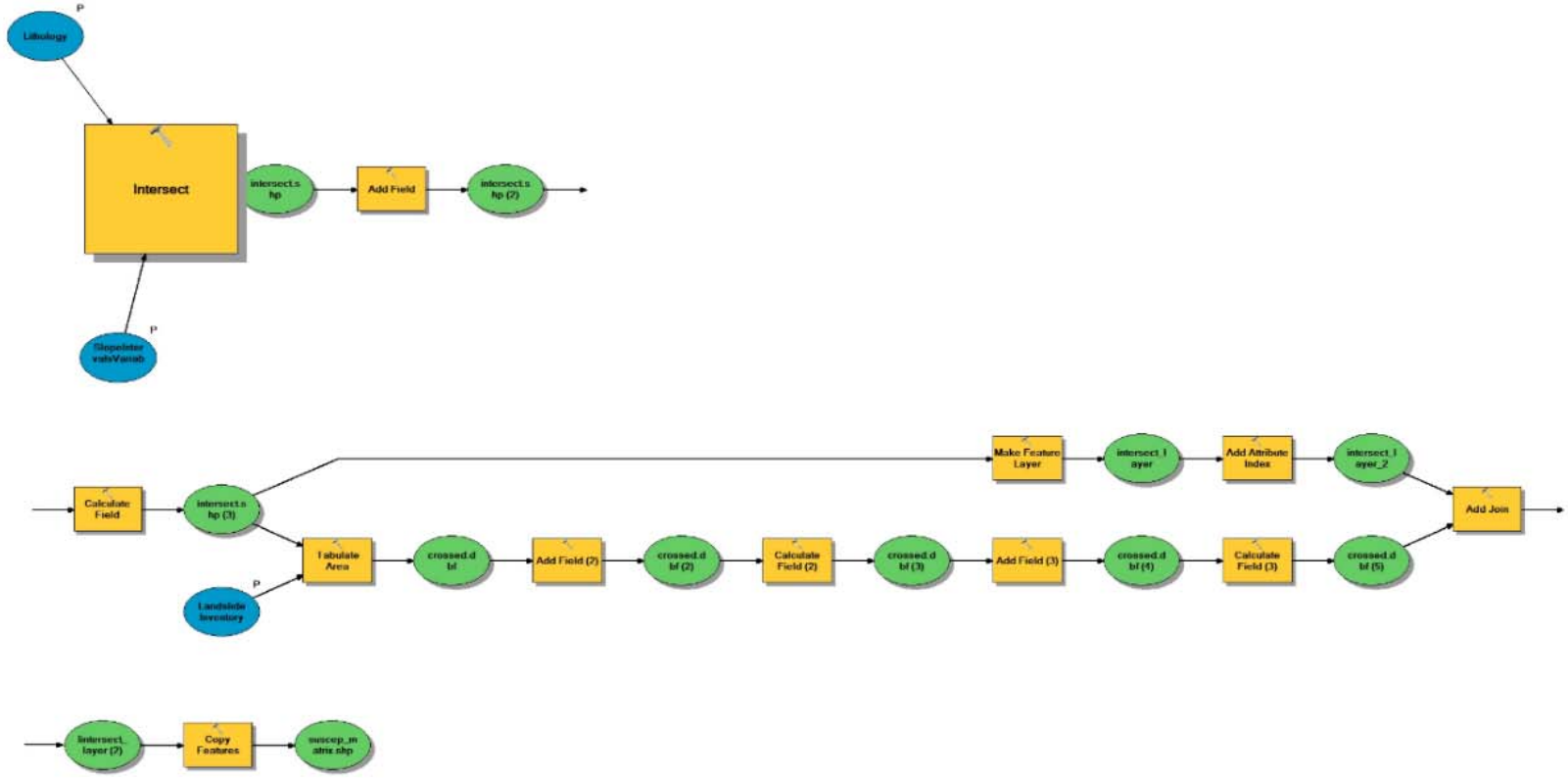

Appendix E – Cle Elum Lake Sediment Textures.

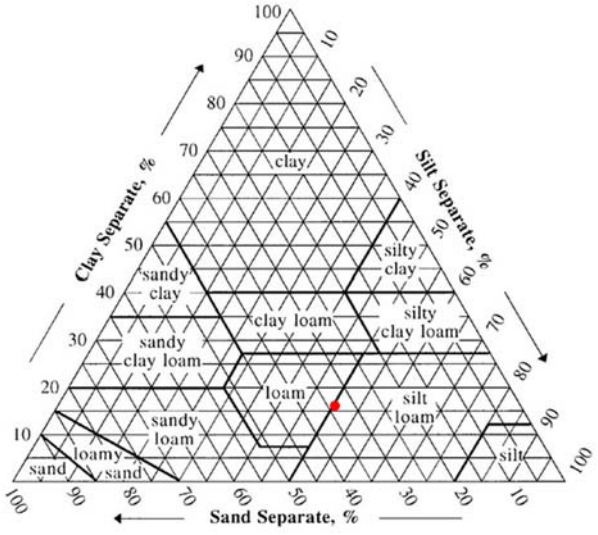

1 - Very Gravelly Loam

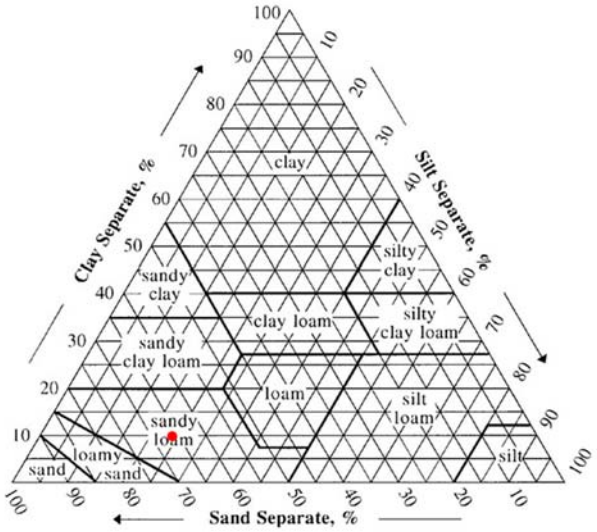

2 - Extremely Gravelly Coarse Sandy Loam

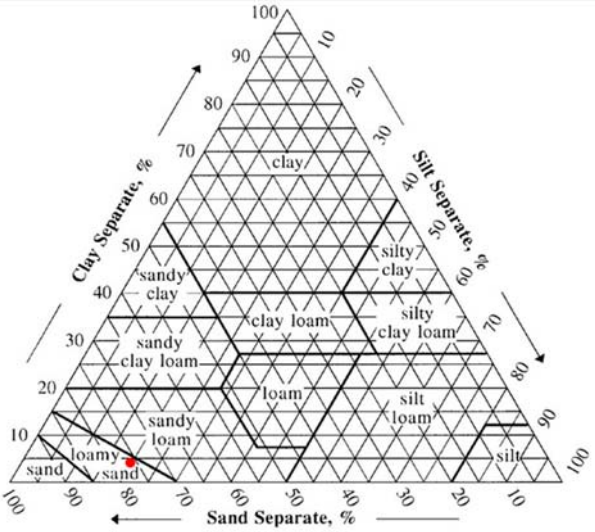

3 - Very Gravelly Loamy Sand

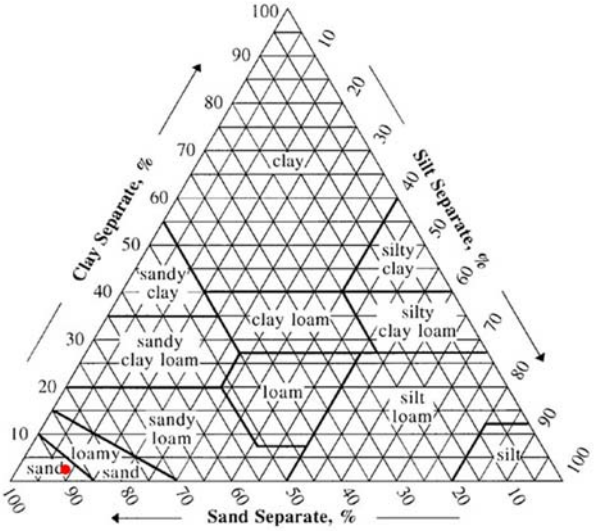

4 - Very Gravelly Fine Sand

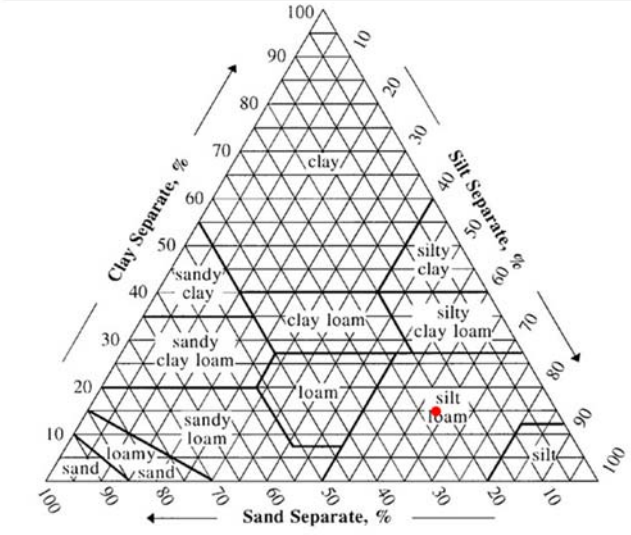

5 - Gravelly Silt Loam

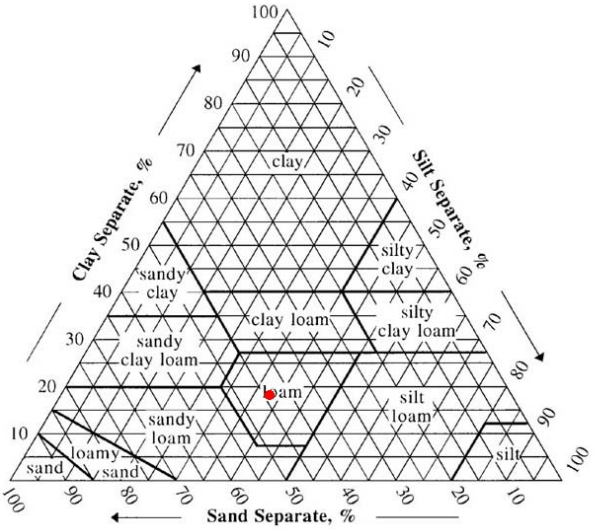

6 - Extremely Gravelly Loam

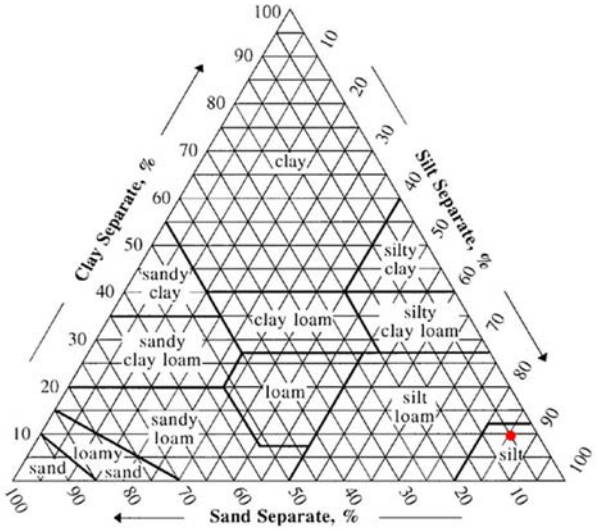

7 - Very Gravelly Silt

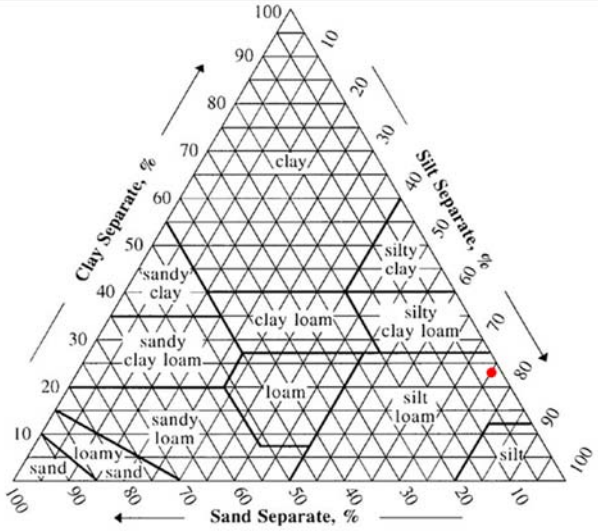

8 - Extremely Gravelly Silt Loam

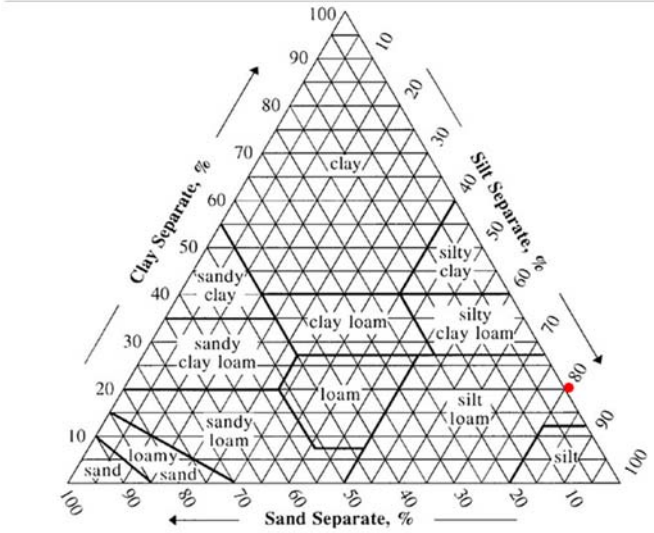

9 - Very Gravelly Silt Loam

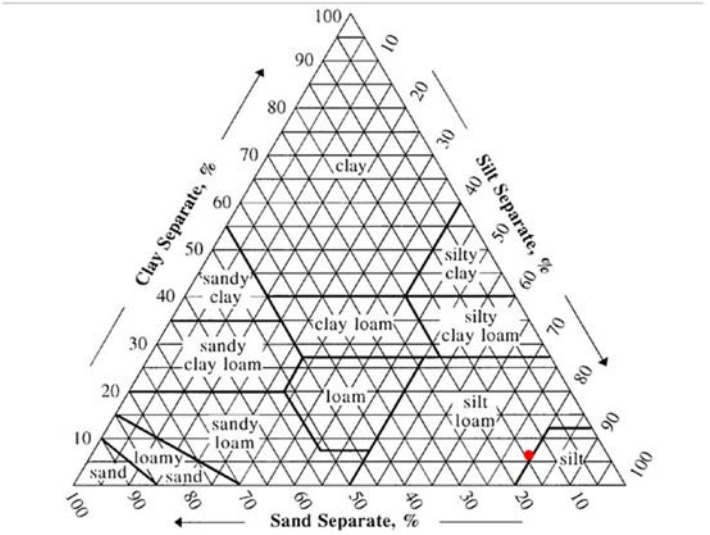

10 - Extremely Gravelly Silt Loam

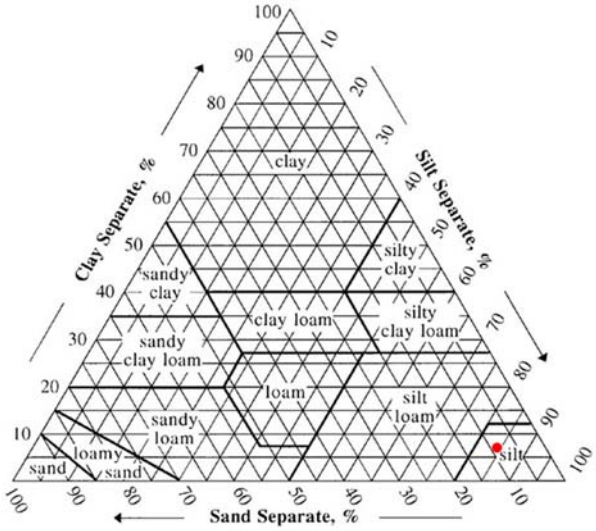

11 - Silt

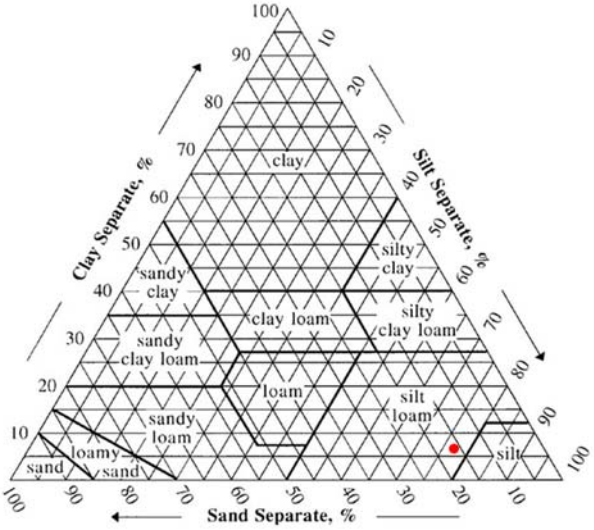

12 - Very Gravelly Silt Loam

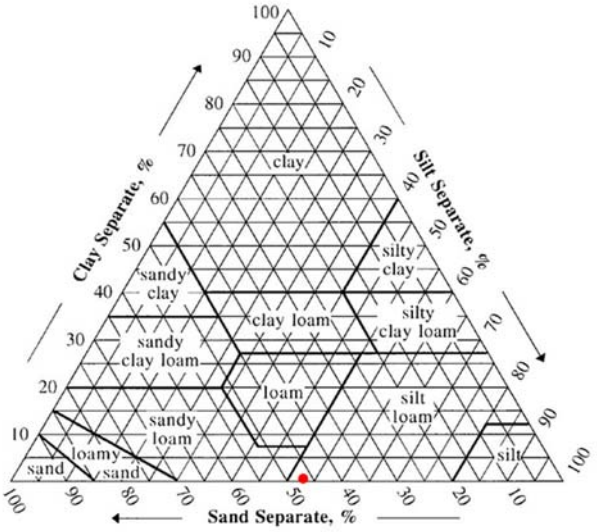

13 - Extremely Gravelly Silt Loam

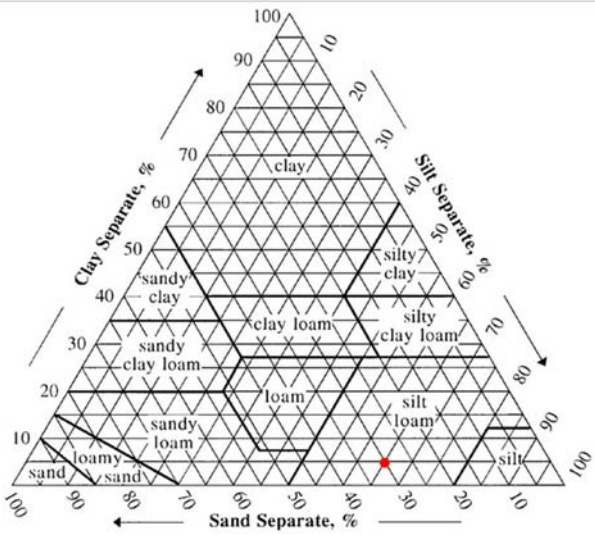

14 - Very Gravelly Silt Loam

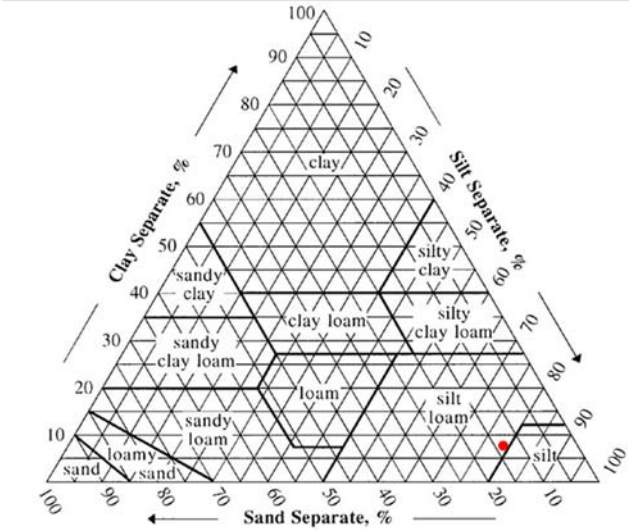

15 - Very Gravelly Silt Loam

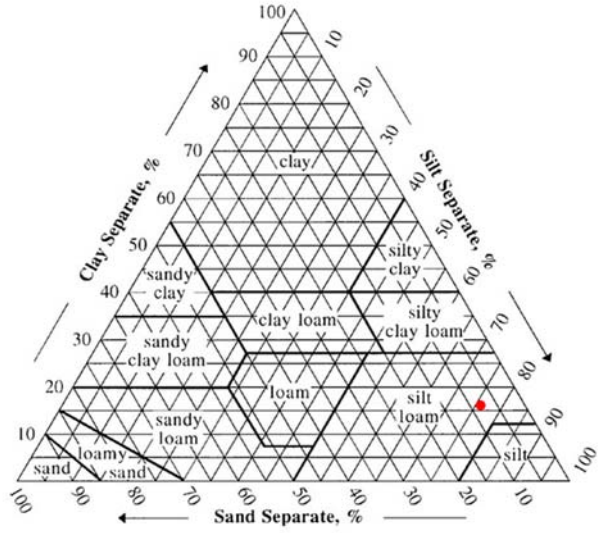

16 - Very Gravelly Silt Loam

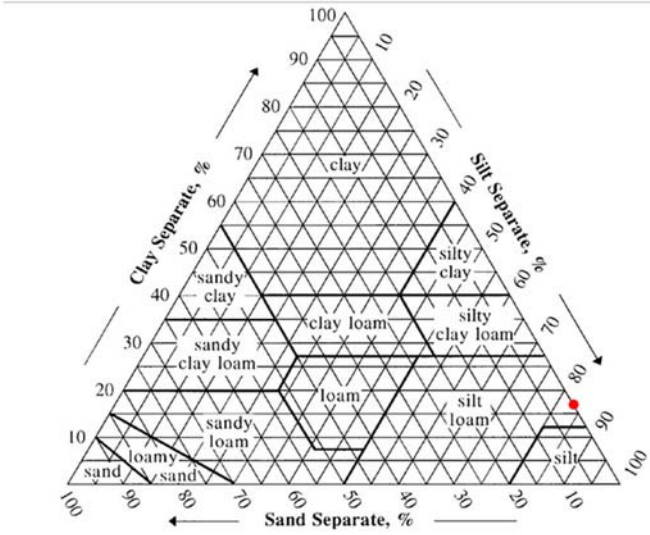

17 - Gravelly Silt Loam

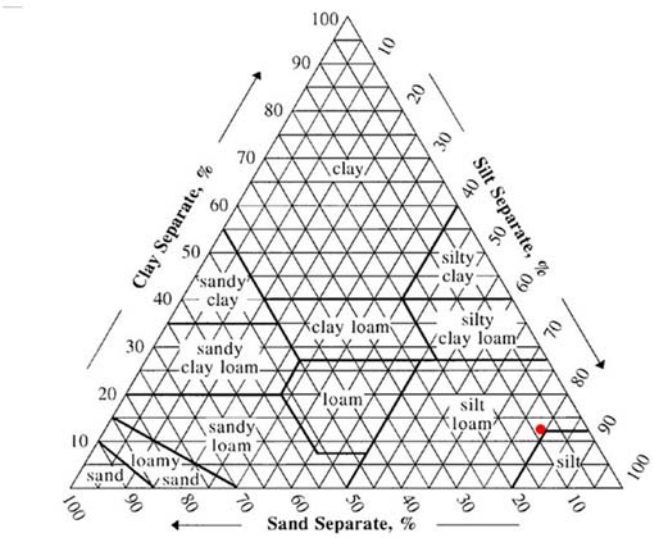

18 - Extremely Gravelly Silt Loam

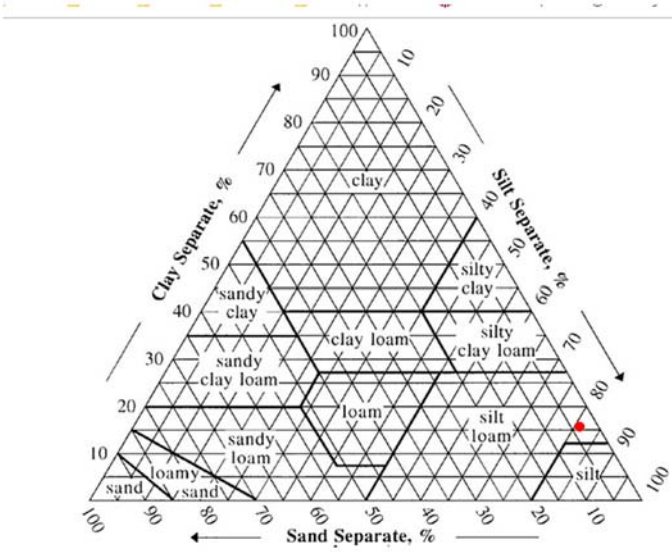

19 - Silt Loam

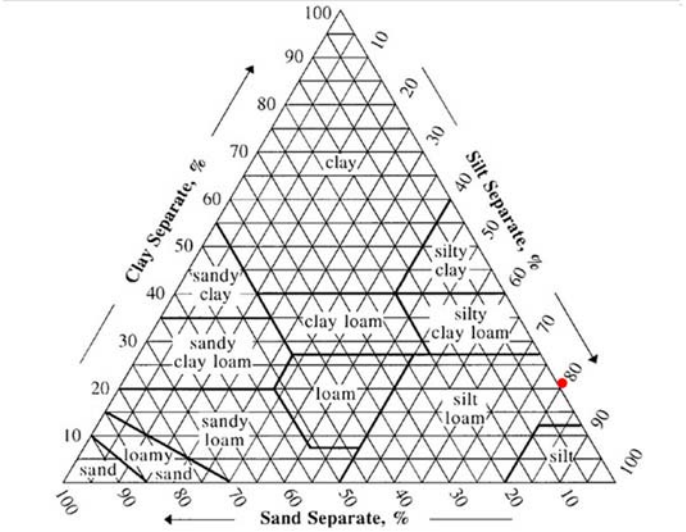

20 - Extremely Gravelly Silt Loam

Appendix E: Cle Elum Lake soil textures (USDA 2019).